ASSESSMENT REPORT TITLE PAGE AND SUMMARY

TITLE OF REPORT: **Assessment Report on Geophysical Work Performed on the BARK Property**

TOTAL COST: **$ 32, 253.00**

AUTHOR(S): **Elena Guszowaty and C.** Mark Rebagliati

SIGNATURE(S):

NOTICE OF WORK PERMIT NUMBER(S)/DATE(S):
STATEMENT OF WORK EVENT NUMBER(S)/DATE(S): **4830543 – Jan 27, 2011**

YEAR OF WORK: **2011**

PROPERTY NAME: **BARK**

CLAIM NAME(S) (on which work was done): **705779, 705788, 705788, 705788, 705790, 705780, 705781, 705782, 705783, 705784, 705785, 705786, 705787, 705822, 705823 and 705824**

COMMODITIES SOUGHT: **Au, Cu**

MINERAL INVENTORY MINFILE NUMBER(S),IF KNOWN:

MINING DIVISION: Omineca Mining **Division**
NTS / BCGS: 93F/07, 93F/08, 93F/09, **93F/10**
LATITUDE: ____53_____ ° ____25_____ ' ____14_____ "
LONGITUDE: ____124_____ ° ____32_____ ' ____20_____ " (at centre of work)
UTM Zone: **10** EASTING: 397,725 NORTHING: **5,920,180**

OWNER(S): **Amarc Resources Ltd.**

MAILING ADDRESS: **15th Floor – 1040 West Georgia Street, Vancouver, BC V6E 4H8**

OPERATOR(S) [who paid for the work]: **Amarc Resources Ltd.**

MAILING ADDRESS: **15th Floor – 1040 West Georgia Street, Vancouver, BC V6E 4H8**

REPORT KEYWORDS (lithology, age, stratigraphy, structure, alteration, mineralization, size and attitude. **Do not use abbreviations or codes**)
Chilcotin Group, basaltic and alkaline volcanic rocks; Hazelton Group – Naglico Formation volcanic and sedimentary rocks

REFERENCES TO PREVIOUS ASSESSMENT WORK AND ASSESSMENT REPORT NUMBERS:
No previous assessment work has been completed on this property

TYPE OF WORK IN THIS REPORT	EXTENT OF WORK (in metric units)	ON WHICH CLAIMS	PROJECT COSTS APPORTIONED (incl. support)
GEOLOGICAL (scale, area)			
Ground, mapping			
Photo interpretation			
GEOPHYSICAL (line-kilometres)			
Ground			
Magnetic			
Electromagnetic			
Induced Polarization			
Radiometric			
Seismic			
Other			
Airborne	369 line-km	All claims listed on page 1	$ 32, 253.00
GEOCHEMICAL (number of samples analysed for ...)			
Soil			
Silt			
Rock			
Other			
DRILLING (total metres, number of holes, size, storage location)			
Core			
Non-core			
RELATED TECHNICAL			
Sampling / Assaying			
Petrographic			
Mineralographic			
Metallurgic			
PROSPECTING (scale/area)			
PREPATORY / PHYSICAL			
Line/grid (km)			
Topo/Photogrammetric (scale, area)			
Legal Surveys (scale, area)			
Road, local access (km)/trail			
Trench (number/metres)			
Underground development (metres)			
Other			
		TOTAL COST	$ 32, 253.00

BC Geological Survey
Assessment Report
32177

Assessment Report on Geophysical Work

Performed on the BARK Property

Located in the Omineca Mining Division

NTS: 93F/07, 93F/08, 93F/09, 93F/10
BCGS: 093F.048, 93F.058

Centred at approximately
53°25' 14" N Latitude
124°32'20" W Longitude
5,920,180 m N; 397,725 m E
UTM NAD 83, Zone 10

Owner/Operator: Amarc Resources Ltd.

Authors:
Elena Guszowaty, BSc (Geol)
Mark Rebagliati, P. Eng

April 20, 2011

TABLE OF CONTENTS

1.0 SUMMARY 1
2.0 INTRODUCTION 2
3.0 LOCATION AND ACCESS 2
4.0 PHYSIOGRAPHY AND CLIMATE 2
5.0 CLAIMS 2
6.0 EXPLORATION HISTORY 5
7.0 REGIONAL GEOLOGY 5
8.0 AIRBORNE GEOPHYSICS 8
9.0 RECOMMENDATIONS 8
10.0 REFERENCES 9
11.0 STATEMENT OF AUTHORS' QUALIFICATIONS 10
12.0 STATEMENT OF COSTS 13

APPENDIX A Airborne Geophysical Report

LIST OF FIGURES

Figure 3.1 Property Location 3
Figure 5.1 Claims 4
Figure 7.1 Regional Geology 6
Figure 7.2 Regional Geology Legend 7

LIST OF TABLES

Table 5.1 BARK claims 5

1.0 SUMMARY

The BARK property is located in central British Columbia, in the Omineca Mining Division, approximately 70 km southwest of Vanderhoof, B.C., on NTS map sheets 93F/07, 08, 09 and 10. The property is accessible by a network of gravel logging roads.

Regional geology shows the property is dominated by Jurassic Hazelton Group volcanic and sedimentary rocks. Hazelton Group volcanic rocks are overlain by Miocene Chilcotin Group alkaline and basaltic volcanic rocks.

An airborne DIGHEM ^{V} electromagnetic/ resistivity/magnetic survey was flown over the claims by Fugro Airborne Surveys Corp., in January 2011 for a total of 369 line-km at a spacing of 200 m. Several magnetic and resistive features were identified and targeted for prospecting, geochemical sampling and ground geophysical surveys.

2.0 INTRODUCTION

This report documents the results of the airborne geophysics performed on the BARK claim group between January 16 and January 19, 2011.

3.0 LOCATION AND ACCESS

The BARK property is situated in central British Columbia, in the Omineca Mining Division. The property is located on NTS maps 93F/07, 93F/08, 93F/09 and 93F/10 and on BCGS maps 093F.048 and 93F.058. The centre of the claim group is approximately 70 km southwest of Vanderhoof, B.C. at 53°25' 14" N Latitude and 124°32'20" W Longitude, or 5,920,180 m N and 397,725 m E (UTM NAD 83, Zone 10), as shown in Figure 3.1.

The property is accessible by road from Vanderhoof via the Yellowhead Highway (Hwy 16) west from Vanderhoof to the Kluskus Forestry Service Road (FSR). The Kluskus FSR intersects the claim block along with a network of lesser forestry roads.

4.0 PHYSIOGRAPHY AND CLIMATE

The BARK property is situated in the Vanderhoof Forest District of the Northern Interior Forest Region. Topography is dominated by gently rolling hills, with numerous lakes, rivers and marshes, with elevations ranging from 950 m to 1,220 m above sea level. The area is forested primarily with Lodgepole Pine, White Spruce, Subalpine Fir (balsam), Douglas fir, Black Spruce and Trembling Aspen (poplar).

Average temperatures in Vanderhoof are 22°C in summer and -12.5°C in winter, annual rainfall averaging 29.2 cm and annual snowfall averaging 176 cm (The Rural Coordination Centre of BC website http://www.rccbc.ca/Vanderhoof-community_overview).

5.0 CLAIMS

The BARK property consists of 15 claims covering approximately 7,000 hectares (Figure 5.1). The claims were staked in February, 2010 and are owned and operated by Amarc Resources Ltd. A list of all claims is given in Table 5.1.

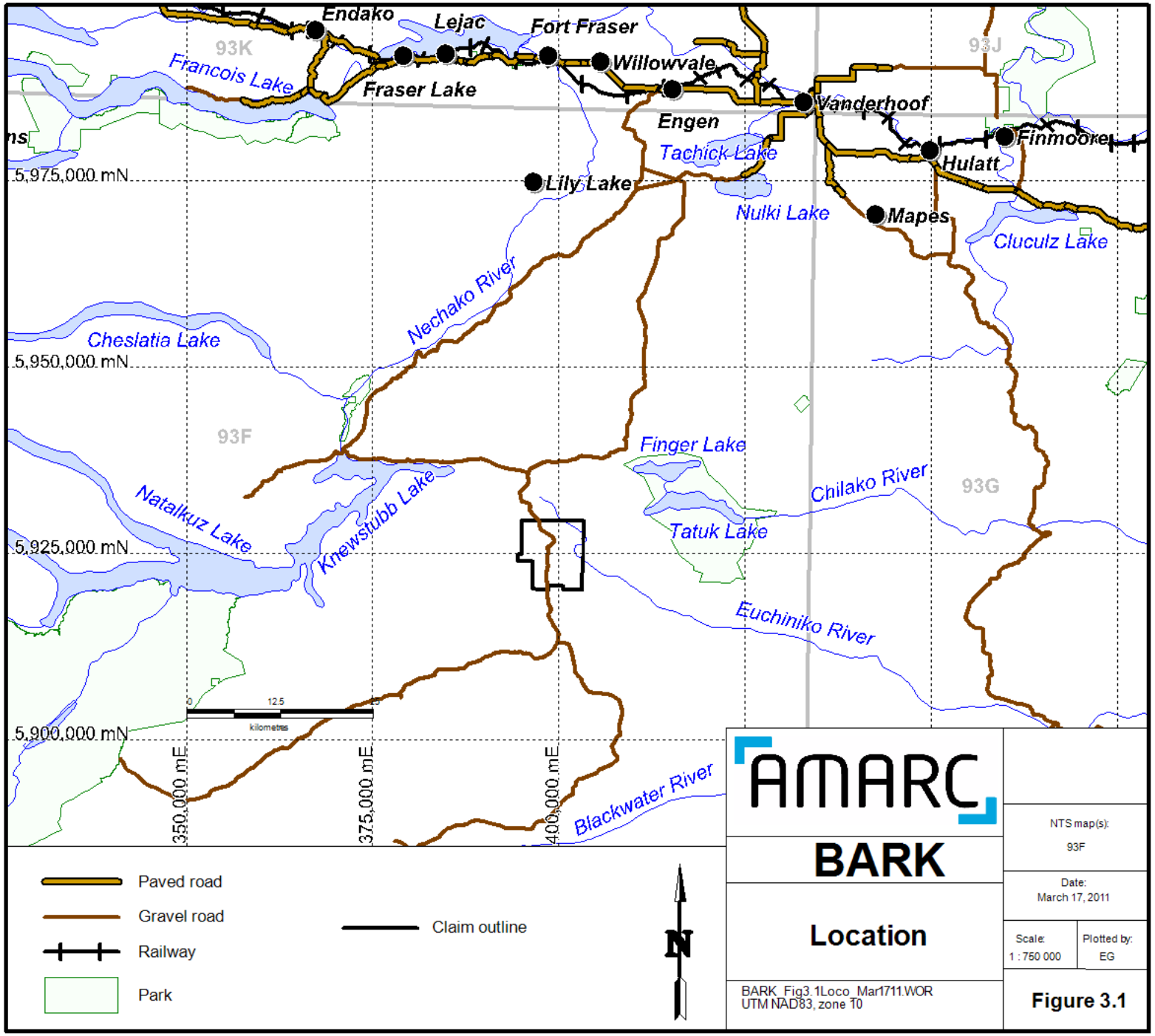
Endako
Lejac
Fort Fraser
Willowvale
Vanderhoof
Finmoore
Hulatt
Engen
Tachick Lake
Fraser Lake
Francois Lake
Lily Lake
Nulki Lake
Mapes
Cluculz Lake
Nechako River
Cheslatia Lake
Finger Lake
Chilako River
Tatuk Lake
Natalkuz Lake
Knewstubb Lake
Euchiniko River
Blackwater River
93K
93J
93F
93G
5,975,000 mN
5,950,000 mN
5,925,000 mN
5,900,000 mN
350,000 mE
375,000 mE
400,000 mE
0
12.5
kilometres
Paved road
Gravel road
Railway
Park
Claim outline
N
AMARC
BARK
Location
NTS map(s):
93F
Date:
March 17, 2011
Scale:
1 : 750 000
Plotted by:
EG
BARK_Fig3.1Loco_Mar1711.WOR
UTM NAD83, zone 10
Figure 3.1

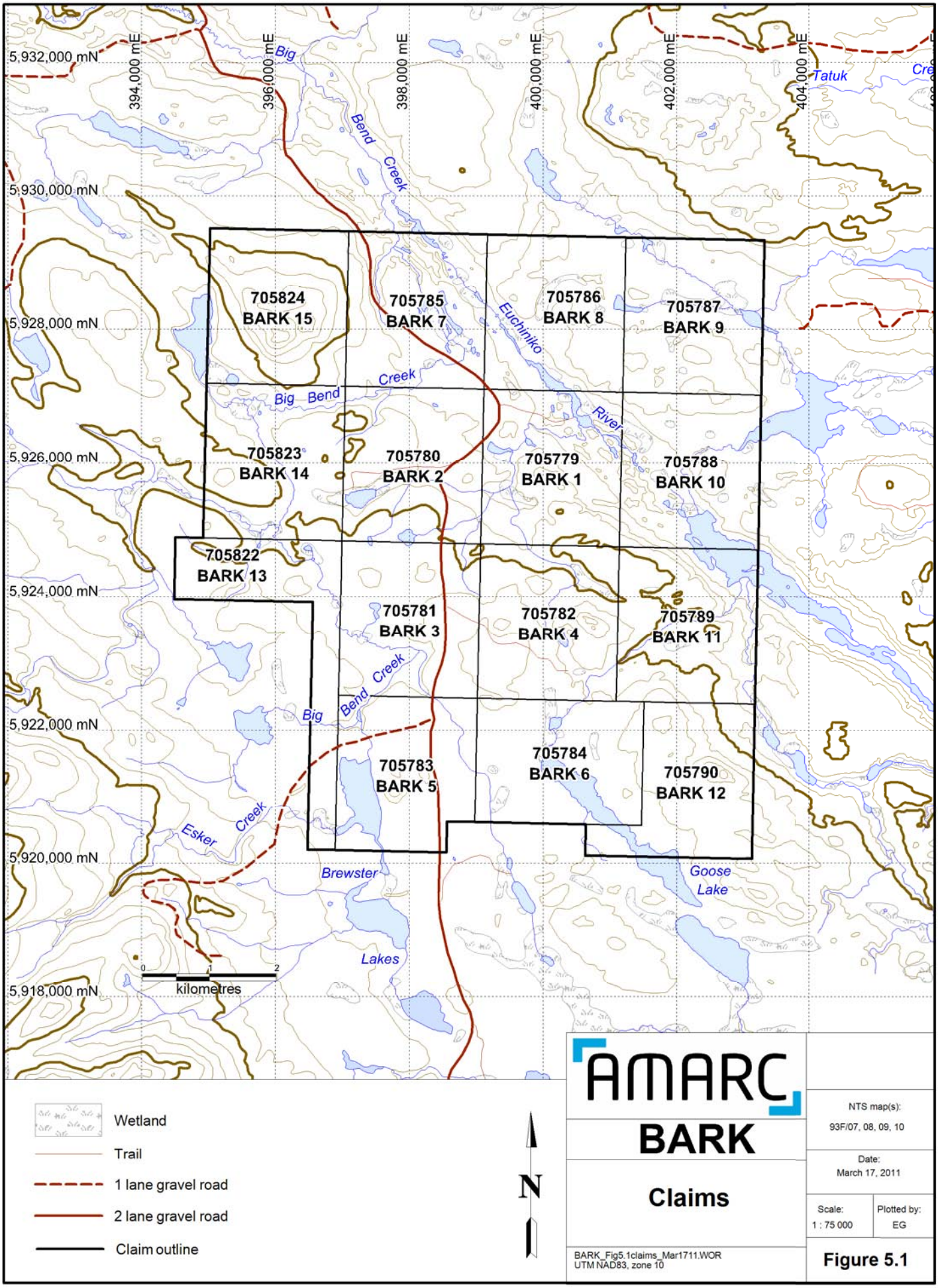
5,932,000 mN
5,930,000 mN
5,928,000 mN
5,926,000 mN
5,924,000 mN
5,922,000 mN
5,920,000 mN
5,918,000 mN
394,000 mE
396,000 mE
398,000 mE
400,000 mE
402,000 mE
404,000 mE
Big Bend Creek
Tatuk
Euchiniko River
Big Bend Creek
Big Bend Creek
Esker Creek
Brewster Lakes
Goose Lake
705824 BARK 15
705785 BARK 7
705786 BARK 8
705787 BARK 9
705823 BARK 14
705780 BARK 2
705779 BARK 1
705788 BARK 10
705822 BARK 13
705781 BARK 3
705782 BARK 4
705789 BARK 11
705783 BARK 5
705784 BARK 6
705790 BARK 12
0
1
2
kilometres
Wetland
Trail
1 lane gravel road
2 lane gravel road
Claim outline
N
AMARC
BARK
Claims
NTS map(s):
93F/07, 08, 09, 10
Date:
March 17, 2011
Scale:
1 : 75 000
Plotted by:
EG
BARK_Fig5.1claims_Mar1711.WOR
UTM NAD83, zone 10
Figure 5.1

Table 5.1 BARK claims

Tenure Number	Claim Name	Owner	Date Recorded	Expiry Date	Area (ha)
705779	BARK 1	Amarc Resources Ltd.	8-Feb-10	8-Feb-12	481.2158
705788	BARK 10	Amarc Resources Ltd.	8-Feb-10	8-Feb-12	481.2338
705789	BARK 11	Amarc Resources Ltd.	8-Feb-10	8-Feb-12	481.4605
705790	BARK 12	Amarc Resources Ltd.	8-Feb-10	8-Feb-12	423.8916
705780	BARK 2	Amarc Resources Ltd.	8-Feb-10	8-Feb-12	481.2049
705781	BARK 3	Amarc Resources Ltd.	8-Feb-10	8-Feb-12	481.4330
705782	BARK 4	Amarc Resources Ltd.	8-Feb-10	8-Feb-12	481.4434
705783	BARK 5	Amarc Resources Ltd.	8-Feb-10	8-Feb-12	462.3910
705784	BARK 6	Amarc Resources Ltd.	8-Feb-10	8-Feb-12	462.3851
705785	BARK 7	Amarc Resources Ltd.	8-Feb-10	8-Feb-12	480.9736
705786	BARK 8	Amarc Resources Ltd.	8-Feb-10	8-Feb-12	480.9841
705787	BARK 9	Amarc Resources Ltd.	8-Feb-10	8-Feb-12	481.0030
705822	BARK 13	Amarc Resources Ltd.	9-Feb-10	9-Feb-12	385.1700
705823	BARK 14	Amarc Resources Ltd.	9-Feb-10	9-Feb-12	481.2100
705824	BARK 15	Amarc Resources Ltd.	9-Feb-10	9-Feb-12	480.9800

6.0 EXPLORATION HISTORY

Only one assessment report has been filed on the area now covered by the BARK property. The report was filed by United Exploration Management Inc. in 2010 for geological and geophysics work. This report is still under review and has not been released to the public.

7.0 REGIONAL GEOLOGY

The entire BARK property occurs in the southern half of the Stikinia terrane along the eastern border (Figure 7.1, 7.2). The regional geology of the claim group is derived from Massey, *et al*., (2005).

The claims are covered by Mesozoic volcanic and sedimentary rocks overlain by Cenozoic volcanic rocks. Cenozoic rocks are primarily alkaline volcanic rock of the Miocene Chilcotin Group (MiCCl), with minor Miocene Chilcotin Group basaltic volcanic rocks (MiCvb).

Mesozoic rocks are dominated by volcanic rocks of the Middle Jurassic Hazelton Group (mJHN) and are described by Massey *et al.* as clinopyroxene- and plagioclase-phyric basaltic and andesitic lava flows, volcanic breccia and conglomerate, volcaniclastic rocks, rare hyaloclastite, and associated sedimentary rocks. Lesser windows of Early to Middle Jurassic Hazelton Group (lJHvl) volcaniclastic and pyroclastic volcanic rocks and Early Jurassic Hazelton Group (lJHNsf) mudstone, siltstone, shale fine clastic sedimentary rocks are located within the property boundary.

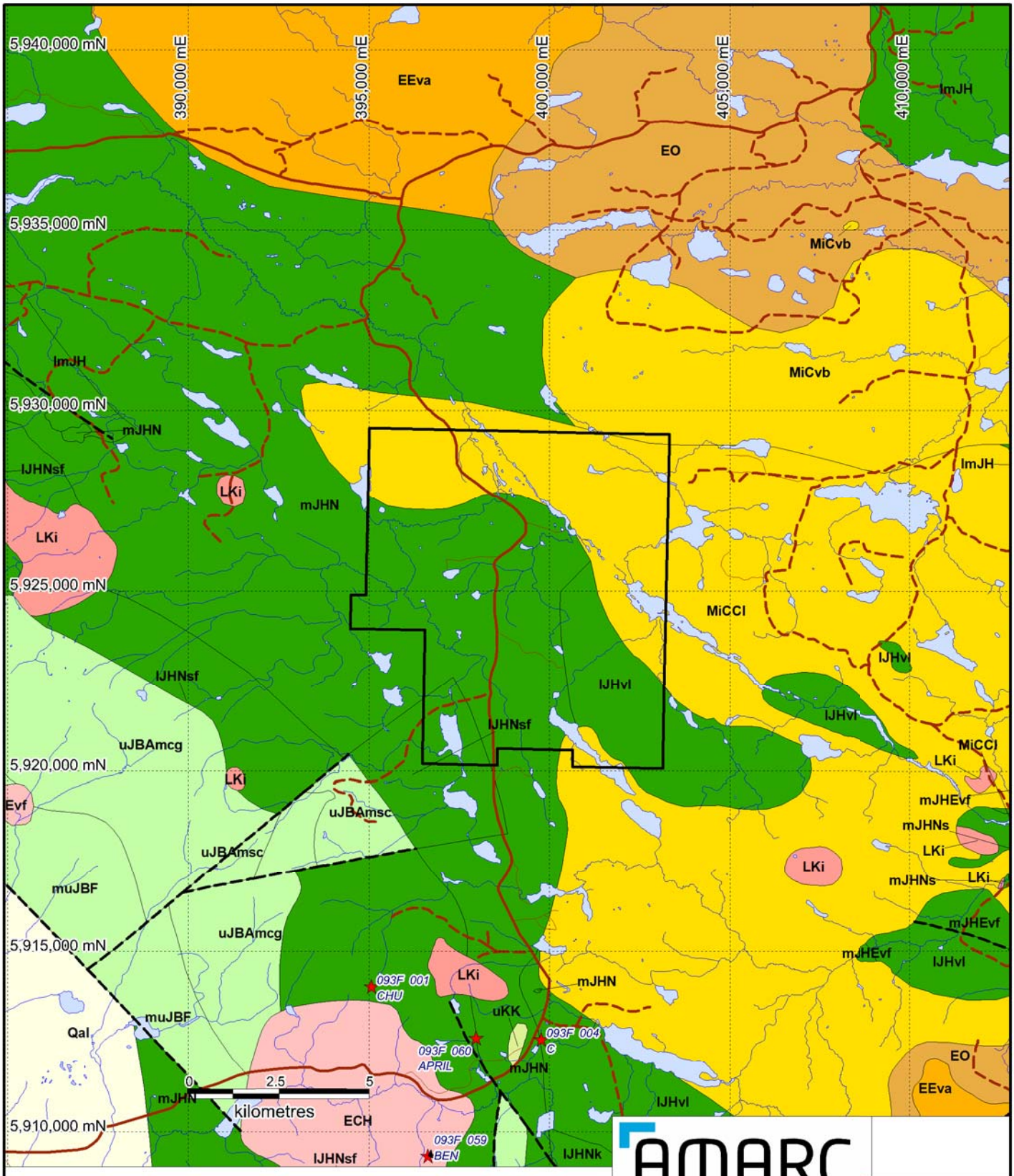

Legend on Figure 7.2

AMARC

BARK

Regional Geology

BARK_Fig7.1RegGeol_Mar1711.WOR
UTM NAD83, zone 10

NTS map(s):
93F/07, 08, 09, 10

Date:
March 17, 2011

Scale:
1 : 150 000

Plotted by:
EG

Figure 7.1

STRATIGRAPHIC UNITS

Quaternary

Qal
unconsolidated till, glaciofluvial deposits, glaciolacustrine deposits, collovium, alluvium

Miocene

MiCvb
Chilcotin Group
basaltic volcanic rocks

MiCCl
Chilcotin Group - Cheslatta Lake Complex
alkaline volcanic rocks

Eocene

EEva
Nechako Plateau Group - Endako Formation
andesitic volcanic rocks

Eocene to Oligocene

EO
Nechako Plateau Group - Oosta Lake Formation
rhyolite, felsic volcanic rocks

Late Cretaceous

uKK
Kasalka Group
andesitic volcanic rocks

Middle to Late Jurassic

uJBAmcg
Bowser Lake Group - Ashman Formation
conglomerate, coarse clastic sedimentary rocks

uJBAmsc
Bowser Lake Group - Ashman Formation
coarse clastic sedimentary rocks

muJBF
Bowser Lake Group - Fawnie Volcanics
undivided volcanic rocks

Middle Jurassic

mJHN
Hazelton Group - Naglico Formation
undivided volcanic rocks

mJHNs
Hazelton Group - Naglico Formation
undivided sedimentary rocks

mJHEvf
Hazelton Group - Entiako Formation
rhyolite, felsic volcanic rocks

Early to Middle Jurassic

lmJH
Hazelton Group
undivided volcanic rocks

lJHvl
Hazelton Group
coarse volcaniclastics and pyroclastic volcanic rocks

Early Jurassic

lJHNsf
Hazelton Group - Nechako Formation
mudstone, siltstone, shale fine clastic sedimentary rocks

lJHNk
Hazelton Group - Nechako Formation
marine sedimentary and volcanic rocks

INTRUSIVE ROCKS

Eocene

ECH
Ch Pluton
granodiorite intrusive rocks

Evf
unnamed intrusive rocks, undivided

Late Cretaceous to Neogene

LKi
intrusive rocks, undivided

★ MINFILE occurrence

Fault

Claim boundary

AMARC

BARK

Regional Geology Legend

Date: March 17, 2011

Plotted by: EG

BARK_Fig7.1RegGeol_Mar1711.WOR
UTM NAD83, zone 10

Figure 7.2

The BARK property does not host any MINFILE occurrences, but several occur in close proximity to the south of the claims. Approximately 6 km south of the property is the Chu showing (MINFILE 093F 001), a molybdenum and copper occurrence characterized by stockworks and disseminated mineralization, thought to be associated with a low Fe porphyry deposit. To the southeast of the Chu showing is the C showing (MINFILE 093F 004) a molybdenum and copper occurrence, with disseminated mineralization, classified as a hydrothermal epigenetic system. Directly to the east of the Chu showing is the April prospect (MINFILE 093F 060), a high sulphidation epithermal Au-Ag-Cu system, dominated by massive and vein-style mineralization. Southwest of the April prospect is the Ben showing (MINFILE 093F 059), a high sulphidation epithermal Au-Ag-Cu occurrence, characterized by vein-style mineralization.

8.0 AIRBORNE GEOPHYSICS

Fugro Airborne Surveys Corp. was contracted to carry out a DIGHEM ^{V} electromagnetic/ resistivity/magnetic survey over the entire BARK property. The survey was flown from January 16 to January 19, 2011 in an AS350-B2 (A-Star) turbine helicopter using the DIGHEM ^{V} electromagnetic system. The helicopter flew at an average airspeed of 100 km/h with an EM sensor height of approximately 35 metres. A total of 369 line-km were flown east-west (90°/270°) at 200 m spacing.

The results of the airborne survey identified several magnetic and resistivity features of interest, warranting further field examination.

9.0 RECOMMENDATIONS

Prospecting, grid geochemical surveys and ground geophysical surveys are recommended to determine if any of the identified magnetic and resistivity features are associated with economic mineralization.

10.0 REFERENCES

Massey, N.W.D., *et al*. (2005) Digital Geology Map of British Columbia, B.C. Ministry of Energy and Mines, Geological Survey Branch, Open File 2005-2, January, 2005.

The Rural Coordination Centre of BC website, http://www.rccbc.ca/Vanderhoof-community_overview, accessed March 7, 2011.

11.0 STATEMENT OF AUTHORS' QUALIFICATIONS

STATEMENT OF QUALIFICATIONS

I, ***Elena Guszowaty***, of Vancouver, British Columbia, hereby certify that:

I am a Geologist working for Amarc Resources Ltd., with offices located at 1020-800 West Pender Street, Vancouver, British Columbia.

1. I received a B.Sc. degree in Earth and Ocean Sciences from the University of British Columbia, Vancouver, British Columbia in 2008.
2. I am an author of this report and am also responsible for the technical figures.

Signed on the 20th day of April, 2011

Elena Guszowaty, B.Sc.

STATEMENT OF QUALIFICATIONS

I, ***C. Mark Rebagliati***, P. Eng., of Vancouver, British Columbia, Canada, do hereby state that:

1. I am a consulting geological engineer and President of Rebagliati Geological Consulting Ltd with offices at 317-2200 Highbury St, Vancouver, British Columbia, Canada.
2. I am a member of the Association of Professional Engineers and Geoscientists of the Province of British Columbia, holding License Number 8352.
3. I graduated with a B.Sc. in geological engineering from Michigan Technological University, Houghton, Michigan, USA in 1969.
4. I have worked as an exploration geologist for a total of 41 years since my graduation from university.
5. I am the Technical Manager directing activities on the BARK Property for Amarc Resources Ltd.

Signed on the 20th day of April, 2011

C. Mark Rebagliati, P. Eng.

12.0 STATEMENT OF COSTS

Exploration Work type					Totals
Office Studies	**List Personnel (Office Only)**	**Days**			
Project Supervision	Mark Rebagliati/ Exploration Mgr	1.00	$2,000.00	$2,000.00	
Map preparation	Gwendolen Ditson	0.25	$600.00	$150.00	
Report preparation	Elena Guszowaty	5.00	$600.00	$3,000.00	
				$5,150.00	**$5,150.00**
Airborne Exploration Surveys	**Description**	**Line km**			
Aeromagnetics	369 line km @ $87/line km	369.0	$87.00	$32,103.00	
				$32,103.00	**$32,103.00**
TOTAL Expenditures					**$37,253.00**

APPENDIX A

Report # 10073-1

DIGHEM ^{V} SURVEY
FOR
AMARC RESOURCES LTD.
BARK PROJECT,
VANDERHOOF AREA, B.C.

NTS: 93F/7,8,9,10;

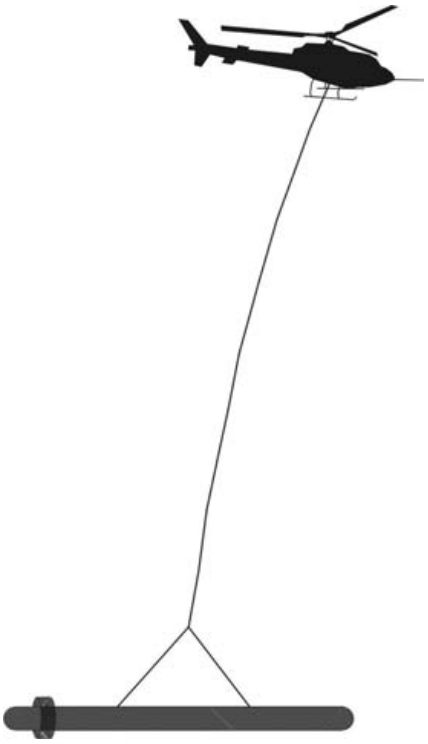

Fugro Airborne Surveys Corp.
Mississauga, Ontario

March 3, 2011

Fugro Airborne Surveys, 2505 Meadowvale Boulevard, Mississauga, Ontario, Canada, L5N 5S2
Phone: 1 905 812 0212, Fax: 1 905 812 1504

SUMMARY

This report describes the logistics, data acquisition, processing, and presentation of results pertaining to a DIGHEM^{V} airborne geophysical survey carried out for Amarc Resources Ltd., over a property located near Vanderhoof, B.C. Total coverage of the survey block amounted to 369 line-km. The survey was flown from January 16 to January 19, 2011.

The purpose of the survey was to map any intrusions or shears in the area that might be favourable for gold deposition, to detect any zones of conductive mineralization or alteration, and to provide information that could be used to map the geology and structure of the Bark Project area. This was accomplished by using a DIGHEM ^{V} multi-coil, multi-frequency electromagnetic system, supplemented by a high sensitivity magnetometer. The information from these sensors was processed to produce maps that display the magnetic and conductive properties of the survey area. A GPS electronic navigation system ensured accurate positioning of the geophysical data with respect to the base maps.

The survey property hosts several anomalous features, some of which are considered to be of moderate priority as exploration targets. Although auriferous targets in this area can be associated with resistive units, rather than conductive units, there are a few inferred bedrock conductors that may also warrant further investigation using appropriate surface exploration techniques. Areas of interest may be assigned priorities on the basis of supporting geophysical, geochemical and/or geological information. After initial investigations have been carried out, it may be necessary to re-evaluate the remaining anomalous responses based on information acquired from the follow-up program.

CONTENTS

1. INTRODUCTION 1.1

2. SURVEY OPERATIONS 2.1

3. SURVEY EQUIPMENT 3.1
   - Electromagnetic System 3.1
   - In-Flight EM System Calibration 3.2
   - Magnetometer 3.3
   - Magnetic Base Station 3.3
   - Navigation (Global Positioning System) 3.5
   - Radar Altimeter 3.6
   - Barometric Pressure and Temperature Sensors 3.7
   - Digital Data Acquisition System 3.7
   - Video Flight Path Recording System 3.7

4. QUALITY CONTROL AND IN-FIELD PROCESSING 4.1

5. DATA PROCESSING 5.1
   - Flight Path Recovery 5.1
   - Electromagnetic Data 5.1
   - Apparent Resistivity 5.2
   - Dielectric Permittivity and Magnetic Permeability Corrections 5.3
   - Resistivity-depth Sections (optional) 5.4
   - Residual Magnetic Intensity 5.5
   - Calculated Vertical Magnetic Gradient 5.5
   - Magnetic Derivatives (optional) 5.6
   - Contour, Colour and Shadow Map Displays 5.6
   - Digital Elevation (optional) 5.7
   - Contour, Colour and Shadow Map Displays 5.8

6. PRODUCTS 6.1
   - Base Maps 6.1
   - Final Products 6.2

7. SURVEY RESULTS 7.1
   - General Discussion 7.1
   - Magnetic Data 7.2
   - Apparent Resistivity 7.3
   - Electromagnetic Anomalies 7.5

Potential Bedrock Conductors 7.7

8. CONCLUSIONS AND RECOMMENDATIONS 8.1

APPENDICES

A. List of Personnel
B. Data Processing Flowcharts
C. Background Information
D. Data Archive Description
E. EM Anomaly List
F. Glossary

1. INTRODUCTION

A DIGHEM V electromagnetic/resistivity/magnetic survey was flown for Amarc Resources Ltd., over the BARK property located near Vanderhoof, B.C. The survey was flown from January 16 to January 19, 2011. The survey area can be located on NTS map sheets 93F/7,8,9,10. (Figure 2.)

Survey coverage consisted of approximately 369 line-km including tie lines. Flight lines were flown east-west (90°/270°) with a line separation of 200 metres. Tie lines were flown orthogonal to the traverse lines (N-S) with a line separation of 2000 metres.

The survey employed the DIGHEM ^{V} electromagnetic system. Ancillary equipment consisted of an optically pumped, high-sensitivity cesium magnetometer, radar and barometric altimeters, a video camera, digital recorders, and an electronic navigation system. The instrumentation was installed in an AS350-B2 turbine helicopter (Registration C-FZTA) that was provided by Questral Helicopters Ltd. The helicopter flew at an average airspeed of 100 km/h with an EM sensor height of approximately 35 metres.

Figure 1: Fugro Airborne Surveys DIGHEM ^{V} EM bird with AS350-B2

2. SURVEY OPERATIONS

The base of operations for the survey was established at the Chu Camp. Table 2-1 lists the corner coordinates of the survey area in NAD83, UTM Zone 10N, central meridian 123°W.

Table 2-1

NAD83 UTM Zone 10N

Block	Corners	X-UTM (E)	Y-UTM (N)
10073-1	1	395000	5929100
BARK Area	2	403000	5929100
	3	403000	5920100
	4	396600	5920100
	5	396600	5923900
	6	394500	5923900
	7	394500	5924900
	8	395000	5924900

f

The survey specifications were as follows:

Parameter	Specifications
Traverse line direction	E-W (90°)
Traverse line spacing	200 m
Tie line direction	N-S (360°)
Tie line spacing	2000 m
Sample interval	10 Hz, 2.75 m @ 100 km/h
Aircraft mean terrain clearance	65 m
EM sensor mean terrain clearance	35m
Mag sensor mean terrain clearance	35 m
Average speed	100 km/h
Navigation (guidance)	±5 m, Real-time GPS
Post-survey flight path	±2 m, Differential GPS

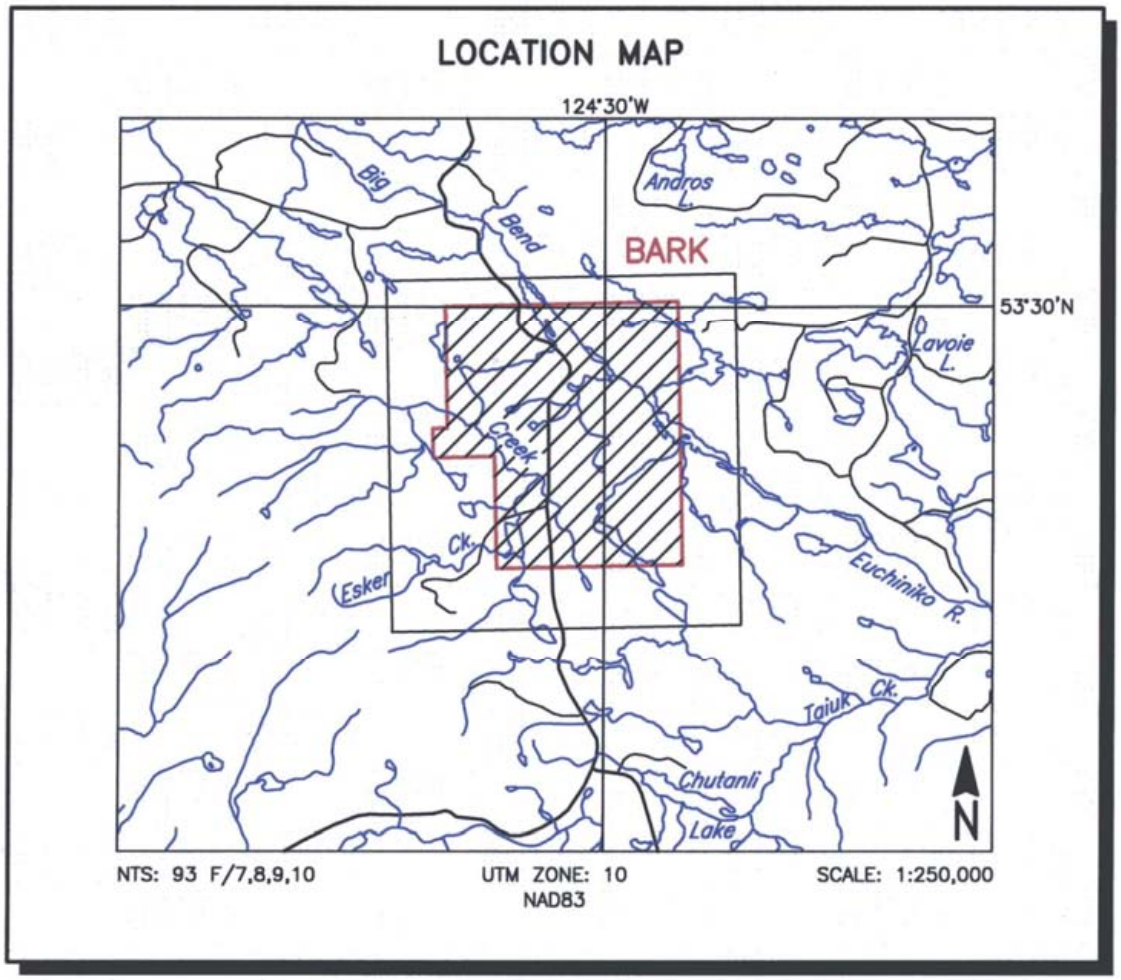

Figure 2
Location Map and Sheet Layout
BARK Project Area
Job # 10073-1

3. SURVEY EQUIPMENT

This section provides a brief description of the geophysical instruments used to acquire the survey data and the calibration procedures employed. The geophysical equipment was installed in an AS350-B2 helicopter. This aircraft provides a safe and efficient platform for surveys of this type.

Electromagnetic System

Model: DIGHEM ^{V}-BKS 51

Type: Towed bird, symmetric dipole configuration operated at a nominal survey altitude of 50 metres. Coil separation is 8 metres for 900 Hz, 1000 Hz, 5500 Hz and 7200 Hz, and 6.3 metres for the 56,000 Hz coil-pair.

Coil orientations, frequencies and dipole moments

Atm^2	orientation		nominal	actual
211	coaxial	/	1000 Hz	1114 Hz
211	coplanar	/	900 Hz	924 Hz
67	coaxial	/	5500 Hz	5495 Hz
56	coplanar	/	7200 Hz	7095 Hz
15	coplanar	/	56,000 Hz	55630 Hz

Channels recorded:
5 in-phase channels
5 quadrature channels
2 monitor channels

Sensitivity:
0.06 ppm at 1000 Hz Cx
0.12 ppm at 900 Hz Cp
0.12 ppm at 5,500 Hz Cx
0.24 ppm at 7,200 Hz Cp
0.60 ppm at 56,000 Hz Cp

Sample rate: 10 per second, equivalent to 1 sample every 2.75 m, at a survey speed of 100 km/h.

The electromagnetic system utilizes a multi-coil coaxial/coplanar technique to energize conductors in different directions. The coaxial coils are vertical with their axes in the flight direction. The coplanar coils are horizontal. The secondary fields are sensed simultaneously by means of receiver coils that are maximum-coupled to their respective transmitter coils. The system yields an in-phase and a quadrature channel from each transmitter-receiver coil-pair.

In-Flight EM System Calibration

Calibration of the system during the survey uses the Fugro AutoCal automatic, internal calibration process. At the beginning and end of each flight, and at intervals during the flight, the system is flown up to high altitude to remove it from any “ground effect” (response from the earth). Any remaining signal from the receiver coils (base level) is measured as the zero level, and is removed from the data collected until the time of the next calibration. Following the zero level setting, internal calibration coils, for which the response phase and amplitude have been determined at the factory, are automatically triggered – one for each frequency. The on-time of the coils is sufficient to determine an accurate response through any ambient noise. The receiver response to each calibration coil “event” is compared to the expected response (from the factory calibration) for both phase angle and amplitude, and any phase and gain corrections are automatically applied to bring the data to the correct value.

In addition, the outputs of the transmitter coils are continuously monitored during the survey, and the gains are adjusted to correct for any change in transmitter output.

Because the internal calibration coils are calibrated at the factory (on a resistive half-space) ground calibrations using external calibration coils on-site are not necessary for system calibration. A check calibration may be carried out on-site to ensure all systems are working correctly. All system calibrations will be carried out in the air, at sufficient altitude that there will be no measurable response from the ground.

The internal calibration coils are rigidly positioned and mounted in the system relative to the transmitter and receiver coils. In addition, when the internal calibration coils are calibrated at the factory, a rigid jig is employed to ensure accurate response from the external coils.

Using real time Fast Fourier Transforms and the calibration procedures outlined above, the data are processed in real time, from measured total field at a high sampling rate, to in-phase and quadrature values at 10 samples per second.

Magnetometer

Model:	Scintrex CS-3 sensor with a Fugro D1344 counter.
Type:	Optically pumped cesium vapour
Sensitivity:	0.01 nT
Sample rate:	10 per second

The magnetometer sensor is housed in the HEM bird, which is flown 28 m below the helicopter.

Magnetic Base Station

Primary

Model:	Fugro CF1 base station with timing provided by integrated GPS	
Sensor type:	Scintrex CS-3	
Counter specifications:	Accuracy:	±0.1 nT
	Resolution:	0.01 nT
	Sample rate	1 Hz

GPS specifications:	Model:	Marconi Allstar
	Type:	Code and carrier tracking of L1 band, 12-channel, C/A code at 1575.42 MHz
	Sensitivity:	-90 dBm, 1.0 second update
	Accuracy:	Manufacturer's stated accuracy for differential corrected GPS is 2 metres

Environmental Monitor specifications:

Temperature:

- Accuracy: ±1.5ºC max
- Resolution: 0.0305ºC
- Sample rate: 1 Hz
- Range: -40ºC to +75ºC

Barometric pressure:

- Model: Motorola MPXA4115AP
- Accuracy: ±3.0º kPa max (-20ºC to 105ºC temp. ranges)
- Resolution: 0.013 kPa
- Sample rate: 1 Hz
- Range: 55 kPa to 108 kPa

Backup

Model:	GEM Systems GSM-19T
Type:	Digital recording proton precession
Sensitivity:	0.10 nT
Sample rate:	3 second intervals

A digital recorder is operated in conjunction with the base station magnetometer to record the diurnal variations of the earth's magnetic field. The clock of the base station is

synchronized with that of the airborne system, using GPS time, to permit subsequent removal of diurnal drift. The Fugro CF1 was the primary magnetic base station. It was located at the Chu Camp, at WGS 84 Latitude 53° 20′ 30.153″ N; Longitude 124° 38′ 52.6998″ W at an orthometric elevation of 1081 m (a.m.s.l.).

Navigation (Global Positioning System)

Airborne Receiver for Real-time Navigation & Guidance

Model:	NovAtel OEM4/V with PNAV 2100 interface
Type:	Code and carrier tracking of L1-C/A code at 1575.42 MHz and L2-P code at 1227.0 MHz. Dual frequency, 24-channel. WAAS enabled.
Sensitivity:	-132 dBm, 10 Hz update
Accuracy:	Manufacturer's stated accuracy is better than 2 metres real-time
Antenna:	Aero AT1675; Mounted on tail of aircraft

Primary Base Station for Post-Survey Differential Correction

Model:	NovAtel OEM4/V
Type:	Code and carrier tracking of L1-C/A code at 1575.42 MHz and L2-P code at 1227.0 MHz. Dual frequency, 24-channel.
Sample rate:	10 Hz update.
Accuracy:	Better than 1 metre in differential mode.

Secondary GPS Base Station

Model:	Marconi Allstar, CMT-1200
Type:	Code and carrier tracking of L1 band, 12-channel, C/A code

	at 1575.42 MHz
Sensitivity:	-90 dBm, 1.0 second update
Accuracy:	Manufacturer's stated accuracy for differential corrected GPS is 2 metres.

The Wide Area Augmentation System (WAAS enabled) NovAtel OEM/V is a line of sight, satellite navigation system that utilizes time-coded signals from at least four of forty-eight available satellites. Both GLONASS and NAVSTAR satellite constellations are used to calculate the position and to provide real time guidance to the helicopter. For flight path processing, a similar NovAtel system was used as the primary base station receiver. The mobile and base station raw XYZ data were recorded, thereby permitting post-survey differential corrections for theoretical accuracies of better than 2 metres. A Marconi Allstar GPS unit, part of the CF-1, was used as a secondary (back-up) base station.

Each base station receiver is able to calculate its own latitude and longitude. For this survey, the primary GPS station was located at latitude 53° 20' 20.96130" N, longitude 124° 38' 48.68810" W, at an elevation of 1081 metres above mean sea level. The secondary GPS unit was located at latitude 53° 20' 30.153" N, longitude 124° 38' 52.6998" W, also at an elevation of 1081 metres.

The GPS records data relative to the WGS84 ellipsoid, which is the basis of the revised North American Datum (NAD83). Conversion software is used to transform the WGS84 Lat/Lon coordinates to the UTM Zone 10N system displayed on the maps.

Radar Altimeter

Manufacturer:	Honeywell/Sperry
Model:	RT300
Type:	Short pulse modulation, 4.3 GHz
Sensitivity:	0.3 m

Sample rate: 2 per second

The radar altimeter measures the vertical distance between the helicopter and the ground except in areas of dense tree cover. This information is used in the processing algorithm that determines conductor depth.

Barometric Pressure and Temperature Sensors

Model:	DIGHEM D 1300	
Type:	Motorola MPX4115AP analog pressure sensor	
	AD592AN high-impedance remote temperature sensors	
Sensitivity:	Pressure:	150 mV/kPa
	Temperature:	100 mV/°C or 10 mV/°C (selectable)
Sample rate:	10 per second	

The D1300 circuit is used in conjunction with one barometric sensor and up to three temperature sensors. Two sensors (baro and temp) are installed in the EM console in the aircraft, to monitor pressure (KPA) and internal operating temperatures (TEMP_INT).

Digital Data Acquisition System

Manufacturer:	Fugro
Model:	HeliDAS – Integrated Data Acquisition System
Recorder:	SanDisk compact flash card (PCMCIA)

The stored data are downloaded to the field workstation PC at the survey base, for verification, backup and preparation of in-field products.

Video Flight Path Recording System

Type:	Axis 2420 Digital Network Camera
Recorder:	Axis 241S Video Server and Tablet Computer
Format:	BIN/BDX

Fiducial numbers are recorded continuously and are displayed on the margin of each image. This procedure ensures accurate correlation of data with respect to visible features on the ground.

4. QUALITY CONTROL AND IN-FIELD PROCESSING

Digital data for each flight were transferred to the field workstation, in order to verify data quality and completeness. A database was created and updated using Geosoft Oasis Montaj and proprietary Fugro Atlas software. This allowed the field personnel to calculate, display and verify both the positional (flight path) and geophysical data on a screen or printer. Records were examined as a preliminary assessment of the data acquired for each flight.

In-field processing of Fugro survey data consists of differential corrections to the airborne GPS data, verification of the flight path, verification of EM calibrations, drift correction of the raw airborne EM data, spike rejection and filtering of all geophysical and ancillary data, verification of the flight videos, calculation of preliminary resistivity data, diurnal correction, and preliminary leveling of magnetic data.

All data, including base station records, were checked on a daily basis, to ensure compliance with the survey contract specifications. Reflights were required if any of the following specifications were not met.

Navigation - Positional (x,y) accuracy of better than 10 m, with a CEP (circular error of probability) of 95%.

Flight Path - No lines to exceed ±25 m departure from nominal line spacing over a continuous distance of more than 1 km, except for reasons of safety.

Clearance - Mean terrain sensor clearance of 35 m, ±10 m, except where precluded by safety considerations, e.g., restricted or populated

areas, severe topography, obstructions, tree canopy, aerodynamic limitations, etc.

Airborne Mag - Aerodynamic magnetometer noise envelope not to exceed 0.5 nT over a distance of more than 1 km. The non-normalized 4th difference not to exceed 1.6 nT over a continuous distance of 1 kilometre excluding areas where this specification is exceeded due to natural anomalies.

Base Mag - Diurnal variations not to exceed 10 nT over a straight-line time chord of 1 minute.

EM - Spheric pulses may occur having strong peaks but narrow widths. The EM data area considered acceptable when their occurrence is less than 10 spheric events exceeding the stated noise specification for a given frequency per 100 samples continuously over a distance of 2,000 metres.

Frequency	Coil Orientation	Peak to Peak Noise Envelope (ppm)
1000Hz	vertical coaxial	5.0
900 Hz	horizontal coplanar	10.0
5500 Hz	vertical coaxial	10.0
7200 Hz	horizontal coplanar	20.0
56,000 Hz	horizontal coplanar	40.0

5. DATA PROCESSING

Flight Path Recovery

The raw range data from at least four satellites are simultaneously recorded by both the base and mobile GPS units. The geographic positions of both units, relative to the model ellipsoid, are calculated from this information. Differential corrections, which are obtained from the base station, are applied to the mobile unit data to provide a post-flight track of the aircraft, accurate to within 2 m. Speed checks of the flight path are also carried out to determine if there are any spikes or gaps in the data.

The corrected WGS84 latitude/longitude coordinates are transformed to the UTM coordinate system used on the final maps. Images or plots are then created to provide a visual check of the flight path.

Electromagnetic Data

EM data are processed at the recorded sample rate of 10 samples/second. Spheric rejection median and Hanning filters are then applied to reduce noise to acceptable levels. EM test profiles are then created to allow the interpreter to select the most appropriate EM anomaly picking controls for a given survey area. The EM picking parameters depend on several factors but are primarily based on the dynamic range of the resistivities within the survey area, and the types and expected geophysical responses of the targets being sought.

The interpretation geophysicist determines initial anomaly picking parameters and thresholds. Anomalous electromagnetic responses that meet the specific criteria are then automatically selected and analysed by computer to provide a preliminary electromagnetic anomaly map. The automatic selection algorithm is intentionally oversensitive to assure that

no meaningful responses are missed. Using the preliminary maps in conjunction with the multi-parameter stacked profiles, the interpreter then classifies the anomalies according to their source and eliminates those that are not substantiated by the data. The final interpreted EM anomaly map will include bedrock, surficial and cultural conductors. A map containing only bedrock conductors can be generated, if desired.

Apparent Resistivity

The apparent resistivities in ohm-m are generated from the in-phase and quadrature EM components for all of the coplanar frequencies, using a pseudo-layer half-space model. The inputs to the resistivity algorithm are the in-phase and quadrature amplitudes of the secondary field. The algorithm calculates the apparent resistivity in ohm-m, and the apparent height of the bird above the conductive source. Any difference between the apparent height and the true height, as measured by the radar altimeter, is called the pseudo-layer and reflects the difference between the real geology and a homogeneous half-space. This difference is often attributed to the presence of a highly resistive upper layer. Any errors in the altimeter reading, caused by heavy tree cover, are included in the pseudo-layer and do not affect the resistivity calculation. The apparent depth estimates, however, will reflect the altimeter errors. Apparent resistivities calculated in this manner may differ from those calculated using other models.

In any areas where the effects of magnetic permeability or dielectric permittivity have suppressed the in-phase responses, the calculated resistivities will be erroneously high. Various algorithms and inversion techniques can be used to partially correct for the effects of permeability and permittivity.

Apparent resistivity maps portray all of the information for a given frequency over the entire survey area. This full coverage contrasts with the electromagnetic anomaly map, which provides information only over interpreted conductors. The large dynamic range afforded by the multiple frequencies makes the apparent resistivity parameter an excellent mapping tool.

The preliminary apparent resistivity maps and images are carefully inspected to identify any lines or line segments that might require base level adjustments. Subtle changes between in-flight calibrations of the system can result in line-to-line differences that are more recognizable in resistive (low signal amplitude) areas. If required, manual level adjustments are carried out to eliminate or minimize resistivity differences that can be attributed, in part, to changes in operating temperatures. These leveling adjustments are usually very subtle, and do not result in the degradation of discrete anomalies.

After the manual leveling process is complete, revised resistivity grids are created. The resulting grids can be subjected to a microleveling technique in order to smooth the data for contouring. The coplanar resistivity parameter has a broad 'footprint' that requires very little filtering.

The calculated resistivities for the 900 Hz, 7200 Hz and 56kHz coplanar frequencies are included in the XYZ and grid archives. Apparent Resistivity maps have been created from the 7200 Hz and 56 kHz data. Values are in ohm-metres on all final products.

Dielectric Permittivity and Magnetic Permeability Corrections[1]

In resistive areas having magnetic rocks, the magnetic and dielectric effects will both generally be present in high-frequency EM data, whereas only the magnetic effect will exist in low-frequency data.

The magnetic permeability is first obtained from the EM data at the lowest frequency, because the ratio of the magnetic response to conductive response is maximized and because displacement currents are negligible. The homogeneous half-space model is used. The computed magnetic permeability is then used along with the in-phase and quadrature response at the highest frequency to obtain the relative dielectric permittivity,

again using the homogeneous half-space model. The highest frequency is used because the ratio of dielectric response to conductive response is maximized. The resistivity can then be determined from the measured in-phase and quadrature components of each frequency, given the relative magnetic permeability and relative dielectric permittivity.

Resistivity-depth Sections (optional)

The apparent resistivities for all frequencies can be displayed simultaneously as coloured resistivity-depth sections. Usually, only the coplanar data are displayed as the close frequency separation between the coplanar and adjacent coaxial data tends to distort the section. The sections can be plotted using the topographic elevation profile as the surface. The digital elevations, in metres a.m.s.l., can be calculated from the GPS Z-value or barometric altimeter, minus the aircraft radar altimeter.

Resistivity-depth sections can be generated in three formats:

(1) Sengpiel resistivity sections, where the apparent resistivity for each frequency is plotted at the depth of the centroid of the in-phase current flow[2]; and,

(2) Differential resistivity sections, where the differential resistivity is plotted at the differential depth[3].

(3) Occam[4] or Multi-layer[5] inversion

---

[1] Huang, H. and Fraser, D.C., 2001 Mapping of the Resistivity, Susceptibility, and Permittivity of the Earth Using a Helicopter-borne Electromagnetic System: Geophysics 106 pg 148-157.

[2] Sengpiel, K.P., 1988, Approximate Inversion of Airborne EM Data from Multilayered Ground: Geophysical Prospecting 36, 446-459.

[3] Huang, H. and Fraser, D.C., 1993, Differential Resistivity Method for Multi-frequency Airborne EM Sounding: presented at Intern. Airb. EM Workshop, Tucson, Ariz.

[4] Constable et al, 1987, Occam's inversion: a practical algorithm for generating smooth models from electromagnetic sounding data: Geophysics, 52, 289-300.

[5] Huang H., and Palacky, G.J., 1991, Damped least-squares inversion of time domain airborne EM data based on singular value decomposition: Geophysical Prospecting, 39, 827-844.

Both the Occam and multi-layer inversions compute the layered earth resistivity model that would best match the measured EM data. The Occam inversion uses a series of thin, fixed layers (usually 20 x 5m and 10 x 10m layers) and computes resistivities to fit the EM data. The multi-layer inversion computes the resistivity and thickness for each of a defined number of layers (typically 3-5 layers) to best fit the data.

Residual Magnetic Intensity

The residual magnetic intensity (RMI) is derived from the total magnetic field (TMF) channels, the diurnal, and the regional magnetic field. The total magnetic intensity is measured in the aircraft, the diurnal is measured from the ground station, and the regional magnetic field is calculated from the IGRF (International Geomagnetic Reference Field).

A fourth difference editing routine is applied to the magnetic data to remove any spikes. The result is then corrected for diurnal variation using the magnetic base station data. The results are then leveled using tie and traverse line intercepts. Manual adjustments are applied to any lines that require leveling, as indicated by shadowed images of the gridded magnetic data.

The low frequency component of the diurnal is extracted from the filtered ground station data and removed from the averaged total magnetic field. The average of the diurnal is then added back in to obtain the resultant total magnetic intensity. The IGRF calculated for the specific survey location and the time of the survey, is then removed from the resultant total magnetic intensity to yield the residual magnetic intensity (RMI). The leveled data are then subjected to a microleveling filter.

Calculated Vertical Magnetic Gradient

The diurnally-corrected residual magnetic field data are subjected to a processing algorithm that enhances the response of magnetic bodies in the upper 500 m and attenuates the response of deeper bodies. The resulting vertical gradient map provides better definition

and resolution of near-surface magnetic units. It also identifies weak magnetic features that may not be evident on the total field or residual magnetic maps. However, regional magnetic variations and changes in lithology may be better defined on the total magnetic field or residual magnetic intensity maps.

Magnetic Derivatives (optional)

The total magnetic field data can be subjected to a variety of filtering techniques to yield maps or images of the following:

enhanced magnetics
second vertical derivative
reduction to the pole/equator
magnetic susceptibility with reduction to the pole
upward/downward continuations
analytic signal

All of these filtering techniques improve the recognition of near-surface magnetic bodies, with the exception of upward continuation. Any of these parameters can be produced on request.

Contour, Colour and Shadow Map Displays

The geophysical data are interpolated onto a regular grid using a modified Akima spline technique. The resulting grid is suitable for image processing and generation of contour maps. The grid cell size is 20% of the line interval.

Colour maps or images are produced by interpolating the grid down to the pixel size. The parameter is then incremented with respect to specific amplitude ranges to provide colour "contour" maps.

Monochromatic shadow maps or images can be generated by employing an artificial sun to cast shadows on a surface defined by the geophysical grid. There are many variations in the shadowing technique. These techniques can be applied to total field or enhanced magnetic data, magnetic derivatives, resistivity, etc. The shadowing technique is also used as a quality control method to detect subtle changes between lines.

Digital Elevation (optional)

The altimeter values (sensor to ground clearance) are subtracted from the differentially corrected and de-spiked GPS-Z values to produce profiles of the orthometric heights (a.m.s.l.) along the survey lines. These values are gridded to produce contour maps showing approximate elevations within the survey area. The calculated digital terrain data are then tie-line leveled and can be adjusted to any known benchmarks in the survey area. Any remaining subtle line-to-line discrepancies are manually removed. After the manual corrections are applied, the digital terrain data are filtered with a microleveling algorithm.

The accuracy of the elevation calculation is directly dependent on the accuracy of the two input parameters, altimeter and GPS-Z. The altimeter values may be erroneous in areas of heavy tree cover, where the altimeter reflects the distance to the tree canopy rather than the ground. The GPS-Z value is primarily dependent on the number of available satellites. Although post-processing of GPS data will yield X and Y accuracies in the order of 1-2 metres, the accuracy of the Z value is usually much less, sometimes in the ±10 metre range. Further inaccuracies might be introduced during the interpolation and gridding process.

The data archive contains the calculated digital elevations above the geoid (a.m.s.l.). Because of the inherent inaccuracies of this method, no guarantee is made or implied that the information displayed is a true representation of the height above sea level. Although this product may be of some use as a general reference, THIS PRODUCT MUST NOT BE USED FOR NAVIGATION PURPOSES.

Contour, Colour and Shadow Map Displays

The geophysical data are interpolated onto a regular grid using a modified Akima spline technique. The resulting grid is suitable for image processing and generation of contour maps. The grid cell size is 20% of the line interval.

Colour maps are produced by interpolating the grid down to the pixel size. The parameter is then incremented with respect to specific amplitude ranges to provide colour "contour" maps.

Monochromatic shadow maps or images can be generated by employing an artificial sun to cast shadows on a surface defined by the geophysical grid. There are many variations in the shadowing technique. These techniques can be applied to total field or enhanced magnetic data, magnetic derivatives, resistivity, etc. The shadowing technique is also used as a quality control method to detect subtle changes between lines.

6. PRODUCTS

This section lists the final maps and products that will be provided under the terms of the survey agreement. Other products can be prepared from the existing dataset, if requested. These include stacked multi-parameter profiles, resistivity-depth sections, inversions, magnetic enhancements or derivatives, percent magnetite, resistivities corrected for magnetic permeability and/or dielectric permittivity, and digital elevation. Most parameters can be displayed as contours, profiles, or in colour; or as digital images in PDF or other file formats.

Base Maps

Base maps of the survey area are produced by scanning published topographic maps to a bitmap (.bmp) format. This process provides a relatively accurate, distortion-free base that facilitates correlation of the navigation data to the map coordinate system. It should be noted that the (older) scanned topographic map shows UTM coordinate lines in the NAD 27 datum, whereas the graticules (crosses) are in the newer NAD 83 system. The difference between the two coordinate systems is seen as a shift of about 200 m to the south and 90 m to the east for the NAD 83 relative to NAD 27. This is not a location error, as the NAD 83 geophysical data are properly positioned relative to the NAD 27 topography. The NAD 27 topographic files were combined with NAD 83 geophysical data for plotting the final maps. All maps were created using the following parameters:

Projection Description:

Datum:	NAD 83
Ellipsoid:	WGS 84; GRS 1980
Projection:	UTM (Zone: 10N)
Central Meridian:	123° W
False Northing:	0
False Easting:	500000
Scale Factor:	0.9996
WGS84 to Local Conversion:	Molodensky

Datum Shifts: DX: 0 DY: 0 DZ: 0

Final Products

The following parameters are presented on a single map sheet at a scale of 1:20,000. All maps include flight lines and topography, unless otherwise indicated. Preliminary products are not listed.

	1 Map Sheet x 2 Sets*	
	Blackline	Colour
EM Anomalies		2x2
Residual Magnetic Intensity		2x2
Calculated Vertical Magnetic Gradient		2x2
Apparent Resistivity 7200 Hz		2x2
Apparent Resistivity 56 kHz		2x2

Additional Products

Digital Archive (see Archive Description)	1 DVD
Survey Report	2 copies + PDF version
Final Digital versions of all maps above	PDF files on Archive
)	

7. SURVEY RESULTS

General Discussion

Table 7-1 summarizes the EM responses in the survey area, with respect to conductance grade and interpretation. For “discrete” conductors (B, D, or T), the apparent conductance and depth values shown in the EM Anomaly list appended to this report have been calculated from “local” in-phase and quadrature amplitudes of the Coaxial 5500 Hz frequency, using a near-vertical, half plane model. Conductance values for the broader (S, H, or E) types have been calculated from absolute amplitudes using a horizontal half-space model.

Wide bedrock conductors or flat-lying conductive units, (S, H, or E) whether from surficial or bedrock sources, may give rise to very broad anomalous responses on the EM profiles. These may not appear on the electromagnetic anomaly map if they have a regional character rather than a locally anomalous character. These broad conductors, which more closely approximate a half-space model, will be maximum coupled to the horizontal (coplanar) coil-pair and should be more evident on the resistivity parameters. Resistivity maps, therefore, may be more valuable than the electromagnetic anomaly maps, in areas where broad or flat-lying conductors are considered to be of importance. All three coplanar resistivity grids are included on the final data archive.

The picking and interpretation procedure relies on several parameters and calculated functions. For this survey, the Coaxial 5500 Hz responses and the mid-frequency difference channels were used as two of the main picking criteria. The 7200 Hz coplanar results were also weighted to provide picks over wider or flat-dipping sources. The quadrature channels provided picks in any areas where the in-phase responses might have been suppressed by magnetite.

Excellent resolution and discrimination of conductors was accomplished by using a fast sampling rate of 0.1 sec and by employing a “common” frequency (5500Hz / 7200Hz) on

two orthogonal coil-pairs (coaxial and coplanar). The resulting difference channel parameters often permit differentiation of bedrock and surficial conductors, even though they may exhibit similar conductance values. Because of the poorly conductive nature of the expected mineralization in the area, the difference calculations were based on the mid frequencies rather than the low frequencies. The lower frequencies tend to “see deeper” in conductive environments, but the higher frequencies respond better to weaker conductors and resistive units, and are probably better suited to this specific target.

Magnetic Data

A Fugro CF-1 cesium vapour magnetometer was operated at the survey base to record diurnal variations of the earth's magnetic field. The clock of the base station was synchronized with that of the airborne system to permit subsequent removal of diurnal drift. A GEM Systems GSM-19T proton precession magnetometer was also operated as a backup unit.

The horizontal gradient enhanced residual magnetic field data (IGRF removed) have been presented as contours on the base maps using a contour interval of 5 nT where gradients permit. The maps show the magnetic properties of the rock units underlying the survey area.

The residual magnetic field data were also subjected to a processing algorithm to produce maps of the calculated vertical gradient. This procedure enhances near-surface magnetic units and suppresses regional gradients. It also provides better definition and resolution of magnetic units and displays weak magnetic features that may not be clearly evident on the residual intensity maps.

There is evidence on the magnetic maps that suggests that the survey area has been subjected to deformation and/or alteration. These structural complexities are evident on the

colour contour maps as variations in magnetic intensity, irregular patterns, and as offsets or changes in strike direction.
If a specific magnetic intensity can be assigned to the rock type that is believed to host the target mineralization, it may be possible to select areas of higher priority on the basis of the magnetic data. This is based on the assumption that the magnetite content of the host rocks will give rise to a limited range of contour values that will permit differentiation of the various lithological units.

The magnetic results have provided valuable information that can be used in conjunction with the other geophysical parameters, to help map the geology and structure in the survey areas.

Apparent Resistivity

Apparent resistivity grids, which display the conductive properties of the survey areas, were produced from the 900 Hz, 7200 Hz, and 56000 Hz coplanar data. The maximum resistivity values, which are calculated for each frequency, are 1080, 8,010 and 30,000 ohm-m respectively. These cut-offs eliminate the erratic higher resistivities that could result from unstable ratios of very small EM amplitudes. All coplanar resistivity data are included on the final data archive.

Both resistive and weakly conductive trends are evident on the near-surface 56 kHz maps. It is interesting to note that some of the well-defined linear magnetic lows are conductive, while other lows are resistive. Note, for example, the broad SE-trending magnetic low that follows the main creek in the NE quadrant of the property. This well-defined magnetic low - topographic low coincides with a pronounced resistivity high. Conversely, the plug-like magnetic high located on the hill near EM response 10050B, is resistive, at least near its southern contact.

In other areas, magnetic highs are more conductive, as evidenced by the conductive/magnetic zone at the eastern end of line 10160. As there is no consistent resistivity/magnetic correlation on the survey block, this suggests that the magnetic and resistivity parameters are sometimes responding to different causative sources; i.e., the EM-derived resistivity is responding to changes in the overburden and near-surface layers, while the magnetic data are reflecting changes in the underlying deeper basement units.

If the target shears are highly silicified and non-porous, these should show as narrow resistive units. These non-magnetic, non-conductive linear trends may prove to be the more attractive targets in the search for quartz-vein mineralization. Conversely, increased porosity, clay alteration, or an increase in sulphide content associated with some shears or faults, could show as more conductive trends. Any plug-like intrusive features, either resistive or conductive, are also considered to be of interest. Any weak EM responses that are associated with the margins of these inferred intrusive units may also warrant further investigation.

There are other resistivity lows and highs in the areas that might also be of interest. Some of these are quite extensive and might reflect "formational" conductors or layers that could be of minor interest as direct exploration targets. However, attention may be focused on areas where these zones appear to be faulted or folded or where anomaly characteristics differ along strike. The broad low resistivity low that dominates the NE corner of the block, indicates a thick, buried conductive layer

Some of the resistive zones could reflect intrusive plugs, flows or caps. These are more evident on the 56 kHz resistivity parameter. Most of these appear to be due to resistive rock units, rather than magnetite suppression, and possibly reflect siliceous (non-magnetic) units. The resistive zones in the vicinity of anomaly 10050B, east of 10080 E, 10018F and 10080G, at the west end of line 10130, east 10130F, near 10240I, and on the tie line at 19030B, are all considered to be potential areas of interest.

Other resistive zones are quite subtle, and could be due to changes in overburden thickness, rather than changes in rock type. However, those that are associated with linear magnetic breaks, contacts, or decreases in magnetite, are considered to be of slightly higher priority.

Electromagnetic Anomalies

Although the targets of interest in this area may be resistive, rather than conductive, discrete EM anomalies were picked, based primarily on the mid-frequency (5500 Hz) coaxial channel. The EM anomalies resulting from this survey appear to fall within one of three general categories. The first type consists of discrete, well-defined anomalies that yield marked inflections on the difference channels. These anomalies are usually attributed to conductive sulphides or graphite, and are generally given a "B" or "D" interpretive symbol, denoting a bedrock source.

The second class of anomalies comprises moderately broad responses that exhibit the characteristics of a half-space and do not yield well-defined inflections on the difference channels. Anomalies in this category are usually given an "S" (at, or near surface) or "H" (buried half-space) interpretive symbol. The lack of a difference channel response usually implies a broad or flat-lying conductive source. Some of these anomalies could reflect buried flat-dipping conductive rock units (shales?), zones of deep weathering, or increased overburden thickness, all of which can yield “non-discrete” signatures. Nearly 90% of the anomalies on the property fall into this category, and are generally considered to be of minor interest.

The effects of conductive overburden are evident over more than half of the survey area. Although the difference channels (DIFI and DIFQ) are extremely valuable in detecting bedrock conductors that are partially masked by conductive overburden, sharp undulations in the bedrock/overburden interface can yield anomalies in the difference channels which

may be interpreted as possible bedrock conductors. Such anomalies usually fall into the "S?" or "B?" classification but may also be given an "E" interpretive symbol, denoting a resistivity contrast at the edge of a conductive unit.

The "?" symbol does not question the validity of an anomaly, but instead indicates some degree of uncertainty as to which is the most appropriate EM source model. This ambiguity results from the combination of effects from two or more conductive sources, such as overburden and bedrock, gradational changes, or moderately shallow dips. The presence of a conductive upper layer has a tendency to mask or alter the characteristics of bedrock conductors, making interpretation difficult. This problem is further exacerbated in the presence of magnetite.

The third anomaly category includes responses that are associated with magnetite. Magnetite can cause suppression or polarity reversals of the in-phase components, particularly at the lower frequencies in resistive areas. Conductive overburden tends to mask many of these negative excursions, particularly at the higher frequencies, but the effects of magnetite-rich rock units are occasionally evident on the EM profiles as suppressions or negative excursions of the lower frequency in-phase channels. Two weak examples can be observed at anomaly 10190D and on line 10140 at fiducial 9390 . In the latter instance there is no appreciable quadrature response to indicate the presence of any conductive material.

Poorly conductive magnetic features can give rise to resistivity anomalies that are only slightly below or slightly above background. If it is expected that poorly conductive economic mineralization could be associated with magnetite-rich units, most of these weakly anomalous features will be of interest. In areas where magnetite causes the in-phase components to become negative, the apparent conductance and depth of EM anomalies will be unreliable. Magnetite effects usually give rise to overstated (higher) resistivity values and understated (too shallow) depth calculations.

As potential targets within the area can be associated faults, alteration zones, or very weakly disseminated sulphides, which may be hosted by non-magnetic quartz-rich units, and which can be overlain by conductive overburden, it is impractical to assess the relative merits of EM anomalies on the basis of conductance. It is recommended that an attempt be made to compile a suite of geophysical "signatures" over any known areas of interest.

Potential Bedrock Conductors

Quartz-vein type auriferous mineralization would not normally give rise to discrete EM conductors, unless it was associated with conductive clay material or semi-massive to massive sulphides. However, electromagnetic anomalies have been picked for this survey area in order to locate any possible conductive sulphide deposits and any conductive faults or shears that could serve as conduits or host units for auriferous mineralization. The electromagnetic anomaly maps show the anomaly locations with the interpreted conductor type, dip, and conductance being indicated by symbols. Direct magnetic correlation is also shown, if it exists.

Table 7-1 shows that nearly 90% of the anomalous responses have been attributed to conductive overburden or flat-lying bedrock units, while only about 8% represent possible discrete bedrock sources. The 356 anomalous EM responses detected by the survey have been assigned a simple colour code on the EM Anomaly map, in order to facilitate source recognition. The thinner dyke-like (D) sources have been assigned a red colour, while the thicker (B) bedrock sources are shown in dark blue. Surficial (S) overburden responses or buried thick layers (H) are shown in green, as are edge effects (E).

Conductor axes have been shown only in areas where the EM anomalies can be correlated from line to line with a reasonable degree of confidence. Most of the anomalous responses are of moderate to strong signal amplitude but they generally yield low conductance values of less than 5 Siemens (mhos). The conductance is based on the mid-frequency coaxial responses, so there could be higher conductance

values than those shown on the map, particularly in the eastern portion, where several anomalies indicate an increase in conductivity at depth, as evidenced by the more conductive 900 Hz responses. These results often suggest a buried flat-dipping layer of clay or conductive bedrock at depth, beneath more resistive cover.

TABLE 7-1 EM ANOMALY STATISTICS

BARK PROJECT AREA

CONDUCTOR GRADE	CONDUCTANCE RANGE SIEMENS (MHOS)	NUMBER OF RESPONSES
7	>100	0
6	50 - 100	0
5	20 - 50	0
4	10 - 20	1
3	5 - 10	2
2	1 - 5	348
1	<1	2
*	INDETERMINATE	4
TOTAL		356

CONDUCTOR MODEL	MOST LIKELY SOURCE	NUMBER OF RESPONSES
D	DISCRETE BEDROCK CONDUCTOR	2
B	DISCRETE BEDROCK CONDUCTOR	27
S	CONDUCTIVE COVER	260
H	ROCK UNIT OR THICK COVER	45
E	EDGE OF WIDE CONDUCTOR	22
L	CULTURE	0
TOTAL		356

(SEE EM MAP LEGEND FOR EXPLANATIONS)

A few of the interpreted discrete bedrock responses are associated with moderately broad zones of low resistivity. Some of these zones appear to be formational in nature, and the contained anomalous responses could simply be due to local changes in conductance within carbonaceous sedimentary units. Therefore, these broad conductive zones may be of minor exploration interest, unless they occur in areas of favourable geology or geochemistry.

The following text very briefly describes some of the more attractive geophysical responses, based on favourable structure, magnetic association, conductance, length, width, or depth extent. Most of these are quite weak or poorly defined. Although some of these could reflect sulphide-type targets, most are considered to be of moderately low priority, given the non-conductive nature of the expected (auriferous) target mineralization.

Anomaly	Type	Mag	Comments
10020A 10050B 10080A 10080B	B? B? B? B?	- - - -	These anomalies are all associated with a circular hill in the northwestern corner of the property. The hill is resistive, and is also magnetic. With the exception of 10050B, these EM anomalies are associated with the non-magnetic, conductive perimeter that encircles the topographic high, and could reflect contact-related concentrations of conductive material. At least three possible breaks can be inferred from the CVG data: SSE along the western flank, SW along the southern flank, and SE through the centre of the plug-like high. The central anomaly, 10050B, is extremely weak, but is associated with a subtle trough within the magnetic high. Anomalies 10080A and 10080B also coincide with subtle magnetic lows. 10080A is more conductive at surface, while 10080B suggests a deeper source.
10080C 19020F	B?	-	To the southeast of the magnetic hill, anomaly 10080C indicates a possible conductor associated with two intersecting faults. Anomaly 19020F, on the tie-line, is nearby, but appears to be related to a separate contact. These responses appear to be more conductive at depth.
10020G	B?	-	Anomaly 10020G is associated with a weak SSW-trending resistivity low, northeast of the main creek valley The CVG map shows that it is also associated with the NE contact of a

Anomaly	Type	Mag	Comments
			lenticular magnetic low.
10030D	B?	11	This moderately broad, poorly defined response is west of the main creek valley, and yields a moderate resistivity low. It could be influenced by conductive overburden, but the 900 Hz resistivity suggests a very thick source or a continuation at depth. There is a weak 11 nT magnetic correlation, but the conductor is actually contained within a broad, SE-trending unit of relatively low magnetic susceptibility.
10060H 10060I 19040H	D B? B?	148 - -	These two closely spaced anomalies are only about 180m apart, but they yield different signatures. Anomaly 10060H suggests a possible thin, E-dipping conductor that correlates with a narrow SSE trending magnetic unit, while 10060I is in a local magnetic low that could reflect alteration. This moderately strong conductive source is also seen on the tie-line at 19040H. Conductivity increases towards the east, to anomaly 10060J, where a buried half-space yields a resistivity of less than 20 ohm-m at an apparent depth of about 30 m. .i
10100G	D	-	A moderately strong, thin, east-dipping source is located near the eastern contact of a SSE-trending magnetic low, which is sandwiched between two SSE magnetic highs. The CVG suggests the presence of a possible fault (160°) that continues SSE through anomaly 10160G.
10110A	D	7	This weak response has been attributed to a buried thin source with a possible dip to the east. It occurs on the eastern flank of a NW trending magnetic low, which is located just south of the non-magnetic halo that encircles the main magnetic plug in the NE corner of the property.
10110B	D	-	Anomaly 10110B is located near the south end of a weak resistivity low. It is contained within the broad unit of low magnetic susceptibility that follows the SE-trending creek valley.
10170E 10180G 10190F 19050G	B? B? B? B?	- 49 35 -	Although these four anomalies are associated with the same SE-trending resistivity low that follows the eastern edge of the main creek valley, the magnetic results tend to suggest that they may not all be related to the same causative source. The magnetic results show a probable E-trending contact between 10170E and 10180G. Resistivity values of

Anomaly	Type	Mag	Comments
			less than 20 ohm-m are observed at surface. The conductive zone appears to extend to the east, but at depth (beneath resistive cover). Anomaly 10190F is flanked on the east by a well defined SE-trending (142°) magnetic trough, that could be an extension of the inferred fault previously noted through 10160G and 10100G.
10210D 10220C 10220B	B? B? B?	- 20 -	Anomaly 10210D is located within a broad, conductive half-space. The coaxial inflection could be due to a change in altitude, but this response is located on the southeastern contact of a NE trending magnetic low. About 365 m to the WSW, 10220B occurs on the opposite edge of the NE trending magnetic low, and could be related to the same non-magnetic unit that hosts 10210D. Anomaly 10220C, to the east, coincides with a subtle magnetic low within the larger magnetic high. Surface resistivities are less than 25 ohm-m on surface, but become more resistive at depth. The complexity of the magnetic patterns tends to enhance the significance of the conductors in this area.
10320F 10340D 10350C	B? B? B?	- 166 106	The magnetic patterns in this area show a linear, dyke-like magnetic feature that strikes approximately 12°. Anomaly 10320F could be due to an edge effect (resistivity contrast) associated with the western flank of this magnetic trend. Anomalies 10340D and 10350C coincide with the peak of the magnetic high, but the conductivity appears to be more surficial and does not continue at depth. The CVG map suggests a moderately complex structure in this area. Weak magnetite effects are evident at 10350E, near the western edge of the creek valley, on the eastern contact of a resistive and magnetic hill.
10370D	B?	-	Anomaly 10370D is possibly due to conductive overburden. However, the depth channels suggest a broad, buried source, that is associated with the low that flanks the eastern contact of the linear, dyke-like magnetic feature that hosts 10340D.
19050D	D	-	This tie-line response was evident as a possible surficial source on the traverse line, 10310G. The more discrete response on the tie-line is the result of a better coupling angle, but this response also suggests a surficial source that strikes ESE. It has been classified as a possible bedrock source because of the moderately sharp coaxial response

Anomaly	Type	Mag	Comments
			and its location in a magnetic low.
19050G	B?	-	This anomaly was described previously as part of a subtle SSE-trending fault zone. It occurs on the south edge of a strong resistivity low.
19050L 19050M 19050O	B? B? B?	157 - 67	These three anomalies are located within a large conductive zone in the northeast corner of the property. The conductive zone is underlain by both magnetic and non-magnetic units, indicating that they may be due to different causative sources. Note the moderate magnetic high between 19050L and 19050M. The firmer is close enough to the magnetic peak to yield a magnetic correlation of 157 nT, but latter is more conductive, yielding resistivities of less than 25 ohm-m at depth. Anomaly 19050O, at the north end of the line, is also magnetic but less conductive.

In the search for auriferous mineralization, the value of EM conductors may be of little importance, unless the gold is known to be associated with conductive material such as sulphides, conductive shears or faults, alteration products, or magnetite-rich zones. As mentioned previously, resistive zones can often be of greater exploration interest, particularly if the host rocks are siliceous. On the BARK survey block, the magnetic parameter appears to have been more effective than the resistivity in delineating rock units and areas of structural deformation that may have influenced local mineral deposition. The resistivity parameter, however, has outlined several resistive units, some of which do not yield magnetic signatures. The two parameters are complementary, and when used together, can help to used to locate the more favourable areas for mineral deposition.

8. CONCLUSIONS AND RECOMMENDATIONS

This report provides a very brief description of the survey results and describes the equipment, data processing procedures and logistics of the airborne survey over the BARK project area, near Vanderhoof, B.C.

The various products accompanying this report display the magnetic and conductive properties of the survey area. It is recommended that a complete assessment and detailed evaluation of the survey results be carried out, in conjunction with all available geophysical, geological and geochemical information.

The magnetic results have provided valuable structural information that can be used to help locate the more favourable areas for structurally controlled gold deposition on the property. In addition to locating a few linear faults and shears, the vertical gradient data have outlined the contacts of both magnetic and non-magnetic units. The latter could reflect felsic intrusions or siliceous breccias that might host auriferous mineralization. In addition, the combined magnetic and resistivity parameters have outlined a few interesting magnetic lows and resistivity highs that could reflect alteration zones or siliceous intrusives.

There were more than 350 anomalous EM responses detected in the survey block, but only a few that might be attributed to increases in conductive sulphide content or clay-altered shears. Most responses are of moderate amplitude, but yield moderately low conductance, generally less than 5 Siemens

In the northern portion of the property, there are two main zones where resistivities of less than 30 ohm-m have been observed on the lower (deeper) 900 Hz frequency.. Some of these broad zones are likely due to (non-magnetic) conductive clay layers or graphitic shales, while some of the more discrete (magnetic) responses could be due to increases in conductive sulphide content. Although the former “formational” zones may be of little economic interest, those in the latter category might warrant additional work.

Other anomalous EM responses coincide with magnetic linears that reflect contacts, faults, or shears. These inferred contacts and structural breaks are considered to be of particular interest as they may have influenced or controlled mineral deposition within the survey area.

The anomalous (resistive) targets and some of the interpreted bedrock conductors defined by the survey should be subjected to further investigation, using appropriate surface exploration techniques. Anomalies that are currently considered to be of moderately low priority may require upgrading if follow-up results are favourable.

Additional processing of existing geophysical data might also be considered, in order to extract the maximum amount of information from the survey results. Current software and imaging techniques can often provide valuable information on structure and lithology, which may not be clearly evident on the colour maps and images provided with this report. These techniques can yield images that define subtle, but significant, structural details.

Respectfully submitted,

FUGRO AIRBORNE SURVEYS CORP.

R10073-1

APPENDIX A

LIST OF PERSONNEL

The following personnel were involved in the acquisition, processing, interpretation and presentation of data, relating to a DIGHEM airborne geophysical survey carried out over the BARK project area, for Amarc Resources Ltd., near Vanderhoof, B.C.

Adriana Pagliero	Project Manager
Gary Ellis	Equipment Operator
Mike Neilly	Equipment Operator
Tim Nykolyaichuk	Equipment Operator
Yuri Mironenko	Data Processor (Office)
Amanda Heydorn	Data Processor (Office)
Richardo White	Data Processor (Office)
Lyn Vanderstarren	Drafting Supervisor
Albina Tonello	Secretary/Expeditor
Matt Richie	Pilot (Questral Helicopters Ltd.)

The survey consisted of 369 km of coverage, flown from January 16 to January 19, 2011.

All personnel are employees of Fugro Airborne Surveys, except for the pilot who is an employee of Questral Helicopters Ltd.

APPENDIX B

DATA PROCESSING FLOWCHARTS

APPENDIX B

Processing Flow Chart - Electromagnetic Data

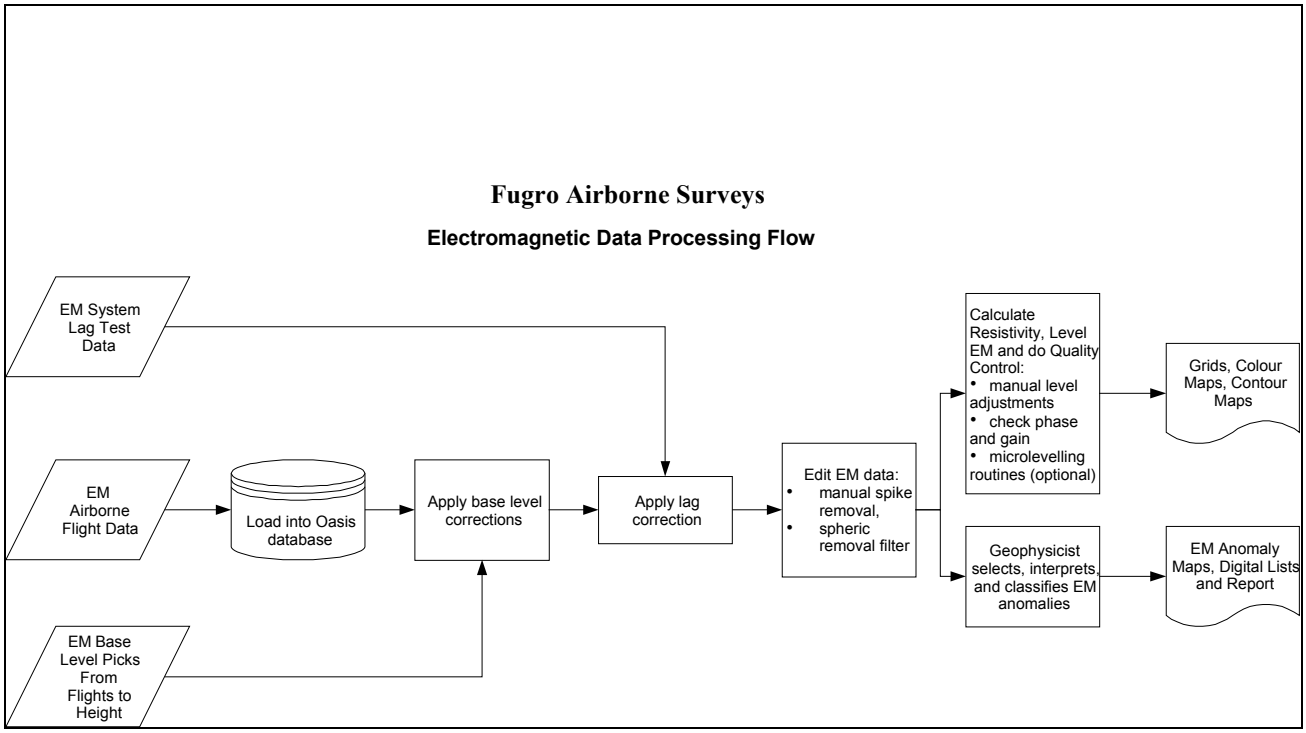

Processing Flow Chart - Magnetic Data

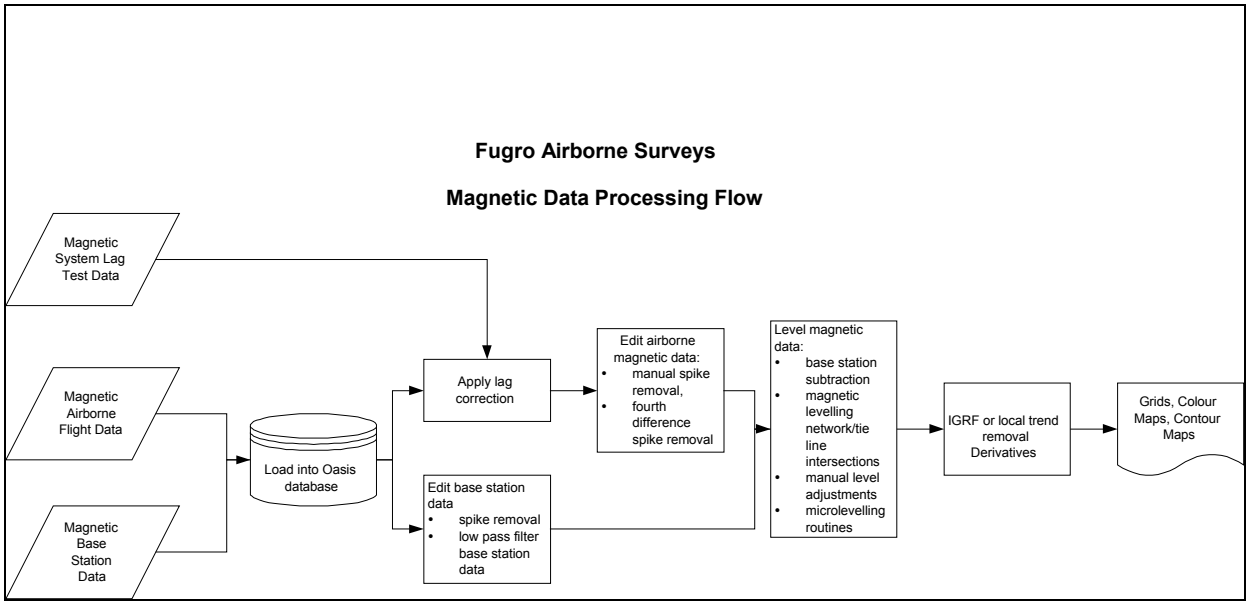

APPENDIX C

BACKGROUND INFORMATION

BACKGROUND INFORMATION

Electromagnetics

Fugro electromagnetic responses fall into two general classes, discrete and broad. The discrete class consists of sharp, well-defined anomalies from discrete conductors such as sulphide lenses and steeply dipping sheets of graphite and sulphides. The broad class consists of wide anomalies from conductors having a large horizontal surface such as flatly dipping graphite or sulphide sheets, saline water-saturated sedimentary formations, conductive overburden and rock, kimberlite pipes and geothermal zones. A vertical conductive slab with a width of 200 m would straddle these two classes.

The vertical sheet (half plane) is the most common model used for the analysis of discrete conductors. The B, D and T type are analyzed according to this model, with the conductance being calculated from the local amplitudes of the coaxial data.. The following section entitled **Discrete Conductor Analysis** describes this model in detail.

The conductive earth (half-space) model is more suitable for broad conductors that carry an S, H, or E type interpretation symbol. Conductance values for these anomalous responses are based on the absolute amplitudes of the selected coplanar channels. Resistivity maps result from the use of this model. A later section entitled **Resistivity Mapping** describes the method further.

Geometric Interpretation

The geophysical interpreter attempts to determine the geometric shape and dip of the conductor. Figure C-1 shows typical HEM anomaly shapes that are used to guide the geometric interpretation.

Discrete Conductor Analysis

The EM anomalies appearing on the electromagnetic map are analyzed by computer to give the conductance (i.e., conductivity-thickness product) in siemens (mhos). The B, D, and T type calculations are based on a vertical sheet model. This is not an unreasonable procedure, because the computed conductance increases as the electrical quality of the conductor increases, regardless of its true shape. HEM anomalies are divided into seven grades of conductance, as shown in Table C-1. The conductance in siemens (mhos) is the reciprocal of resistance in ohms.

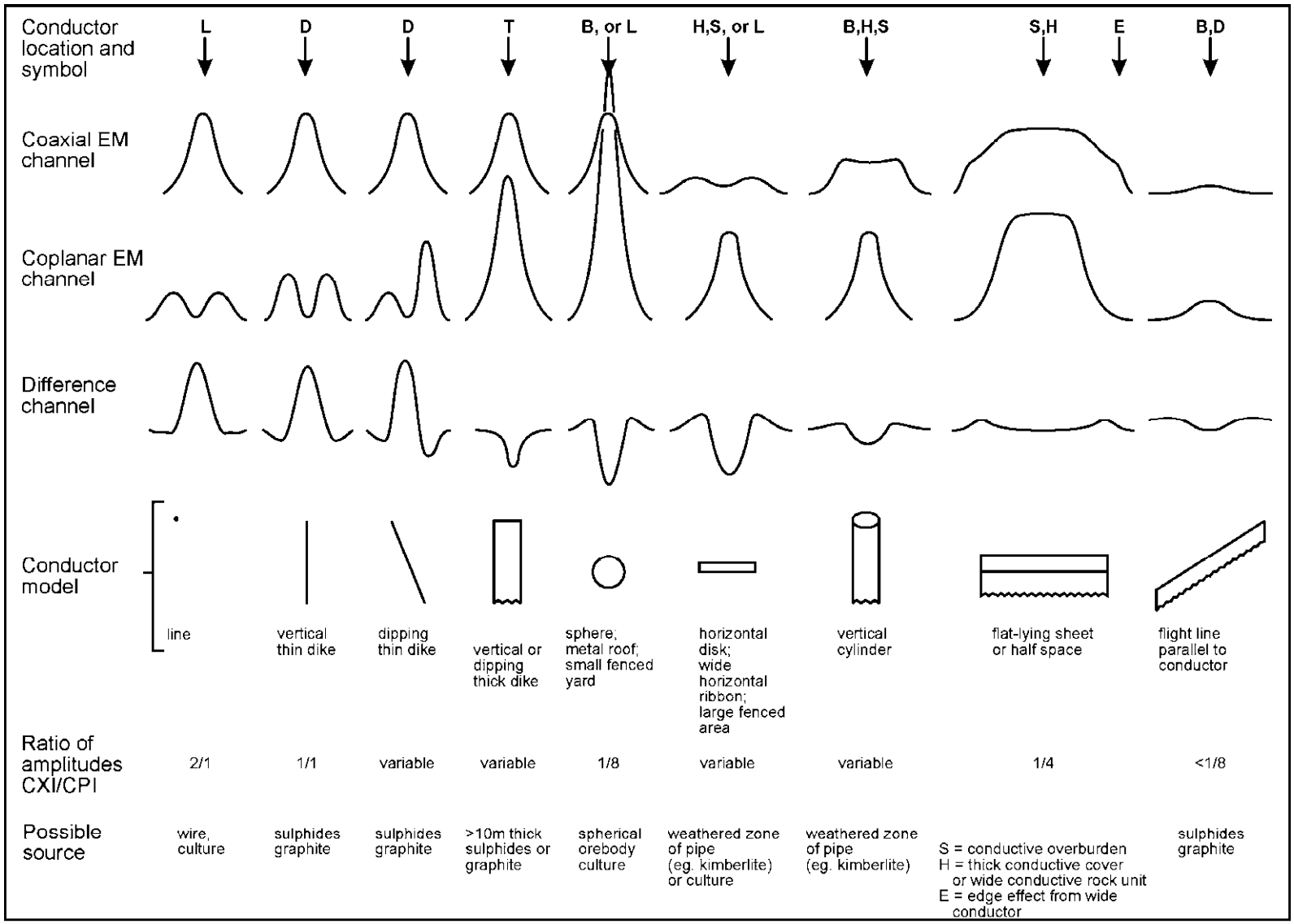

Typical HEM anomaly shapes
Figure C-1

The conductance value is a geological parameter because it is a characteristic of the conductor alone. It generally is independent of frequency, flying height or depth of burial, apart from the averaging over a greater portion of the conductor as height increases. Small anomalies from deeply buried strong conductors are not confused with small anomalies from shallow weak conductors because the former will have larger conductance values.

Table C-1. EM Anomaly Grades

Anomaly Grade	Siemens
7	> 100
6	50 - 100
5	20 - 50
4	10 - 20
3	5 - 10
2	1 - 5
1	< 1

Conductive overburden generally produces broad EM responses which may not be shown as anomalies on the geophysical maps. However, patchy conductive overburden in otherwise resistive areas can yield discrete anomalies with a conductance grade (cf. Table C-1) of 1, 2 or even 3 for conducting clays that have resistivities as low as 50 ohm-m. In areas where ground resistivities are less than 10 ohm-m, anomalies caused by weathering variations and similar causes can have any conductance grade. The anomaly shapes from the multiple coils often allow such conductors to be recognized, and these are indicated by the letters S, H, and sometimes E on the geophysical maps (see EM legend on maps).

For bedrock conductors, the higher anomaly grades indicate increasingly higher conductances. Examples: the New Insco copper discovery (Noranda, Canada) yielded a grade 5 anomaly, as did the neighbouring copper-zinc Magusi River ore body; Mattabi (copper-zinc, Sturgeon Lake, Canada) and Whistle (nickel, Sudbury, Canada) gave grade 6; and the Montcalm nickel-copper discovery (Timmins, Canada) yielded a grade 7 anomaly. Graphite and sulphides can span all grades but, in any particular survey area, field work may show that the different grades indicate different types of conductors.

Strong conductors (i.e., grades 6 and 7) are characteristic of massive sulphides or graphite. Moderate conductors (grades 4 and 5) typically reflect graphite or sulphides of a less massive character, while weak bedrock conductors (grades 1 to 3) can signify poorly connected graphite or heavily disseminated sulphides. Grades 1 and 2 conductors may not respond to ground EM equipment using frequencies less than 2000 Hz.

The presence of sphalerite or gangue can result in ore deposits having weak to moderate conductances. As an example, the three million ton lead-zinc deposit of Restigouche Mining Corporation near Bathurst, Canada, yielded a well-defined grade 2 conductor. The 10 percent by volume of sphalerite occurs as a coating around the fine-grained massive pyrite, thereby inhibiting electrical conduction. Faults, fractures and shear zones may

produce anomalies that typically have low conductances (e.g., grades 1 to 3). Conductive rock formations can yield anomalies of any conductance grade. The conductive materials in such rock formations can be salt water, weathered products such as clays, original depositional clays, and carbonaceous material.

For each interpreted electromagnetic anomaly on the geophysical maps, a letter identifier and an interpretive symbol are plotted beside the EM grade symbol. In areas where anomalies are crowded, the letter identifiers and interpretive symbols may be obliterated. The EM grade symbols, however, will always be discernible, and any obliterated information can be obtained from the anomaly listing appended to this report.

The conductance measurement is considered more reliable than the depth estimate. There are a number of factors that can produce an error in the depth estimate, including the averaging of topographic variations by the altimeter, overlying conductive overburden, and the location and attitude of the conductor relative to the flight line. Conductor location and attitude can provide an erroneous depth estimate because the stronger part of the conductor may be deeper or to one side of the flight line, or because it has a shallow dip. A heavy tree cover can also produce errors in depth estimates. This is because the depth estimate is computed as the distance of the bird from the conductor, minus the altimeter reading. The altimeter can lock onto the top of a dense forest canopy. This situation yields an erroneously large depth estimate but does not affect the conductance estimate.

Dip symbols are used to indicate the direction of dip of conductors. These symbols are used only when the anomaly shapes are unambiguous, which usually requires a fairly resistive environment.

A further interpretation is often presented on the EM map by means of the line-to-line correlation of bedrock anomalies, which is based on a comparison of anomaly shapes on adjacent lines. This provides conductor axes that may define the geological structure over portions of the survey area. The absence of conductor axes in an area implies that anomalies could not be correlated from line to line with reasonable confidence.

The electromagnetic anomalies are designed to provide a correct impression of conductor quality by means of the conductance grade symbols. The symbols can stand alone with geology when planning a follow-up program. The actual conductance values are printed in the attached anomaly list for those who wish quantitative data. The map provides an interpretation of conductors in terms of length, strike and dip, geometric shape, conductance, and thickness. The accuracy is comparable to an interpretation from a high quality ground EM survey having the same line spacing.

The appended EM anomaly list provides a tabulation of anomalies in ppm, conductance, and depth for the vertical sheet or horizontal sheet models. The vertical sheet model (B, D, and T types) uses the local coaxial amplitudes for the calculation. Values for the horizontal sheet model (S, H, and E types) are calculated from the absolute amplitudes of the selected coplanar channels. No conductance or depth estimates are shown for weak anomalous

responses that are not of sufficient amplitude to yield reliable calculations, or where magnetite effects have caused negative in-phase responses.

Questionable Anomalies

The EM maps may contain anomalous responses that are displayed as asterisks (*). These responses denote weak anomalies of indeterminate conductance, which may reflect one of the following: a weak conductor near the surface, a strong conductor at depth (e.g., 100 to 120 m below surface) or to one side of the flight line, or aerodynamic noise. Those responses that have the appearance of valid bedrock anomalies on the flight profiles are indicated by appropriate interpretive symbols (see EM legend on maps). The others probably do not warrant further investigation unless their locations are of considerable geological interest.

The Thickness Parameter

A comparison of coaxial and coplanar shapes can provide an indication of the thickness of a steeply dipping conductor. The amplitude of the coplanar anomaly (e.g., CPI channel) increases relative to the coaxial anomaly (e.g., CXI) as the apparent thickness increases, i.e., the thickness in the horizontal plane. (The thickness is equal to the conductor width if the conductor dips at 90 degrees and strikes at right angles to the flight line.) This report refers to a conductor as thin when the thickness is likely to be less than 5 m, and thick when in excess of 10 m. Thick conductors are indicated on the EM map by parentheses "( )". For base metal exploration in steeply dipping geology, thick conductors can be high priority targets because many massive sulphide ore bodies are thick. The system cannot sense the thickness when the strike of the conductor is subparallel to the flight line, when the conductor has a shallow dip, when the anomaly amplitudes are small, or when the resistivity of the environment is less than 100 ohm-m.

Resistivity Mapping

Resistivity mapping is useful in areas where broad or flat lying conductive units are of interest. One example of this is the clay alteration that is associated with Carlin-type deposits in the south west United States. The resistivity parameter was able to identify the clay alteration zone over the Cove deposit. The alteration zone appeared as a strong resistivity low on the 900 Hz resistivity parameter. The 7,200 Hz and 56,000 Hz resistivities showed more detail in the covering sediments, and delineated a range front fault. This is typical in many areas of the southwest United States, where conductive near surface sediments, which may sometimes be alkalic, attenuate the higher frequencies.

Resistivity mapping has proven successful for locating diatremes in diamond exploration. Weathering products from relatively soft kimberlite pipes produce a resistivity contrast with the unaltered host rock. In many cases weathered kimberlite pipes were associated with

thick conductive layers that contrasted with overlying or adjacent relatively thin layers of lake bottom sediments or overburden.

Areas of widespread conductivity are commonly encountered during surveys. These conductive zones may reflect alteration zones, shallow-dipping sulphide or graphite-rich units, saline ground water, or conductive overburden. In such areas, EM amplitude changes can be generated by decreases of only 5 m in survey altitude, as well as by increases in conductivity. The typical flight record in conductive areas is characterized by in-phase and quadrature channels that are continuously active. Local EM peaks reflect either increases in conductivity of the earth or decreases in survey altitude. For such conductive areas, apparent resistivity profiles and contour maps are necessary for the correct interpretation of the airborne data. The advantage of the resistivity parameter is that anomalies caused by altitude changes are virtually eliminated, so the resistivity data reflect only those anomalies caused by conductivity changes. The resistivity analysis also helps the interpreter to differentiate between conductive bedrock and conductive overburden. For example, discrete conductors will generally appear as narrow lows on the contour map and broad conductors (e.g., overburden) will appear as wide lows.

The apparent resistivity is calculated using the pseudo-layer (or buried) half-space model defined by Fraser (1978)[6]. This model consists of a resistive layer overlying a conductive half-space. The depth channels give the apparent depth below surface of the conductive material. The apparent depth is simply the apparent thickness of the overlying resistive layer. The apparent depth (or thickness) parameter will be positive when the upper layer is more resistive than the underlying material, in which case the apparent depth may be quite close to the true depth.

The apparent depth will be negative when the upper layer is more conductive than the underlying material, and will be zero when a homogeneous half-space exists. The apparent depth parameter must be interpreted cautiously because it will contain any errors that might exist in the measured altitude of the EM bird (e.g., as caused by a dense tree cover). The inputs to the resistivity algorithm are the in-phase and quadrature components of the coplanar coil-pair. The outputs are the apparent resistivity of the conductive half-space (the source) and the sensor-source distance. The flying height is not an input variable, and the output resistivity and sensor-source distance are independent of the flying height when the conductivity of the measured material is sufficient to yield significant in-phase as well as quadrature responses. The apparent depth, discussed above, is simply the sensor-source distance minus the measured altitude or flying height. Consequently, errors in the measured altitude will affect the apparent depth parameter but not the apparent resistivity parameter.

---

[6] Resistivity mapping with an airborne multicoil electromagnetic system: Geophysics, v. 43, p.144-172

The apparent depth parameter is a useful indicator of simple layering in areas lacking a heavy tree cover. Depth information has been used for permafrost mapping, where positive apparent depths were used as a measure of permafrost thickness. However, little quantitative use has been made of negative apparent depths because the absolute value of the negative depth is not a measure of the thickness of the conductive upper layer and, therefore, is not meaningful physically. Qualitatively, a negative apparent depth estimate usually shows that the EM anomaly is caused by conductive overburden. Consequently, the apparent depth channel can be of significant help in distinguishing between overburden and bedrock conductors.

Interpretation in Conductive Environments

Environments having low background resistivities (e.g., below 30 ohm-m for a 900 Hz system) yield very large responses from the conductive ground. This usually prohibits the recognition of discrete bedrock conductors. However, Fugro data processing techniques produce three parameters that contribute significantly to the recognition of bedrock conductors in conductive environments. These are the in-phase and quadrature difference channels (DIFI and DIFQ, which are available only on systems with “common” frequencies on orthogonal coil pairs), and the resistivity and depth channels (RES and DEP) for each coplanar frequency.

The EM difference channels (DIFI and DIFQ) eliminate most of the responses from conductive ground, leaving responses from bedrock conductors, cultural features (e.g., telephone lines, fences, etc.) and edge effects. Edge effects often occur near the perimeter of broad conductive zones. This can be a source of geologic noise. While edge effects yield anomalies on the EM difference channels, they do not produce resistivity anomalies. Consequently, the resistivity channel aids in eliminating anomalies due to edge effects. On the other hand, resistivity anomalies will coincide with the most highly conductive sections of conductive ground, and this is another source of geologic noise. The recognition of a bedrock conductor in a conductive environment therefore is based on the anomalous responses of the two difference channels (DIFI and DIFQ) and the resistivity channels (RES). The most favourable situation is where anomalies coincide on all channels.

The DEP channels, which give the apparent depth to the conductive material, also help to determine whether a conductive response arises from surficial material or from a conductive zone in the bedrock. When these channels ride above the zero level on the depth profiles (i.e., depth is negative), it implies that the EM and resistivity profiles are responding primarily to a conductive upper layer, i.e., conductive overburden. If the DEP channels are below the zero level, it indicates that a resistive upper layer exists, and this usually implies the existence of a bedrock conductor. If the low frequency DEP channel is below the zero level and the high frequency DEP is above, this suggests that a bedrock conductor occurs beneath conductive cover.

Reduction of Geologic Noise

Geologic noise refers to unwanted geophysical responses. For purposes of airborne EM surveying, geologic noise refers to EM responses caused by conductive overburden and magnetic permeability. It was mentioned previously that the EM difference channels (i.e., channel DIFI for in-phase and DIFQ for quadrature) tend to eliminate the response of conductive overburden.

Magnetite produces a form of geological noise on the in-phase channels. Rocks containing less than 1% magnetite can yield negative in-phase anomalies caused by magnetic permeability. When magnetite is widely distributed throughout a survey area, the in-phase EM channels may continuously rise and fall, reflecting variations in the magnetite percentage, flying height, and overburden thickness. This can lead to difficulties in recognizing deeply buried bedrock conductors, particularly if conductive overburden also exists. However, the response of broadly distributed magnetite generally vanishes on the in-phase difference channel DIFI. This feature can be a significant aid in the recognition of conductors that occur in rocks containing accessory magnetite.

EM Magnetite Mapping

The information content of HEM data consists of a combination of conductive eddy current responses and magnetic permeability responses. The secondary field resulting from conductive eddy current flow is frequency-dependent and consists of both in-phase and quadrature components, which are positive in sign. On the other hand, the secondary field resulting from magnetic permeability is independent of frequency and consists of only an in-phase component which is negative in sign. When magnetic permeability manifests itself by decreasing the measured amount of positive in-phase, its presence may be difficult to recognize. However, when it manifests itself by yielding a negative in-phase anomaly (e.g., in the absence of eddy current flow), its presence is assured. In this latter case, the negative component can be used to estimate the percent magnetite content.

A magnetite mapping technique, based on the low frequency coplanar data, can be complementary to magnetometer mapping in certain cases. Compared to magnetometry, it is far less sensitive but is more able to resolve closely spaced magnetite zones, as well as providing an estimate of the amount of magnetite in the rock. The method is sensitive to 1/4% magnetite by weight when the EM sensor is at a height of 30 m above a magnetitic half-space. It can individually resolve steep dipping narrow magnetite-rich bands that are separated by 60 m. Unlike magnetometry, the EM magnetite method is unaffected by remanent magnetism or magnetic latitude.

The EM magnetite mapping technique provides estimates of magnetite content that are usually correct within a factor of 2 when the magnetite is fairly uniformly distributed. EM magnetite maps can be generated when magnetic permeability is evident as negative in-phase responses on the data profiles.

Like magnetometry, the EM magnetite method maps only bedrock features, provided that the overburden is characterized by a general lack of magnetite. This contrasts with resistivity mapping which portrays the combined effect of bedrock and overburden.

The Susceptibility Effect

When the host rock is conductive, the positive conductivity response will usually dominate the secondary field, and the susceptibility effect[7] will appear as a reduction in the in-phase, rather than as a negative value. The in-phase response will be lower than would be predicted by a model using zero susceptibility. At higher frequencies the in-phase conductivity response also gets larger, so a negative magnetite effect observed on the low frequency might not be observable on the higher frequencies, over the same body. The susceptibility effect is most obvious over discrete magnetite-rich zones, but also occurs over uniform geology such as a homogeneous half-space.

High magnetic susceptibility will affect the calculated apparent resistivity, if only conductivity is considered. Standard apparent resistivity algorithms use a homogeneous half-space model, with zero susceptibility. For these algorithms, the reduced in-phase response will, in most cases, make the apparent resistivity higher than it should be. It is important to note that there is nothing wrong with the data, nor is there anything wrong with the processing algorithms. The apparent difference results from the fact that the simple geological model used in processing does not match the complex geology.

Measuring and Correcting the Magnetite Effect

Theoretically, it is possible to calculate (forward model) the combined effect of electrical conductivity and magnetic susceptibility on an EM response in all environments. The difficulty lies, however, in separating out the susceptibility effect from other geological effects when deriving resistivity and susceptibility from EM data.

Over a homogeneous half-space, there is a precise relationship between in-phase, quadrature, and altitude. These are often resolved as phase angle, amplitude, and altitude. Within a reasonable range, any two of these three parameters can be used to calculate the half space resistivity. If the rock has a positive magnetic susceptibility, the in-phase component will be reduced and this departure can be recognized by comparison to the other parameters.

The algorithm used to calculate apparent susceptibility and apparent resistivity from HEM data, uses a homogeneous half-space geological model. Non half-space geology, such as horizontal layers or dipping sources, can also distort the perfect half-

[7] Magnetic susceptibility and permeability are two measures of the same physical property. Permeability is generally given as relative permeability, μ_r, which is the permeability of the substance divided by the permeability of free space ($4 \pi \times 10^{-7}$). Magnetic susceptibility k is related to permeability by $k=\mu^r-1$. Susceptibility is a unitless measurement, and is usually reported in units of 10^{-6}. The typical range of susceptibilities is –1 for quartz, 130 for pyrite, and up to 5×10^5 for magnetite, in 10^{-6} units (Telford et al, 1986).

space relationship of the three data parameters. While it may be possible to use more complex models to calculate both rock parameters, this procedure becomes very complex and time-consuming. For basic HEM data processing, it is most practical to stick to the simplest geological model.

Magnetite reversals (reversed in-phase anomalies) have been used for many years to calculate an "FeO" or magnetite response from HEM data (Fraser, 1981). However, this technique could only be applied to data where the in-phase was observed to be negative, which happens when susceptibility is high and conductivity is low.

Applying Susceptibility Corrections

Resistivity calculations done with susceptibility correction may change the apparent resistivity. High-susceptibility conductors, which were previously masked by the susceptibility effect in standard resistivity algorithms, may become evident. In this case the susceptibility corrected apparent resistivity is a better measure of the actual resistivity of the earth. However, other geological variations, such as a deep resistive layer, can also reduce the in-phase by the same amount. In this case, susceptibility correction would not be the best method. Different geological models can apply in different areas of the same data set. The effects of susceptibility, and other effects that can create a similar response, must be considered when selecting the resistivity algorithm.

Susceptibility from EM vs Magnetic Field Data

The response of the EM system to magnetite may not match that from a magnetometer survey. First, HEM-derived susceptibility is a rock property measurement, like resistivity. Magnetic data show the total magnetic field, a measure of the potential field, not the rock property. Secondly, the shape of an anomaly depends on the shape and direction of the source magnetic field. The electromagnetic field of HEM is much different in shape from the earth's magnetic field. Total field magnetic anomalies are different at different magnetic latitudes; HEM susceptibility anomalies have the same shape regardless of their location on the earth.

In far northern latitudes, where the magnetic field is nearly vertical, the total magnetic field measurement over a thin vertical dike is very similar in shape to the anomaly from the HEM-derived susceptibility (a sharp peak over the body). The same vertical dike at the magnetic equator would yield a negative magnetic anomaly, but the HEM susceptibility anomaly would show a positive susceptibility peak.

Effects of Permeability and Dielectric Permittivity

Resistivity algorithms that assume free-space magnetic permeability and dielectric permittivity, do not yield reliable values in highly magnetic or highly resistive areas. Both magnetic polarization and displacement currents cause a decrease in the in-

phase component, often resulting in negative values that yield erroneously high apparent resistivities. The effects of magnetite occur at all frequencies, but are most evident at the lowest frequency. Conversely, the negative effects of dielectric permittivity are most evident at the higher frequencies, in resistive areas.

The table below shows the effects of varying permittivity over a resistive (10,000 ohm-m) half space, at frequencies of 56,000 Hz (DIGHEM^{V}) and 140,000 Hz (RESOLVE).

Apparent Resistivity Calculations
Effects of Permittivity on In-phase/Quadrature/Resistivity

Freq (Hz)	Coil	Sep (m)	Thres (ppm)	Alt (m)	In Phase	Quad Phase	App Res	App Depth (m)	Permittivity
56,000	CP	6.3	0.1	30	7.3	35.3	10118	-1.0	1 Air
56,000	CP	6.3	0.1	30	3.6	36.6	19838	-13.2	5 Quartz
56,000	CP	6.3	0.1	30	-1.1	38.3	81832	-25.7	10 Epidote
56,000	CP	6.3	0.1	30	-10.4	42.3	76620	-25.8	20 Granite
56,000	CP	6.3	0.1	30	-19.7	46.9	71550	-26.0	30 Diabase
56,000	CP	6.3	0.1	30	-28.7	52.0	66787	-26.1	40 Gabbro
140,000	CP	7.94	0.1	30	52.1	159.1	8710	0.2	1 Air
140,000	CP	7.94	0.1	30	16.1	180.4	29215	-18.5	5 Quartz
140,000	CP	7.94	0.1	30	-27.0	211.9	102876	-26.9	10 Epidote
140,000	CP	7.94	0.1	30	-103.6	287.0	84044	-27.2	20 Granite
140,000	CP	7.94	0.1	30	-166.0	371.5	70766	-27.5	30 Diabase
140,000	CP	7.94	0.1	30	-215	459.3	61433	-27.6	40 Gabbro

Methods have been developed (Huang and Fraser, 2000, 2001) to correct apparent resistivities for the effects of permittivity and permeability. The corrected resistivities yield more credible values than if the effects of permittivity and permeability are disregarded.

Recognition of Culture

Cultural responses include all EM anomalies caused by man-made metallic objects. Such anomalies may be caused by inductive coupling or current gathering. The concern of the interpreter is to recognize when an EM response is due to culture. Points of consideration

used by the interpreter, when coaxial and coplanar coil-pairs are operated at a common frequency, are as follows:

1. The CPPL channel monitors 60 Hz radiation. An anomaly on this channel shows that the conductor is radiating power. Such an indication is normally a guarantee that the conductor is cultural. However, care must be taken to ensure that the conductor is not a geologic body that strikes across a power line, carrying leakage currents.

2. A flight that crosses a "line" (e.g., fence, telephone line, etc.) yields a centre-peaked coaxial anomaly and an m-shaped coplanar anomaly.[8] When the flight crosses the cultural line at a high angle of intersection, the amplitude ratio of coaxial/coplanar response is 2. Such an EM anomaly can only be caused by a line. The geologic body that yields anomalies most closely resembling a line is the vertically dipping thin dike. Such a body, however, yields an amplitude ratio of 1 rather than 2. Consequently, an m-shaped coplanar anomaly with a CXI/CPI amplitude ratio of 2 is virtually a guarantee that the source is a cultural line.

3. A flight that crosses a sphere or horizontal disk yields centre-peaked coaxial and coplanar anomalies with a CXI/CPI amplitude ratio (i.e., coaxial/coplanar) of 1/8. In the absence of geologic bodies of this geometry, the most likely conductor is a metal roof or small fenced yard.[9] Anomalies of this type are virtually certain to be cultural if they occur in an area of culture.

4. A flight that crosses a horizontal rectangular body or wide ribbon yields an m-shaped coaxial anomaly and a centre-peaked coplanar anomaly. In the absence of geologic bodies of this geometry, the most likely conductor is a large fenced area.[5] Anomalies of this type are virtually certain to be cultural if they occur in an area of culture.

5. EM anomalies that coincide with culture, as seen on the video display, are usually caused by culture. However, care is taken with such coincidences because a geologic conductor could occur beneath a fence, for example. In this example, the fence would be expected to yield an m-shaped coplanar anomaly as in case #2 above. If, instead, a centre-peaked coplanar anomaly occurred, there would be concern that a thick geologic conductor coincided with the cultural line.

6. Thee above description of anomaly shapes is valid when the culture is not conductively coupled to the environment. In this case, the anomalies arise from

---

[8] See Figure C-1 presented earlier.

[9] It is a characteristic of EM that geometrically similar anomalies are obtained from: (1) a planar conductor, and (2) a wire that forms a loop having dimensions identical to the perimeter of the equivalent planar conductor.

inductive coupling to the EM transmitter. However, when the environment is quite conductive (e.g., less than 100 ohm-m at 900 Hz), the cultural conductor may be conductively coupled to the environment. In this latter case, the anomaly shapes tend to be governed by current gathering. Current gathering can completely distort the anomaly shapes, thereby complicating the identification of cultural anomalies. In such circumstances, the interpreter can only rely on the radiation channel and the video records

Magnetic Responses

The measured total magnetic field provides information on the magnetic properties of the earth materials in the survey area. This information can be used to locate magnetic bodies of direct interest for exploration, and for structural and lithological mapping.

The total magnetic field response reflects the abundance of magnetic material in the source. Magnetite is the most common magnetic mineral. Other minerals such as ilmenite, pyrrhotite, franklinite, chromite, hematite, arsenopyrite, limonite and pyrite are also magnetic, but to a lesser extent than magnetite on average.

In some geological environments, an EM anomaly with magnetic correlation has a greater likelihood of being produced by sulphides than one that is non-magnetic. However, sulphide ore bodies may be non-magnetic (e.g., the Kidd Creek deposit near Timmins, Canada) as well as magnetic (e.g., the Mattabi deposit near Sturgeon Lake, Canada).

Iron ore deposits will be anomalously magnetic in comparison to surrounding rock due to the concentration of iron minerals such as magnetite, ilmenite and hematite.

Changes in magnetic susceptibility often allow rock units to be differentiated based on the total magnetic field. Geophysical classifications may differ from geological classifications if various magnetite levels exist within one general geological classification. Geometric considerations of the source such as shape, dip and depth, inclination of the earth's field and remanent magnetization will complicate such an analysis.

In general, mafic lithologies contain more magnetite and are therefore more magnetic than many sediments which tend to be weakly magnetic. Metamorphism and alteration can also increase or decrease the magnetization of a rock unit.

Textural differences on a total field magnetic contour, colour or shadow map due to the frequency of activity of the magnetic parameter resulting from inhomogeneities in the distribution of magnetite within the rock, may define certain lithologies. For example, near surface volcanics may display highly complex contour patterns with little line-to-line correlation.

Rock units may be differentiated based on the plan shapes of their total or residual magnetic field responses. Mafic intrusive plugs can appear as isolated "bulls-eye"

anomalies. Granitic intrusives appear as sub-circular zones, and may have contrasting rings due to contact metamorphism. Generally, granitic terrain will lack a pronounced strike direction, although granite gneiss may display strike.

Linear north-south units are theoretically not well defined on total magnetic field maps in equatorial regions, due to the low inclination of the earth's magnetic field. However, most stratigraphic units will have variations in composition along strike that will cause the units to appear as a series of alternating magnetic highs and lows.

Faults and shear zones may be characterized by alteration that causes destruction of magnetite (e.g., weathering) that produces a contrast with surrounding rock. Structural breaks may be filled by magnetite-rich, fracture filling material, as is the case with diabase dikes, or by non-magnetic felsic material.

Faulting can also be identified by patterns in the magnetic contours or colours. Faults and dikes tend to appear as lineaments and often have strike lengths of several kilometres. Offsets in narrow, magnetic, stratigraphic trends also delineate structure. Sharp contrasts in magnetic lithologies may arise due to large displacements along strike-slip or dip-slip faults.

APPENDIX D

DATA ARCHIVE DESCRIPTION

APPENDIX D

ARCHIVE DESCRIPTION

Reference: CDVD00681
# of DVD's: 1
Archive Date: March 3, 2011

This archive contains FINAL data and grids of an airborne Dighem^{V} electromagnetic and magnetic geophysical survey over the Bark Area (Block1), Vanderhoof, B.C., conducted by FUGRO AIRBORNE SURVEYS CORP. on behalf of Amarc Resources Ltd., flown from January 16 -19, 2011

Job # 10073

******* Disc 1 of 1 *******

\GRIDS Grids in Geosoft format

CVG-1.GRD	- Calculated Vertical Magnetic Gradient nT/m
MAG-1.GRD	- Residual Magnetic Intensity nT
RES900-1.GRD	- Apparent Resistivity 900 Hz ohm·m
RES7200-1.GRD	- Apparent Resistivity 7200 Hz ohm·m
RES56K-1.GRD	- Apparent Resistivity 56k Hz ohm·m

\LINEDATA

Bark.GDB	- Data archive in Geosoft GDB format
Bark.XYZ	- Data archive in Geosoft ASCII format
AEM_Bark.XYZ	- Anomaly archive in ASCII format

\MAPS Final colour maps in Geosoft PDF format

AEM-1.PDF	- Electromagnetic Anomalies with Interpretation
CVG-1.PDF	- Calculated Vertical Magnetic Gradient nT/m
MAG-1.PDF	- Residual Magnetic Intensity nT
RES900-1.PDF	- Apparent Resistivity 900 Hz ohm•m
RES7200-1.PDF	- Apparent Resistivity 7200 Hz ohm•

\REPORT

10073-1.PDF	- Survey Report

****

GEOSOFT GDB and XYZ ARCHIVE SUMMARY

# CHANNEL NAME	TIME	UNITS	DESCRIPTION
1 x	0.1	m	eastings NAD83 (Zone 10N)

2 y		0.1	m	northings NAD83 (Zone 10N)
3 fid		0.1	synchronization counter	
4 longitude		0.1	degrees	longitude WGS84
5 latitude		0.1	degrees	latitude WGS84
6 flight		0.1	flight number	
7 date		0.1	flight date (yyyy/mm/dd)	
8 altrad_bird		0.1	m	calculated bird height above ground from radar altimeter
9 gpsz		0.1	m	survey height above spheroid
10 dtm		0.1	m	terrain with respect to ellipsoid
11 diurnal_filt		0.1	nT	ground magnetic intensity
12 diurnal_cor		0.1	nT	diurnal correction - base removed
13 mag_raw		0.1	nT	total magnetic field - spike rejected
14 mag_lag		0.1	nT	total magnetic field - corrected for lag
15 mag_diu		0.1	nT	total magnetic field - diurnal variation removed
16 igrf		0.1	nT	international geomagnetic reference field
17 mag_rmi	0.1	nT	residual magnetic intensity - final	
18 cpi900_filt		0.1	ppm	coplanar inphase 900 Hz - unlevelled
19 cpq900_filt		0.1	ppm	coplanar quadrature 900 Hz - unlevelled
20 cxi1000_filt		0.1	ppm	coaxial inphase 1000 Hz - unlevelled
21 cxq1000_filt		0.1	ppm	coaxial quadrature 1000 Hz - unlevelled
22 cxi5500_filt		0.1	ppm	coaxial inphase 5500 Hz - unlevelled
23 cxq5500_filt		0.1	ppm	coaxial quadrature 5500 Hz - unlevelled
24 cpi7200_filt		0.1	ppm	coplanar inphase 7200 Hz - unlevelled
25 cpq7200_filt		0.1	ppm	coplanar quadrature 7200 Hz -unlevelled
26 cpi56k_filt		0.1	ppm	coplanar inphase 56 kHz - unlevelled
27 cpq56k_filt		0.1	ppm	coplanar quadrature 56 kHz - unlevelled
28 cpi900		0.1	ppm	coplanar inphase 900 Hz
29 cpq900		0.1	ppm	coplanar quadrature 900 Hz
30 cxi1000		0.1	ppm	coaxial inphase 1000 Hz
31 cxq1000		0.1	ppm	coaxial quadrature 1000 Hz
32 cxi5500		0.1	ppm	coaxial inphase 5500 Hz
33 cxq5500		0.1	ppm	coaxial quadrature 5500 Hz
34 cpi7200		0.1	ppm	coplanar inphase 7200 Hz
35 cpq7200		0.1	ppm	coplanar quadrature 7200 Hz
36 cpi56k		0.1	ppm	coplanar inphase 56 kHz
37 cpq56k		0.1	ppm	coplanar quadrature 56 kHz
38 res900		0.1	ohm·m	apparent resistivity - 900 Hz
39 res7200		0.1	ohm·m	apparent resistivity - 7200 Hz
40 res56k		0.1	ohm·m	apparent resistivity - 56 kHz
41 dep900		0.1	m	apparent depth - 900 Hz
42 dep7200		0.1	m	apparent depth - 7200 Hz
43 dep56k		0.1	m	apparent depth - 56 kHz
44 difi		0.1	difference channel based on cxi1000/cpi900	
45 difq		0.1	difference channel based on cxq1000/cpq900	
46 cppl		0.1	coplanar powerline monitor	
47 cxsp		0.1	coaxial spherics monitor	
48 cpsp		0.1	coplanar spherics monitor	

FUGRO ANOMALY SUMMARY

# CHANNEL NAME	TIME	UNITS	DESCRIPTION
1 Easting	0.10	m	easting NAD83 (Zone 10N)
2 Northing	0.10	m	northing NAD83 (Zone 10N)
3 FID	1.00		Synchronization Counter
4 FLT	0.10		Flight
5 MHOS	0.10	siemens	Conductance (see report for model used)
6 DEPTH	0.10	m	Depth (see report for model used)
7 MAG	0.10	nT	Mag Correlation, local amplitude
8 CXI1	0.10	ppm	Inphase Coaxial 1000 Hz, local amplitude
9 CXQ1	0.10	ppm	Quadrature Coaxial 1000 Hz, local amplitude

10 CPI1	0.10	ppm	Inphase Coplanar 900 Hz, absolute amplitude
11 CPQ1	0.10	ppm	Quadrature Coplanar 900 Hz, absolute amplitude
12 CPI2	0.10	ppm	Inphase Coplanar 7200 Hz, absolute amplitude
13 CPQ2	0.10	ppm	Quadrature Coplanar 7200 Hz, absolute amplitude
14 LET	0.10	Anomaly Identifier	
15 SYM	0.10	Anomaly Interpretation Symbol	
16 GRD	0.10		Anomaly Grade

The coordinate system for all grids and the data archive is projected as follows

Datum	NAD83	
Spheroid	GRS80	
Central meridian	123 West (Z10N)	
False easting	500000	
False northing	0	
Scale factor	0.9996	
Northern parallel	N/A	
Base parallel	N/A	
WGS84 to local conversion method		Molodensky
Delta X shift	0	
Delta Y shift	0	
Delta Z shift	0	

If you have any problems with this archive please contact

Processing Manager
FUGRO AIRBORNE SURVEYS CORP.
2505 Meadowvale Blvd.
Mississauga, Ontario
Canada L5N 5S2
Tel (905) 812-0212
Fax (905) 812-1504
E-mail toronto@fugroairborne.com

APPENDIX E

EM ANOMALY LIST

EM Anomaly List : 10073-1, BARK Block, B.C.

CX=COAXIAL,CP=COPLANAR			Note: EM amplitudes are local for types B,D,T and are absolute for all others		Estimated depth may be unreliable because the strongest part of the conductor may be deeper or to one side of the flight line, or because of a shallow dip or magnetite/overburden effects							
Label Fid		**Interp**	**XUTM (m), YUTM (m)**	**CXI5500_LLEVHz Real (ppm)**	**CXQ5500_LLEVHz Quad (ppm)**	**CPI7200_LLEVHz Real (ppm)**	**CPQ7200_LLEVHz Quad (ppm)**	**CPI56K_LLEVHz Real (ppm)**	**CPQ56K_LLEVHz Quad (ppm)**	**Conductance (siemens)**	**Depth (metres)**	**Magnetic Corr. (nT)**
LINE 10010		**FLIGHT 1**										
A	2483.3	H	395277.8,5929012.8	36.3	32.9	142.6	109.4	219.4	76.4	1.5	12.3	---
B	2434.8	S	397049.9,5929005.1	23.3	29.4	106.3	111.0	215.3	74.2	1.0	0.4	---
C	2413.1	H	397750.5,5928998.5	29.0	19.1	123.1	66.0	140.4	38.9	1.9	23.4	---
D	2383.6	S?	398849.0,5928996.4	37.9	45.4	173.1	166.7	285.3	84.8	1.1	0.0	---
E	2347.3	H	400252.6,5928999.0	31.9	33.0	140.5	119.9	247.5	141.4	1.4	11.5	---
F	2323.6	S?	401125.3,5929006.7	63.1	64.6	245.8	243.0	485.9	234.9	1.0	0.3	51.8
G	2300.6	H	401996.0,5928993.3	46.2	33.6	180.2	125.6	306.8	206.6	1.7	7.9	---
LINE 10020		**FLIGHT 1**										
A	2557.2	B?	395025.9,5928800.5	5.1	4.1	31.9	27.2	34.8	0.0	1.5	21.1	---
B	2571.3	E	395517.6,5928805.9	25.9	35.5	107.9	109.7	233.3	117.4	1.0	3.9	39.8
C	2587.4	S	396135.9,5928800.1	25.1	48.0	136.5	164.8	341.1	203.4	1.0	0.0	55.7
D	2611.1	S	397001.1,5928793.6	6.8	19.6	68.7	57.8	114.2	36.4	1.0	1.1	---
E	2635.0	S?	397962.4,5928793.8	31.6	25.5	155.4	76.8	173.4	45.2	1.1	1.3	5.5
F	2664.4	S?	399030.9,5928800.7	43.9	52.8	210.8	169.8	300.0	75.0	1.2	0.0	---
G	2705.1	B?	400416.5,5928802.6	13.9	12.7	45.1	49.1	87.4	62.6	1.7	22.4	---
H	2743.1	S	401795.6,5928803.0	55.5	37.0	235.5	117.1	270.6	71.0	1.1	0.0	---
I	2753.4	H	402184.0,5928798.5	70.3	77.9	293.7	285.4	645.3	432.4	1.5	5.0	94.9
LINE 10030		**FLIGHT 1**										
A	3232.5	S	395196.8,5928603.6	40.2	30.3	142.3	84.9	179.7	34.7	1.3	0.0	---
B	3225.1	E	395510.9,5928626.9	34.7	33.5	108.2	95.8	221.0	121.2	1.0	5.4	80.6
C	3184.8	S	396957.8,5928598.4	30.8	42.1	130.3	143.0	259.1	88.0	1.0	3.1	---

- Appendix E.2 -

EM Anomaly List : 10073-1, BARK Block, B.C.

CX=COAXIAL,CP=COPLANAR			Note: EM amplitudes are local for types B,D,T and are absolute for all others		Estimated depth may be unreliable because the strongest part of the conductor may be deeper or to one side of the flight line, or because of a shallow dip or magnetite/overburden effects							
Label Fid		Interp	XUTM (m), YUTM (m)	CXI5500_LLEVHz Real (ppm)	CXQ5500_LLEVHz Quad (ppm)	CPI7200_LLEVHz Real (ppm)	CPQ7200_LLEVHz Quad (ppm)	CPI56K_LLEVHz Real (ppm)	CPQ56K_LLEVHz Quad (ppm)	Conductance (siemens)	Depth (metres)	Magnetic Corr. (nT)
D	3151.9	B?	398044.8,5928606.9	6.6	1.6	36.8	26.0	67.2	2.5	2.8	29.1	11.2
E	3123.4	S?	399148.6,5928604.8	19.5	26.9	96.0	74.5	136.5	25.3	1.3	0.0	---
F	3087.6	H	400460.5,5928596.7	44.2	59.7	191.5	197.2	410.6	261.1	1.4	4.5	---
G	3071.9	S?	401008.3,5928608.7	36.5	46.9	151.6	151.3	311.3	130.6	1.0	0.0	---
H	3046.2	H	401942.2,5928599.8	40.8	31.1	184.1	80.5	200.0	39.7	2.4	13.6	---
LINE 10040		**FLIGHT 3**										
A	3624.8	H	395328.0,5928407.0	38.2	44.4	177.3	148.5	302.8	119.5	1.5	10.7	---
B	3606.0	S?	395930.6,5928399.4	42.7	49.0	199.7	164.7	284.9	127.1	1.0	2.7	---
C	3581.5	S	396647.9,5928404.1	20.5	47.4	113.3	176.0	342.0	162.9	1.0	0.0	---
D	3543.5	H	397833.4,5928403.4	26.2	14.2	110.0	52.6	127.6	50.3	2.0	25.6	9.5
E	3534.9	E	398164.1,5928403.7	29.5	31.3	122.2	115.0	230.3	110.0	1.0	0.0	26.5
F	3507.0	S	399273.8,5928403.1	12.9	15.3	70.5	58.9	100.9	27.1	1.0	0.0	---
G	3456.3	S	401169.1,5928401.2	32.4	38.1	139.7	145.2	284.1	95.2	1.0	0.0	7.0
H	3433.9	H	401988.6,5928401.8	73.0	60.2	283.5	233.7	481.8	214.4	1.7	2.5	---
LINE 10050		**FLIGHT 3**										
A	3158.6	S?	395470.5,5928202.2	26.5	21.3	85.9	70.3	144.2	65.0	1.0	0.0	---
B	3181.4	B?	396240.1,5928200.9	11.7	11.0	19.4	22.9	40.4	11.8	1.5	15.9	---
C	3219.3	H	397858.9,5928199.8	26.5	15.6	107.4	64.4	157.4	76.1	1.7	15.5	15.8
D	3260.4	S	399457.7,5928201.9	24.6	24.4	102.2	102.8	183.3	55.9	1.0	0.0	7.7
E	3324.7	H	401821.1,5928198.6	38.5	30.2	147.4	130.4	268.9	119.4	1.4	9.9	6.5
F	3335.3	E	402235.2,5928199.2	63.6	53.8	225.3	208.9	400.1	154.6	1.0	2.2	10.7
G	3339.1	S?	402381.1,5928199.9	73.8	57.1	275.1	209.1	405.2	144.5	1.0	0.0	---

EM Anomaly List : 10073-1, BARK Block, B.C.

CX=COAXIAL,CP=COPLANAR			Note: EM amplitudes are local for types B,D,T and are absolute for all others		Estimated depth may be unreliable because the strongest part of the conductor may be deeper or to one side of the flight line, or because of a shallow dip or magnetite/overburden effects							
Label Fid		Interp	XUTM (m), YUTM (m)	CXI5500_LLEVHz Real (ppm)	CXQ5500_LLEVHz Quad (ppm)	CPI7200_LLEVHz Real (ppm)	CPQ7200_LLEVHz Quad (ppm)	CPI56K_LLEVHz Real (ppm)	CPQ56K_LLEVHz Quad (ppm)	Conductance (siemens)	Depth (metres)	Magnetic Corr. (nT)
LINE 10060	**FLIGHT 3**											
A	3089.9	S?	395239.0,5928004.8	34.4	46.5	142.1	183.8	343.3	132.7	1.0	1.4	46.3
B	3080.7	H	395572.7,5927999.9	17.7	15.6	65.6	58.2	124.7	70.1	1.2	12.3	---
C	3058.5	S	396259.6,5928000.4	6.3	15.8	28.3	64.6	141.2	106.2	1.0	0.0	---
D	3024.1	H	397159.6,5928002.1	28.4	26.7	117.5	108.7	228.0	89.4	1.3	10.5	---
E	3002.9	H	397885.3,5928008.9	35.3	20.7	127.7	81.5	176.8	81.0	1.7	13.3	---
F	2960.2	S	399546.7,5927999.1	23.2	29.7	88.5	125.2	230.9	102.7	1.0	0.0	7.3
G	2947.8	S	400038.7,5927994.4	28.8	27.2	101.8	104.3	191.8	72.2	1.0	0.0	---
H	2933.3	D	400574.1,5928000.2	14.8	20.6	15.5	64.5	126.1	63.7	1.1	10.5	147.9
I	2928.4	B?	400753.8,5927995.4	16.4	12.7	71.4	34.6	55.7	102.3	2.2	22.3	---
J	2901.6	H	401752.3,5928009.1	42.4	26.5	156.0	108.4	244.9	114.3	1.6	18.3	---
K	2895.2	E	401986.8,5928002.4	53.8	45.4	207.4	187.6	396.7	198.3	1.0	0.0	44.1
L	2875.5	H	402708.0,5927997.8	57.4	46.3	228.8	178.2	350.7	139.3	1.7	7.2	---
LINE 10070	**FLIGHT 3**											
A	2628.2	H	395752.3,5927795.9	38.7	31.6	169.7	130.9	273.4	89.6	1.6	6.5	---
B	2659.0	H	396811.3,5927788.2	19.2	11.4	83.6	50.3	126.0	45.3	1.6	13.5	---
C	2688.5	H	398089.7,5927806.1	18.1	10.3	82.1	56.0	118.2	40.5	1.4	19.4	---
D	2727.2	S	399613.2,5927806.7	24.1	32.9	91.7	143.6	268.4	134.3	1.0	0.0	28.5
E	2743.3	S?	400220.2,5927800.6	42.8	42.6	165.3	169.7	319.2	119.5	1.0	0.0	---
F	2760.7	H	400854.3,5927803.6	40.7	31.7	163.0	132.0	256.3	97.4	1.5	4.2	26.6
G	2777.1	S?	401505.2,5927796.3	41.5	47.6	158.2	203.2	395.5	201.8	1.0	0.0	86.1
H	2788.6	E	401964.5,5927798.2	37.0	38.5	144.0	157.7	286.9	110.5	1.0	0.0	---
I	2800.1	S	402394.7,5927800.6	20.8	18.8	78.1	93.1	169.8	68.8	1.0	0.0	---
J	2805.5	S?	402614.1,5927797.2	25.2	31.9	95.4	132.4	265.8	129.3	1.0	0.0	---

EM Anomaly List : 10073-1, BARK Block, B.C.

CX=COAXIAL,CP=COPLANAR			Note: EM amplitudes are local for types B,D,T and are absolute for all others		Estimated depth may be unreliable because the strongest part of the conductor may be deeper or to one side of the flight line, or because of a shallow dip or magnetite/overburden effects							
Label Fid		**Interp**	**XUTM (m), YUTM (m)**	**CXI5500_LLEVHz Real (ppm)**	**CXQ5500_LLEVHz Quad (ppm)**	**CPI7200_LLEVHz Real (ppm)**	**CPQ7200_LLEVHz Quad (ppm)**	**CPI56K_LLEVHz Real (ppm)**	**CPQ56K_LLEVHz Quad (ppm)**	**Conductance (siemens)**	**Depth (metres)**	**Magnetic Corr. (nT)**
LINE 10080		**FLIGHT 3**										
A	2523.4	B?	395853.3,5927612.1	19.5	18.1	81.8	98.5	172.7	65.6	1.8	17.9	---
B	2515.1	B?	396119.2,5927593.4	11.8	12.5	31.7	38.8	82.8	70.7	1.3	23.4	---
C	2485.8	B?	397033.7,5927602.8	11.4	1.2	45.3	0.0	0.0	0.0	5.4	16.8	---
D	2469.1	H	397642.4,5927600.1	19.8	16.7	81.5	76.3	180.2	72.7	1.2	13.9	---
E	2380.4	H	400909.4,5927598.9	40.4	44.1	178.4	172.6	329.5	165.4	1.4	16.1	142.9
F	2355.6	S	401776.4,5927606.6	32.1	40.5	148.0	156.8	293.8	118.2	1.0	0.4	14.8
G	2327.5	S	402790.7,5927597.6	24.2	44.2	118.8	185.3	359.4	182.0	1.0	5.8	---
LINE 10090		**FLIGHT 3**										
A	1914.1	S	395624.5,5927396.6	29.8	36.7	131.2	140.8	268.7	90.0	1.0	0.0	---
B	1933.4	S	396363.8,5927408.6	32.4	34.4	143.9	124.7	233.8	60.7	1.1	0.0	12.2
C	1945.0	H	396863.3,5927406.6	25.8	16.3	112.3	62.6	157.7	54.8	1.8	14.9	15.8
D	1948.1	E	396996.4,5927403.0	25.5	19.7	97.1	86.9	174.5	62.3	1.0	3.9	---
E	1963.4	H	397613.0,5927399.2	25.2	24.5	111.9	98.2	232.4	164.7	1.3	20.0	---
F	2020.9	S	399793.0,5927404.4	17.2	29.6	75.1	140.1	256.6	141.3	1.0	0.0	---
G	2026.7	S	400019.8,5927402.3	18.2	44.2	67.0	168.4	387.8	286.7	1.0	0.0	---
H	2038.8	H	400458.8,5927402.1	34.0	27.1	113.4	99.2	195.2	76.2	1.3	12.8	---
I	2068.5	S?	401566.5,5927402.5	33.8	32.9	128.0	122.9	212.9	55.0	1.1	0.0	---
J	2081.8	S	402085.0,5927400.3	22.9	36.8	100.2	150.7	286.9	134.3	1.0	0.0	---
K	2093.4	S	402511.9,5927394.7	27.2	45.8	124.7	181.2	331.6	150.3	1.0	0.0	---
LINE 10100		**FLIGHT 3**										
A	1847.3	S	395064.5,5927202.2	37.5	78.8	161.9	293.5	582.2	311.0	1.0	0.0	46.5
B	1838.1	S	395403.9,5927207.0	43.5	85.8	198.8	315.5	622.7	257.1	1.0	0.0	---

EM Anomaly List : 10073-1, BARK Block, B.C.

CX=COAXIAL,CP=COPLANAR			Note: EM amplitudes are local for types B,D,T and are absolute for all others	Estimated depth may be unreliable because the strongest part of the conductor may be deeper or to one side of the flight line, or because of a shallow dip or magnetite/overburden effects								
Label Fid		**Interp**	**XUTM (m), YUTM (m)**	**CXI5500_LLEVHz Real (ppm)**	**CXQ5500_LLEVHz Quad (ppm)**	**CPI7200_LLEVHz Real (ppm)**	**CPQ7200_LLEVHz Quad (ppm)**	**CPI56K_LLEVHz Real (ppm)**	**CPQ56K_LLEVHz Quad (ppm)**	**Conductance (siemens)**	**Depth (metres)**	**Magnetic Corr. (nT)**
C	1807.5	S	396497.2,5927203.5	39.9	56.3	165.8	198.2	366.7	131.1	1.0	3.3	8.3
D	1737.9	S	399183.2,5927202.9	8.4	22.6	38.8	85.5	165.8	110.7	1.0	0.0	---
E	1720.1	S	399892.0,5927194.7	13.6	27.2	53.8	103.3	193.8	106.1	1.0	0.0	---
F	1702.8	S	400601.2,5927200.5	20.3	23.1	93.1	73.9	144.5	41.6	1.0	0.0	---
G	1679.2	/	401552.3,5927207.3	12.7	9.9	44.5	36.8	58.7	19.2	1.9	17.3	---
H	1671.9	E	401830.7,5927197.2	54.2	83.7	184.3	270.0	536.3	335.9	1.0	0.0	140.2
I	1645.1	S	402810.6,5927214.7	19.8	35.3	91.6	122.5	225.5	78.7	1.0	0.6	---
LINE 10110		**FLIGHT 3**										
A	1389.7	B?	395535.2,5927000.4	12.0	12.6	23.7	32.8	57.6	43.3	1.4	23.0	6.7
B	1524.4	B?	400645.8,5927007.8	15.9	8.8	24.5	12.6	19.2	0.0	3.2	17.7	---
C	1551.5	H	401628.7,5927001.3	47.3	61.3	181.5	237.5	440.3	206.6	1.2	0.0	---
LINE 10120		**FLIGHT 3**										
A	1236.2	S	398034.5,5926810.9	20.8	28.1	94.1	114.7	206.2	74.7	1.0	0.0	6.8
B	1161.5	S?	400716.3,5926807.2	34.5	45.8	143.9	201.8	378.8	225.3	1.0	0.0	---
C	1151.4	S?	401106.7,5926795.5	33.2	50.7	131.4	195.9	384.5	175.5	1.0	0.0	---
D	1133.2	S?	401776.2,5926810.1	32.6	40.8	142.3	180.7	335.1	164.6	1.0	1.6	49.7
LINE 10130		**FLIGHT 3**										
A	812.0	S?	395981.6,5926594.3	37.4	52.4	166.3	172.9	343.0	151.0	1.0	0.2	---
B	837.7	S	396799.3,5926595.4	21.6	48.2	100.4	170.8	351.1	203.8	1.0	0.0	---
C	856.2	S	397432.8,5926594.5	11.9	52.6	59.6	196.4	466.9	438.8	1.0	0.0	34.0
D	868.5	S	397834.5,5926595.3	19.9	33.5	100.4	114.8	203.9	71.7	1.0	1.6	12.9
E	897.7	S	398837.3,5926599.3	22.0	41.4	111.6	154.5	302.5	138.8	1.0	3.3	---
F	935.9	S	400117.0,5926597.8	12.6	30.4	64.2	123.6	235.9	147.0	1.0	0.8	35.7

EM Anomaly List : 10073-1, BARK Block, B.C.

CX=COAXIAL,CP=COPLANAR			Note: EM amplitudes are local for types B,D,T and are absolute for all others		Estimated depth may be unreliable because the strongest part of the conductor may be deeper or to one side of the flight line, or because of a shallow dip or magnetite/overburden effects							
Label Fid		**Interp**	**XUTM (m), YUTM (m)**	**CXI5500_LLEVHz Real (ppm)**	**CXQ5500_LLEVHz Quad (ppm)**	**CPI7200_LLEVHz Real (ppm)**	**CPQ7200_LLEVHz Quad (ppm)**	**CPI56K_LLEVHz Real (ppm)**	**CPQ56K_LLEVHz Quad (ppm)**	**Conductance (siemens)**	**Depth (metres)**	**Magnetic Corr. (nT)**
G	951.9	S	400648.2,5926604.1	28.2	40.6	120.9	159.8	310.2	163.6	1.0	0.0	---
H	969.9	S?	401251.3,5926600.0	73.6	116.9	249.9	425.3	815.5	364.7	1.0	0.0	---
I	994.9	S	402071.1,5926593.7	44.2	78.9	180.6	295.2	591.0	344.5	1.0	0.0	106.0
LINE 10140		**FLIGHT 2**										
A	9507.3	H	396080.5,5926403.5	30.7	34.6	111.2	128.7	258.1	126.5	1.1	16.3	---
B	9488.9	S?	396633.5,5926401.1	24.7	49.7	101.7	202.9	424.4	283.4	1.0	2.2	73.2
C	9477.6	S	396974.0,5926397.1	27.2	68.4	110.6	277.2	599.9	412.2	1.0	0.0	5.3
D	9441.7	H	398021.0,5926404.9	21.9	38.0	95.1	149.2	294.8	138.5	1.0	11.5	17.0
E	9411.7	H	398896.0,5926406.8	28.2	42.9	104.3	157.6	306.3	117.4	1.0	6.8	---
F	9348.1	S?	400852.0,5926402.1	33.3	47.2	121.6	170.4	306.2	181.7	1.0	0.0	---
G	9328.2	S	401480.4,5926401.7	46.9	76.2	184.1	296.1	586.9	339.8	1.0	0.0	8.1
H	9296.1	S	402480.8,5926402.1	51.8	99.8	216.5	393.4	766.1	465.8	1.0	0.0	---
LINE 10150		**FLIGHT 2**										
A	9059.0	H	396185.2,5926209.9	35.7	39.5	108.0	131.3	271.2	143.0	1.1	14.3	---
B	9128.2	S	398911.8,5926206.8	24.8	37.6	100.0	151.4	291.7	124.8	1.0	0.0	---
C	9141.1	S?	399425.4,5926190.0	24.9	64.5	104.6	261.4	576.1	343.8	1.0	0.0	95.4
D	9205.6	S	401985.0,5926205.7	33.0	42.8	136.3	156.2	286.6	102.6	1.0	0.0	---
LINE 10160		**FLIGHT 2**										
A	8974.1	S	395076.9,5925993.5	26.6	47.9	132.6	185.7	371.1	188.0	1.0	2.4	31.1
B	8947.2	S	395837.8,5926001.2	46.6	102.0	183.2	399.3	856.7	635.3	1.0	0.0	---
C	8938.6	S	396114.6,5926004.2	27.6	27.3	104.4	102.3	195.7	63.4	1.0	1.3	---
D	8905.8	S	397094.2,5926006.6	44.3	122.2	200.7	510.6	1105.7	671.3	1.0	0.0	42.6
E	8828.2	S?	399442.1,5926006.0	27.4	56.4	121.3	221.3	447.8	258.3	1.0	0.0	37.9

EM Anomaly List : 10073-1, BARK Block, B.C.

CX=COAXIAL,CP=COPLANAR			Note: EM amplitudes are local for types B,D,T and are absolute for all others		Estimated depth may be unreliable because the strongest part of the conductor may be deeper or to one side of the flight line, or because of a shallow dip or magnetite/overburden effects							
Label Fid		**Interp**	**XUTM (m), YUTM (m)**	**CXI5500_LLEVHz Real (ppm)**	**CXQ5500_LLEVHz Quad (ppm)**	**CPI7200_LLEVHz Real (ppm)**	**CPQ7200_LLEVHz Quad (ppm)**	**CPI56K_LLEVHz Real (ppm)**	**CPQ56K_LLEVHz Quad (ppm)**	**Conductance (siemens)**	**Depth (metres)**	**Magnetic Corr. (nT)**
F	8817.8	S	399767.1,5925995.5	20.2	40.1	90.2	171.0	308.1	161.9	1.0	1.1	10.2
G	8738.0	S	402122.5,5926002.7	42.1	41.3	161.2	147.1	281.7	109.5	1.0	0.0	---
H	8709.7	H	403038.2,5925989.7	51.7	35.0	176.2	118.3	257.5	125.6	1.7	4.1	284.3
LINE 10170		**FLIGHT 2**										
A	8482.2	S	396670.6,5925804.0	22.8	24.7	86.9	99.3	192.8	74.2	1.0	0.0	---
B	8526.3	S	398279.1,5925804.4	34.0	56.1	136.6	215.0	421.4	158.6	1.0	0.0	---
C	8543.8	S	398928.5,5925796.4	22.2	39.7	100.5	171.6	321.1	127.7	1.0	1.0	7.4
D	8558.5	S	399503.5,5925794.8	19.5	31.5	89.2	126.9	250.7	121.7	1.0	1.3	8.7
E	8628.4	B?	402169.4,5925797.4	2.8	6.5	77.2	0.5	29.6	0.0	0.8	2.5	---
F	8650.9	H	402930.1,5925798.1	35.6	29.9	130.1	112.5	270.2	212.6	1.4	6.4	---
LINE 10180		**FLIGHT 2**										
A	8224.1	S?	395656.9,5925600.0	33.9	59.3	143.6	230.5	443.5	224.9	1.0	3.8	14.9
B	8183.6	S?	396764.5,5925596.5	41.5	59.6	153.3	220.5	435.0	211.4	1.0	0.0	---
C	8152.2	S	397719.1,5925606.2	56.6	64.2	216.5	235.5	420.7	133.9	1.1	0.0	---
D	8125.2	S	398518.8,5925603.3	48.3	64.9	188.8	245.1	447.1	177.7	1.0	0.0	---
E	8092.3	S	399479.0,5925602.9	25.0	45.6	110.6	178.8	362.6	201.5	1.0	0.0	68.7
F	8052.1	S	400623.5,5925605.5	5.9	14.3	28.6	61.1	124.4	90.7	1.0	10.1	5.5
G	8001.7	B?	402244.9,5925604.5	4.8	3.6	12.4	11.1	23.3	0.0	---	---	49.0
H	7978.0	H	402920.9,5925631.3	36.3	25.7	124.9	92.9	218.8	154.8	1.5	6.5	---
LINE 10190		**FLIGHT 2**										
A	7711.4	S	395108.0,5925398.3	30.4	30.2	118.2	102.6	197.1	64.1	1.0	0.0	---
B	7767.4	S	397272.8,5925407.8	46.8	64.4	181.6	231.7	447.5	158.0	1.0	0.0	---
C	7779.4	H	397678.6,5925394.4	60.7	51.8	236.4	182.0	357.1	111.2	1.7	4.6	---

EM Anomaly List : 10073-1, BARK Block, B.C.

CX=COAXIAL,CP=COPLANAR			Note: EM amplitudes are local for types B,D,T and are absolute for all others		Estimated depth may be unreliable because the strongest part of the conductor may be deeper or to one side of the flight line, or because of a shallow dip or magnetite/overburden effects							
Label	Fid	Interp	XUTM (m), YUTM (m)	CXI5500_LLEVHz Real (ppm)	CXQ5500_LLEVHz Quad (ppm)	CPI7200_LLEVHz Real (ppm)	CPQ7200_LLEVHz Quad (ppm)	CPI56K_LLEVHz Real (ppm)	CPQ56K_LLEVHz Quad (ppm)	Conductance (siemens)	Depth (metres)	Magnetic Corr. (nT)
D	7834.9	S?	399865.5,5925398.5	18.7	44.6	75.1	180.7	391.2	253.5	1.0	0.0	53.3
E	7850.5	S	400388.7,5925403.7	6.8	14.2	34.6	69.5	137.0	66.9	1.0	0.0	42.6
F	7904.7	B?	402454.1,5925397.9	5.1	1.5	14.5	6.1	1.1	0.0	2.3	23.0	34.9
LINE 10200		**FLIGHT 2**										
A	7642.4	S	395372.7,5925198.9	46.2	64.9	191.8	234.2	451.0	184.8	1.0	0.0	---
B	7624.6	S	395933.7,5925201.9	27.6	42.0	124.8	170.4	320.4	131.6	1.0	3.3	9.3
C	7582.9	H	397286.0,5925202.6	51.2	44.1	198.7	155.5	298.2	84.6	1.6	3.7	---
D	7495.5	S	400063.8,5925199.4	15.8	31.5	63.3	131.5	273.5	170.3	1.0	0.0	64.2
E	7475.3	S	400661.5,5925198.1	13.7	25.8	67.9	119.2	229.1	110.4	1.0	1.2	---
F	7414.9	S?	402420.7,5925204.3	27.7	42.8	112.0	167.4	344.2	174.8	1.0	0.0	---
G	7407.8	S	402658.1,5925196.1	25.1	23.1	96.5	89.4	166.9	51.2	1.0	7.7	---
LINE 10210		**FLIGHT 2**										
A	7131.4	E	394933.3,5924996.5	15.9	28.8	71.5	119.1	243.1	135.6	1.0	5.5	---
B	7149.1	S	395600.1,5925002.4	34.3	43.7	146.6	167.0	308.8	105.2	1.0	0.0	---
C	7158.1	S?	395939.0,5924996.0	43.4	67.2	165.2	258.0	527.5	277.1	1.0	0.0	---
D	7195.5	B?	397256.9,5925001.2	14.4	15.1	44.1	53.5	99.5	40.6	1.5	17.7	---
E	7230.6	S?	398561.2,5924999.6	37.7	30.8	157.5	107.7	210.8	76.0	1.0	0.0	---
F	7284.0	S	400562.4,5925008.0	14.7	32.6	71.3	142.8	295.9	153.2	1.0	2.6	---
G	7329.9	S?	402389.3,5925000.5	28.0	37.7	119.0	150.0	280.3	123.5	1.0	0.0	---
LINE 10220		**FLIGHT 2**										
A	7037.2	S?	395697.7,5924801.4	40.9	51.9	186.1	197.3	362.6	118.5	1.0	2.0	8.0
B	6999.7	B?	396975.7,5924804.6	9.4	1.2	53.2	49.4	59.6	0.8	4.3	25.6	---
C	6986.9	B?	397385.6,5924799.4	24.0	26.7	95.3	58.2	75.4	0.0	1.6	0.0	20.0

EM Anomaly List : 10073-1, BARK Block, B.C.

CX=COAXIAL,CP=COPLANAR			Note: EM amplitudes are local for types B,D,T and are absolute for all others		Estimated depth may be unreliable because the strongest part of the conductor may be deeper or to one side of the flight line, or because of a shallow dip or magnetite/overburden effects							
Label	**Fid**	**Interp**	**XUTM (m), YUTM (m)**	**CXI5500_LLEVHz Real (ppm)**	**CXQ5500_LLEVHz Quad (ppm)**	**CPI7200_LLEVHz Real (ppm)**	**CPQ7200_LLEVHz Quad (ppm)**	**CPI56K_LLEVHz Real (ppm)**	**CPQ56K_LLEVHz Quad (ppm)**	**Conductance (siemens)**	**Depth (metres)**	**Magnetic Corr. (nT)**
D	6952.3	S?	398492.0,5924794.9	38.2	36.0	170.0	130.2	239.2	91.3	1.0	0.0	---
E	6882.5	S	400717.7,5924810.2	10.4	31.6	55.7	130.9	297.1	175.7	1.0	0.3	---
F	6822.4	H	402634.9,5924803.5	43.4	70.7	188.4	280.1	536.7	324.3	1.1	0.0	---
LINE 10230		**FLIGHT 2**										
A	6604.5	S	397020.8,5924596.6	27.2	24.7	109.0	94.0	183.9	58.7	1.0	2.2	---
B	6615.2	S?	397451.2,5924603.9	37.0	32.2	140.3	126.2	217.8	59.4	1.1	0.0	49.3
C	6640.5	S?	398418.2,5924595.1	33.9	33.7	140.7	130.4	233.2	106.2	1.0	4.2	7.5
D	6660.3	S	399175.9,5924597.7	15.6	29.4	72.7	128.6	263.4	123.6	1.0	0.0	---
E	6690.3	S	400318.8,5924607.2	11.5	14.4	45.3	64.6	126.1	64.7	1.0	2.5	---
F	6719.0	S	401471.3,5924608.8	9.9	15.2	45.5	66.4	118.5	38.1	1.0	0.0	---
G	6750.4	S	402778.1,5924600.3	44.5	83.8	198.0	328.4	652.5	432.5	1.0	0.0	---
LINE 10240		**FLIGHT 2**										
A	6332.5	S	394801.4,5924398.9	16.6	27.4	75.3	107.5	207.3	96.9	1.0	0.0	---
B	6301.7	S?	395793.4,5924397.8	45.2	61.0	185.9	226.0	404.6	209.3	1.0	0.0	8.5
C	6293.9	S	396062.5,5924409.9	39.2	61.2	170.8	236.5	424.4	167.7	1.0	0.0	---
D	6254.6	S?	397427.0,5924398.6	28.7	34.2	94.4	126.1	246.5	103.8	1.0	5.1	53.9
E	6233.6	S	398118.9,5924401.7	35.0	72.1	150.2	279.1	570.3	292.9	1.0	0.0	---
F	6191.5	S	399485.6,5924404.2	16.4	29.1	67.5	121.3	244.0	118.8	1.0	4.7	---
G	6167.6	S	400271.3,5924407.8	16.6	34.0	74.9	134.5	272.3	141.2	1.0	3.8	132.0
H	6158.9	S?	400549.6,5924400.3	29.0	54.6	120.6	203.7	408.7	219.2	1.0	0.0	---
I	6151.1	E	400815.2,5924398.3	11.3	25.9	31.0	93.6	218.0	203.6	1.0	2.1	---
J	6129.6	S	401486.0,5924399.0	14.4	30.7	57.6	124.3	259.7	128.8	1.0	5.9	---
K	6110.4	S	402026.5,5924400.1	17.2	41.1	84.3	176.9	349.7	181.7	1.0	5.4	15.2
L	6080.4	S	402860.6,5924395.4	25.7	61.6	116.9	251.5	549.9	368.0	1.0	0.0	---

EM Anomaly List : 10073-1, BARK Block, B.C.

CX=COAXIAL,CP=COPLANAR			Note: EM amplitudes are local for types B,D,T and are absolute for all others		Estimated depth may be unreliable because the strongest part of the conductor may be deeper or to one side of the flight line, or because of a shallow dip or magnetite/overburden effects							
Label Fid		**Interp**	**XUTM (m), YUTM (m)**	**CXI5500_LLEVHz Real (ppm)**	**CXQ5500_LLEVHz Quad (ppm)**	**CPI7200_LLEVHz Real (ppm)**	**CPQ7200_LLEVHz Quad (ppm)**	**CPI56K_LLEVHz Real (ppm)**	**CPQ56K_LLEVHz Quad (ppm)**	**Conductance (siemens)**	**Depth (metres)**	**Magnetic Corr. (nT)**
LINE 10250		**FLIGHT 2**										
A	5844.0	S	396210.4,5924194.4	24.5	37.4	107.3	139.8	265.1	115.9	1.0	0.0	---
B	5901.6	S	398426.8,5924198.6	32.2	54.1	146.7	206.3	380.0	163.3	1.0	0.0	---
C	5932.4	S?	399550.4,5924195.4	13.9	35.4	63.3	157.3	338.1	201.9	1.0	1.2	---
D	5946.4	E	400035.9,5924208.2	8.3	18.3	30.7	76.8	171.6	120.8	1.0	1.8	---
E	5965.6	S	400756.1,5924205.2	32.7	66.1	153.9	254.7	513.8	273.8	1.0	0.0	16.4
F	6000.7	S	402047.4,5924199.8	11.7	23.2	44.1	80.8	163.3	83.9	1.0	0.0	---
G	6021.1	S	402843.6,5924198.8	12.4	17.5	53.9	68.7	134.3	68.4	1.0	0.0	12.6
LINE 10260		**FLIGHT 2**										
A	5684.8	S?	396400.7,5924016.4	33.6	64.3	146.6	256.0	513.1	305.2	1.0	0.0	20.0
B	5668.4	S?	396920.1,5924002.1	24.6	34.7	96.6	126.9	234.5	83.6	1.0	0.0	---
C	5638.5	H	397882.4,5924003.7	32.7	41.3	133.3	154.8	301.8	143.7	1.2	7.8	---
D	5576.9	S	399761.1,5924002.3	9.9	21.3	37.1	86.7	186.9	124.6	1.0	0.0	---
E	5559.2	S?	400306.1,5923997.8	12.8	31.2	52.7	123.7	280.1	187.8	1.0	3.2	42.7
F	5537.8	S	400987.1,5923998.3	17.1	32.4	91.3	135.3	255.5	125.6	1.0	0.0	14.7
G	5499.6	S	402227.9,5924003.5	10.7	25.3	57.5	106.9	206.9	92.8	1.0	3.1	8.8
LINE 10270		**FLIGHT 2**										
A	5266.9	S	396980.9,5923804.4	19.5	27.5	72.4	92.0	175.2	69.8	1.0	0.0	---
B	5280.0	S	397495.9,5923802.5	29.1	49.9	123.4	179.0	354.0	159.4	1.0	0.0	---
C	5317.9	S	398910.5,5923800.6	15.3	27.4	69.9	100.9	180.6	71.0	1.0	2.6	---
D	5341.8	S	399865.9,5923801.3	11.2	26.3	49.7	96.9	190.6	97.3	1.0	0.0	---
E	5375.4	S	401137.0,5923800.7	15.3	28.9	76.2	105.9	188.3	74.4	1.0	0.0	7.7
F	5403.1	S	402235.8,5923796.5	7.3	22.3	38.6	81.9	170.1	84.1	1.0	4.4	19.8

EM Anomaly List : 10073-1, BARK Block, B.C.

CX=COAXIAL,CP=COPLANAR			Note: EM amplitudes are local for types B,D,T and are absolute for all others		Estimated depth may be unreliable because the strongest part of the conductor may be deeper or to one side of the flight line, or because of a shallow dip or magnetite/overburden effects							
Label Fid		**Interp**	**XUTM (m), YUTM (m)**	**CXI5500_LLEVHz Real (ppm)**	**CXQ5500_LLEVHz Quad (ppm)**	**CPI7200_LLEVHz Real (ppm)**	**CPQ7200_LLEVHz Quad (ppm)**	**CPI56K_LLEVHz Real (ppm)**	**CPQ56K_LLEVHz Quad (ppm)**	**Conductance (siemens)**	**Depth (metres)**	**Magnetic Corr. (nT)**
LINE 10280		**FLIGHT 2**										
A	5128.4	S?	399103.5,5923604.8	17.5	46.5	82.8	188.1	389.8	198.5	1.0	6.4	---
B	5112.9	S	399575.6,5923609.2	17.9	39.6	89.2	150.1	288.2	124.9	1.0	4.2	---
C	5091.9	S	400200.4,5923604.1	12.4	32.5	54.9	124.2	268.0	142.9	1.0	3.3	35.1
D	5049.5	S	401370.0,5923610.4	14.4	29.6	79.2	107.6	181.8	65.1	1.0	4.2	---
E	5026.6	S	402042.9,5923592.5	7.7	35.9	37.3	140.8	301.7	352.3	1.0	0.0	5.1
F	5016.1	S	402402.0,5923603.1	7.0	28.6	28.4	101.1	238.9	220.2	1.0	0.0	11.0
G	5004.8	S	402763.2,5923610.9	7.2	22.3	27.1	78.8	174.3	120.4	1.0	0.0	26.3
LINE 10290		**FLIGHT 2**										
A	4805.1	S	397347.1,5923402.6	23.8	49.4	101.6	193.9	418.2	248.4	1.0	0.0	---
B	4823.6	S?	398070.2,5923396.8	22.7	28.1	96.9	111.3	205.1	70.4	1.0	0.0	---
C	4864.4	S	399764.2,5923404.2	17.1	28.9	74.2	117.6	232.0	124.4	1.0	0.0	---
D	4875.7	S?	400220.8,5923397.7	14.7	18.9	66.9	76.4	132.3	40.5	1.0	0.0	---
E	4912.5	S	401640.1,5923397.3	7.8	11.4	39.9	50.1	92.9	33.0	1.0	0.0	---
LINE 10300		**FLIGHT 2**										
A	4566.1	S	397483.2,5923208.4	21.4	35.7	94.1	138.2	271.7	135.6	1.0	0.0	---
B	4512.7	S	399333.9,5923201.8	10.7	30.2	51.1	123.9	275.3	188.8	1.0	8.0	10.1
C	4495.1	S	399879.0,5923203.9	22.7	51.5	85.5	196.9	414.3	331.5	1.0	0.0	---
D	4483.7	S?	400240.4,5923208.7	25.8	44.8	129.9	181.7	317.2	144.5	1.0	0.0	---
E	4444.1	E	401496.6,5923204.6	9.5	25.8	48.8	99.4	197.8	129.2	1.0	8.3	---
F	4416.4	S	402364.0,5923211.6	21.3	49.7	119.4	204.6	356.8	167.1	1.0	0.0	---

EM Anomaly List : 10073-1, BARK Block, B.C.

CX=COAXIAL,CP=COPLANAR			Note: EM amplitudes are local for types B,D,T and are absolute for all others		Estimated depth may be unreliable because the strongest part of the conductor may be deeper or to one side of the flight line, or because of a shallow dip or magnetite/overburden effects							
Label Fid		Interp	XUTM (m), YUTM (m)	CXI5500_LLEVHz Real (ppm)	CXQ5500_LLEVHz Quad (ppm)	CPI7200_LLEVHz Real (ppm)	CPQ7200_LLEVHz Quad (ppm)	CPI56K_LLEVHz Real (ppm)	CPQ56K_LLEVHz Quad (ppm)	Conductance (siemens)	Depth (metres)	Magnetic Corr. (nT)
LINE 10310	**FLIGHT 2**											
A	4180.1	S?	396887.8,5922993.1	20.3	18.2	80.6	74.8	136.0	51.7	1.0	3.3	---
B	4207.3	S	397967.1,5922998.7	23.2	34.9	111.5	139.8	255.0	121.2	1.0	0.4	6.0
C	4252.1	S	399534.0,5922996.1	13.3	31.7	75.6	139.8	262.6	139.1	1.0	0.0	14.5
D	4275.2	S?	400454.8,5923002.8	15.0	36.1	81.3	156.2	296.3	135.9	1.0	0.0	14.8
E	4297.4	S?	401284.6,5922996.6	10.1	19.8	50.7	90.4	159.7	76.2	1.0	1.9	114.6
F	4313.8	S	401947.7,5922997.8	11.5	24.3	67.3	104.4	194.9	92.0	1.0	5.3	5.3
G	4339.1	S?	402934.5,5923001.3	35.9	62.9	173.9	243.7	393.9	130.8	1.1	0.0	---
LINE 10320	**FLIGHT 2**											
A	4103.6	H	397028.7,5922804.9	24.1	26.3	102.1	91.7	179.8	84.3	1.3	16.0	---
B	4071.9	S	398036.4,5922811.8	24.8	35.3	110.7	132.1	232.2	75.0	1.0	0.0	---
C	4053.6	S	398662.3,5922792.3	14.5	35.9	69.8	141.7	272.6	117.3	1.0	2.2	---
D	4027.6	S	399521.4,5922798.2	11.6	30.9	41.9	109.2	232.5	175.3	1.0	3.6	21.0
E	3993.7	S	400566.8,5922797.4	13.9	39.5	49.4	147.4	310.3	244.7	1.0	0.0	---
F	3976.8	B?	401116.1,5922800.2	5.3	16.1	46.6	54.7	81.7	32.3	0.4	1.7	---
G	3974.2	S?	401205.1,5922805.1	24.4	41.1	120.0	172.9	271.1	100.8	1.0	0.3	9.0
H	3949.8	S	401988.1,5922802.7	9.4	20.6	45.6	82.6	158.0	74.9	1.0	2.0	---
I	3917.7	S?	402924.2,5922808.7	19.4	46.2	87.0	189.8	370.4	273.8	1.0	0.0	38.1
LINE 10330	**FLIGHT 2**											
A	3710.4	S	397287.9,5922597.2	20.3	29.8	97.1	125.1	227.9	110.5	1.0	0.0	---
B	3743.7	S	398564.7,5922597.1	19.1	38.2	100.9	169.7	300.2	136.4	1.0	2.0	---
C	3777.8	S	399851.0,5922591.4	12.2	27.8	61.2	120.1	224.8	111.5	1.0	0.6	---
D	3808.3	S	401004.9,5922594.7	24.1	38.1	128.7	153.6	244.1	99.8	1.0	0.0	91.5

EM Anomaly List : 10073-1, BARK Block, B.C.

CX=COAXIAL,CP=COPLANAR			Note: EM amplitudes are local for types B,D,T and are absolute for all others		Estimated depth may be unreliable because the strongest part of the conductor may be deeper or to one side of the flight line, or because of a shallow dip or magnetite/overburden effects							
Label Fid		**Interp**	**XUTM (m), YUTM (m)**	**CXI5500_LLEVHz Real (ppm)**	**CXQ5500_LLEVHz Quad (ppm)**	**CPI7200_LLEVHz Real (ppm)**	**CPQ7200_LLEVHz Quad (ppm)**	**CPI56K_LLEVHz Real (ppm)**	**CPQ56K_LLEVHz Quad (ppm)**	**Conductance (siemens)**	**Depth (metres)**	**Magnetic Corr. (nT)**
E	3843.5	S	402223.1,5922603.8	10.7	23.4	64.3	99.0	175.6	73.2	1.0	1.7	---
LINE 10340		**FLIGHT 2**										
A	3592.6	S	398025.6,5922409.6	43.2	69.5	209.2	294.3	497.7	241.4	1.0	0.0	---
B	3550.4	S	399474.2,5922395.7	10.8	55.0	59.1	276.0	609.3	615.2	1.0	0.0	---
C	3538.2	S	399869.4,5922397.5	14.5	30.9	84.6	149.8	259.6	121.6	1.0	4.4	22.3
D	3506.1	B?	400893.3,5922405.7	0.6	1.9	39.7	27.3	13.7	7.6	---	---	166.0
E	3496.8	S	401190.9,5922400.7	26.7	72.5	124.5	324.2	621.3	406.0	1.0	0.0	---
F	3455.4	S	402326.5,5922397.0	14.1	30.4	82.0	140.5	245.7	128.4	1.0	5.4	---
LINE 10350		**FLIGHT 2**										
A	3238.3	S?	397951.3,5922205.2	44.9	73.8	214.1	328.5	542.6	308.6	1.0	0.0	---
B	3290.4	S	399870.6,5922205.6	14.2	25.2	74.0	116.7	200.2	95.2	1.0	1.4	23.1
C	3316.7	B?	400792.5,5922198.7	2.9	0.4	22.8	1.9	6.3	0.0	---	---	105.8
D	3331.6	S?	401356.8,5922191.9	19.0	57.8	108.5	268.3	495.8	298.7	1.0	0.0	26.5
E	3353.6	E	402105.0,5922186.7	-2.6	24.9	12.9	123.8	205.2	257.9	1.0	0.0	---
F	3358.7	S	402295.4,5922194.0	11.2	25.4	73.2	118.7	200.1	82.0	1.0	0.0	---
G	3373.2	S	402865.2,5922200.0	14.6	31.4	77.3	136.6	253.9	137.0	1.0	0.0	20.9
LINE 10360		**FLIGHT 2**										
A	3001.4	S	397205.9,5922005.9	25.0	34.1	122.3	144.0	245.9	116.5	1.0	3.9	---
B	2949.3	S	399025.8,5922002.2	14.7	53.7	83.0	259.9	523.3	498.7	1.0	0.0	6.1
C	2915.5	S	400177.8,5922001.9	19.7	57.9	110.1	276.0	543.4	330.8	1.0	0.0	---
D	2903.3	E	400593.5,5922000.7	14.7	33.1	69.2	149.0	283.2	179.7	1.0	0.0	---
E	2895.1	S?	400870.1,5922008.8	25.3	31.7	123.6	123.0	211.6	98.9	1.0	0.0	43.1
F	2874.3	S	401535.7,5922006.2	17.7	60.4	103.3	296.6	572.4	394.7	1.0	0.0	---

EM Anomaly List : 10073-1, BARK Block, B.C.

CX=COAXIAL,CP=COPLANAR			Note: EM amplitudes are local for types B,D,T and are absolute for all others		Estimated depth may be unreliable because the strongest part of the conductor may be deeper or to one side of the flight line, or because of a shallow dip or magnetite/overburden effects							
Label	**Fid**	**Interp**	**XUTM (m), YUTM (m)**	**CXI5500_LLEVHz Real (ppm)**	**CXQ5500_LLEVHz Quad (ppm)**	**CPI7200_LLEVHz Real (ppm)**	**CPQ7200_LLEVHz Quad (ppm)**	**CPI56K_LLEVHz Real (ppm)**	**CPQ56K_LLEVHz Quad (ppm)**	**Conductance (siemens)**	**Depth (metres)**	**Magnetic Corr. (nT)**
G	2857.9	S?	402004.6,5922010.2	1.6	38.8	14.7	179.3	345.0	493.9	1.0	0.0	109.9
H	2849.6	S	402246.0,5921997.8	6.2	21.7	43.4	102.4	203.7	123.7	1.0	0.0	---
I	2824.9	S	402942.5,5922003.9	15.4	22.8	76.9	91.0	156.7	58.0	1.0	2.7	---
LINE 10370		**FLIGHT 2**										
A	2631.0	S	397462.8,5921787.3	23.0	27.7	113.3	117.8	212.1	83.9	1.0	0.0	---
B	2688.2	S	399720.9,5921807.9	16.2	28.7	85.3	125.0	221.8	108.4	1.0	0.8	---
C	2709.6	E	400597.1,5921800.4	19.1	29.0	75.0	121.9	212.3	106.1	1.0	0.0	19.2
D	2717.4	B?	400927.4,5921799.2	4.2	1.2	23.4	0.0	4.3	1.7	---	---	---
E	2744.3	S	402036.0,5921803.7	5.3	12.8	26.9	57.3	110.0	57.2	1.0	1.9	59.2
LINE 10380		**FLIGHT 2**										
A	2529.6	S	397440.9,5921603.1	19.6	20.8	92.6	86.5	155.1	53.8	1.0	2.8	---
B	2461.8	S	399639.2,5921607.1	17.8	41.7	93.3	183.4	344.8	229.9	1.0	2.7	---
C	2448.4	S	400060.5,5921600.9	25.4	54.9	126.6	231.6	441.5	267.1	1.0	0.0	37.9
D	2431.4	E	400630.4,5921601.7	24.0	37.3	97.4	157.4	279.9	138.0	1.0	3.3	75.6
E	2423.7	S?	400879.2,5921611.7	35.8	44.7	175.6	182.8	289.1	97.2	1.0	3.0	---
F	2386.5	S	402060.6,5921595.9	11.5	32.6	62.7	146.3	283.1	159.9	1.0	7.0	68.3
LINE 10390		**FLIGHT 2**										
A	2135.8	S	397237.0,5921398.8	25.5	33.8	117.0	114.7	208.2	66.1	1.0	0.0	9.5
B	2204.2	S	400081.1,5921403.0	25.3	55.6	109.3	212.7	432.2	216.3	1.0	0.0	---
C	2218.7	S?	400692.8,5921404.3	25.8	33.5	125.1	118.5	196.7	57.9	1.0	0.0	125.3
D	2232.1	S	401246.3,5921392.2	7.9	24.2	43.5	87.3	180.8	96.3	1.0	0.0	---
E	2253.7	S	402101.8,5921395.1	6.6	17.0	38.2	58.8	117.6	52.3	1.0	0.0	22.9

EM Anomaly List : 10073-1, BARK Block, B.C.

CX=COAXIAL,CP=COPLANAR			Note: EM amplitudes are local for types B,D,T and are absolute for all others		Estimated depth may be unreliable because the strongest part of the conductor may be deeper or to one side of the flight line, or because of a shallow dip or magnetite/overburden effects							
Label Fid		Interp	XUTM (m), YUTM (m)	CXI5500_LLEVHz Real (ppm)	CXQ5500_LLEVHz Quad (ppm)	CPI7200_LLEVHz Real (ppm)	CPQ7200_LLEVHz Quad (ppm)	CPI56K_LLEVHz Real (ppm)	CPQ56K_LLEVHz Quad (ppm)	Conductance (siemens)	Depth (metres)	Magnetic Corr. (nT)
LINE 10400		**FLIGHT 2**										
A	2037.0	S?	397239.4,5921204.1	37.7	49.3	168.0	197.0	340.9	123.7	1.0	0.0	27.1
B	1976.1	S	399179.6,5921192.2	21.3	65.2	114.1	271.3	580.2	418.1	1.0	0.0	---
C	1956.5	S	399822.8,5921196.7	23.0	47.6	105.3	205.0	387.0	223.0	1.0	0.0	---
D	1933.0	S?	400548.2,5921202.3	40.1	54.3	167.0	201.3	350.2	123.6	1.0	0.0	---
E	1887.9	S	401941.1,5921199.5	17.0	44.8	82.5	186.4	371.4	287.6	1.0	0.0	---
F	1860.7	S	402754.6,5921199.9	7.5	22.5	40.9	93.4	197.1	146.4	1.0	6.3	5.2
LINE 10410		**FLIGHT 2**										
A	1631.7	S	397289.2,5920995.8	31.2	38.6	131.3	143.3	255.3	83.2	1.0	0.0	---
B	1688.4	S?	399458.2,5921000.1	28.9	55.7	118.6	207.9	407.9	231.7	1.0	0.0	92.7
C	1698.7	S?	399847.9,5921007.8	32.0	65.9	124.5	237.2	475.3	315.5	1.0	0.0	16.0
D	1720.9	S	400651.0,5920998.2	24.3	34.0	106.7	125.7	226.6	76.2	1.0	0.0	46.0
E	1771.0	S	402555.0,5921000.3	16.3	29.7	69.7	112.0	222.6	129.7	1.0	0.0	---
LINE 10420		**FLIGHT 2**										
A	1372.6	S?	397404.1,5920802.0	42.5	55.4	168.6	217.7	410.0	148.4	1.0	0.0	---
B	1353.2	S	398009.2,5920777.1	24.1	45.7	104.7	182.5	384.7	228.7	1.0	0.0	---
C	1324.2	S	398902.4,5920808.0	25.7	43.7	109.0	174.0	360.3	228.7	1.0	0.0	33.9
D	1297.1	S	399715.7,5920806.2	34.5	51.7	144.2	206.3	408.0	193.2	1.0	0.0	9.6
E	1257.6	S	400826.1,5920807.3	17.9	31.0	74.2	123.2	283.8	152.8	1.0	0.0	---
F	1242.3	S	401254.2,5920798.5	13.5	21.0	60.3	87.7	189.8	82.7	1.0	0.0	---
LINE 10430		**FLIGHT 2**										
A	968.0	S?	397112.6,5920590.0	33.1	61.1	143.3	246.6	594.5	322.0	1.0	0.0	---

EM Anomaly List : 10073-1, BARK Block, B.C.

CX=COAXIAL,CP=COPLANAR			Note: EM amplitudes are local for types B,D,T and are absolute for all others		Estimated depth may be unreliable because the strongest part of the conductor may be deeper or to one side of the flight line, or because of a shallow dip or magnetite/overburden effects							
Label Fid		**Interp**	**XUTM (m), YUTM (m)**	**CXI5500_LLEVHz Real (ppm)**	**CXQ5500_LLEVHz Quad (ppm)**	**CPI7200_LLEVHz Real (ppm)**	**CPQ7200_LLEVHz Quad (ppm)**	**CPI56K_LLEVHz Real (ppm)**	**CPQ56K_LLEVHz Quad (ppm)**	**Conductance (siemens)**	**Depth (metres)**	**Magnetic Corr. (nT)**
B	1015.6	S	398969.6,5920601.6	20.3	29.8	82.3	131.1	295.2	162.4	1.0	0.0	---
C	1028.4	S	399505.3,5920603.5	20.5	28.4	93.3	118.1	253.5	115.2	1.0	0.0	---
D	1065.2	S	401046.5,5920601.8	14.8	24.3	59.8	99.1	233.8	104.5	1.0	0.0	---
E	1096.7	S	402248.7,5920601.7	15.2	20.1	75.4	91.5	195.8	86.0	1.0	0.0	---
LINE 10440		**FLIGHT 2**										
A	872.2	H	397017.8,5920408.7	24.6	40.7	104.2	166.3	444.9	298.8	1.0	0.0	---
B	849.4	S	397814.8,5920407.3	31.2	43.2	130.3	174.6	419.6	254.8	1.0	0.0	16.7
C	800.9	S?	399406.4,5920410.1	30.1	35.6	125.3	140.3	299.9	95.8	1.0	0.0	31.5
D	772.9	S	400330.2,5920402.0	33.3	62.5	152.7	253.9	607.4	340.5	1.0	0.0	15.8
E	704.5	S	402693.3,5920387.4	19.4	37.3	91.7	159.0	414.2	244.7	1.0	0.0	---
LINE 10450		**FLIGHT 2**										
A	457.3	H	396658.0,5920188.5	27.4	30.6	101.9	110.6	346.5	243.1	1.2	17.3	45.6
B	487.6	H	397722.3,5920200.5	23.1	27.4	105.5	108.6	275.9	139.3	1.2	12.6	---
C	522.2	S?	399008.6,5920207.7	19.2	31.8	86.3	133.3	341.0	127.9	1.0	0.0	80.4
D	534.4	S	399491.0,5920200.4	25.5	38.0	107.7	145.2	389.2	180.4	1.0	0.0	39.0
E	556.5	S	400311.0,5920202.5	12.7	25.5	52.4	101.8	295.5	172.5	1.0	0.0	---
F	587.6	S	401488.7,5920190.8	15.9	26.9	74.5	110.9	305.6	137.8	1.0	0.0	24.5
G	609.6	S	402268.3,5920201.4	18.0	26.8	74.2	110.5	297.6	153.0	1.0	0.0	---
H	626.7	S	402860.2,5920197.2	15.9	27.5	81.1	117.7	321.0	161.0	1.0	0.0	---
LINE 19010		**FLIGHT 1**										
A	449.3	S	394800.9,5924413.0	11.2	23.7	80.1	130.7	242.6	122.8	1.0	0.0	---

EM Anomaly List : 10073-1, BARK Block, B.C.

CX=COAXIAL,CP=COPLANAR			Note: EM amplitudes are local for types B,D,T and are absolute for all others	Estimated depth may be unreliable because the strongest part of the conductor may be deeper or to one side of the flight line, or because of a shallow dip or magnetite/overburden effects								
Label Fid		**Interp**	**XUTM (m), YUTM (m)**	**CXI5500_LLEVHz Real (ppm)**	**CXQ5500_LLEVHz Quad (ppm)**	**CPI7200_LLEVHz Real (ppm)**	**CPQ7200_LLEVHz Quad (ppm)**	**CPI56K_LLEVHz Real (ppm)**	**CPQ56K_LLEVHz Quad (ppm)**	**Conductance (siemens)**	**Depth (metres)**	**Magnetic Corr. (nT)**
LINE 19020	**FLIGHT 1**											
A	888.4	S	396804.7,5921858.0	14.8	35.0	77.8	157.4	287.3	152.9	1.0	0.0	27.9
B	856.2	S	396798.8,5923082.2	21.9	33.1	103.0	142.3	254.1	139.3	1.0	6.3	---
C	790.2	S	396804.1,5925522.9	25.0	46.3	139.1	198.9	361.3	159.9	1.0	0.0	---
D	763.1	S?	396806.9,5926519.9	24.8	75.1	135.8	325.0	681.7	433.0	1.0	0.0	25.0
E	743.2	E	396802.2,5927239.6	39.9	36.0	173.2	163.1	324.2	144.2	1.0	3.3	---
F	738.8	B?	396812.3,5927400.2	7.5	0.9	1.3	0.7	0.7	0.0	3.7	30.4	---
G	729.4	H	396797.6,5927749.1	22.7	13.6	112.0	71.0	163.8	71.2	1.6	16.8	---
H	707.2	S?	396805.1,5928483.8	19.3	29.3	87.4	125.9	226.1	109.3	1.0	3.0	37.4
LINE 19030	**FLIGHT 1**											
A	1058.7	S?	398799.2,5920825.4	16.3	46.4	93.6	170.5	318.9	220.5	1.0	5.1	90.5
B	1073.6	S?	398799.5,5921373.7	10.7	39.3	62.8	142.5	299.7	224.9	1.0	0.0	---
C	1133.6	S	398801.9,5923685.9	10.3	28.8	61.5	104.0	177.9	75.6	1.0	0.0	---
D	1179.3	S?	398801.5,5925509.7	18.9	22.6	80.0	76.8	119.4	30.3	1.0	0.0	---
E	1204.4	S?	398798.8,5926492.1	20.3	33.5	81.0	123.2	216.7	86.9	1.0	1.7	---
F	1261.5	E	398814.8,5928764.4	26.2	46.1	103.2	173.6	342.4	209.6	1.0	0.0	8.4
G	1268.0	S?	398806.8,5929017.1	31.5	28.9	111.1	103.0	171.5	48.6	1.0	0.0	---
LINE 19040	**FLIGHT 1**											
A	1775.3	S	400793.7,5920782.4	30.1	69.9	90.9	184.7	389.1	228.6	1.0	0.0	---
B	1767.5	S?	400797.2,5921068.8	27.1	49.4	84.8	109.5	187.1	64.2	1.0	0.0	13.2
C	1759.2	S	400798.6,5921350.6	31.0	55.3	101.4	125.4	214.4	72.5	1.0	0.0	35.5
D	1721.2	S?	400803.4,5922627.3	23.9	60.7	72.0	163.1	313.9	167.9	1.0	2.0	---
E	1668.6	S	400795.0,5924197.8	25.2	50.3	76.9	106.0	194.5	75.6	1.0	0.0	---

EM Anomaly List : 10073-1, BARK Block, B.C.

CX=COAXIAL,CP=COPLANAR			Note: EM amplitudes are local for types B,D,T and are absolute for all others		Estimated depth may be unreliable because the strongest part of the conductor may be deeper or to one side of the flight line, or because of a shallow dip or magnetite/overburden effects							
Label Fid		**Interp**	**XUTM (m), YUTM (m)**	**CXI5500_LLEVHz Real (ppm)**	**CXQ5500_LLEVHz Quad (ppm)**	**CPI7200_LLEVHz Real (ppm)**	**CPQ7200_LLEVHz Quad (ppm)**	**CPI56K_LLEVHz Real (ppm)**	**CPQ56K_LLEVHz Quad (ppm)**	**Conductance (siemens)**	**Depth (metres)**	**Magnetic Corr. (nT)**
F	1647.8	S	400792.3,5924908.2	17.7	41.5	45.1	92.2	169.8	72.6	1.0	3.6	15.0
G	1590.4	S	400794.6,5926828.0	35.3	59.9	107.5	148.6	289.7	150.1	1.0	0.0	---
H	1558.3	B?	400796.0,5927951.9	6.3	2.6	32.8	19.9	35.2	28.9	2.2	20.5	---
I	1535.9	E	400797.1,5928712.7	46.5	78.3	153.8	183.9	378.0	246.9	1.0	0.0	11.1
J	1527.2	H	400799.3,5929006.8	50.9	71.8	183.4	156.6	353.1	195.6	1.5	5.0	---
LINE 19050		**FLIGHT 1**										
A	1922.1	S?	402801.0,5920335.3	24.4	28.6	75.9	114.6	221.5	110.9	1.0	1.8	---
B	1941.3	S	402802.1,5921069.4	12.7	23.3	44.8	78.2	168.1	94.4	1.0	0.0	8.8
C	1970.4	S?	402813.2,5922101.5	11.8	21.1	50.0	64.8	119.8	53.0	1.0	0.0	---
D	1995.4	B?	402803.2,5923072.8	18.2	4.6	45.7	28.1	10.1	0.0	5.4	14.9	---
E	2011.7	E	402798.6,5923659.9	4.8	19.2	25.0	75.1	173.0	114.8	1.0	0.0	---
F	2038.2	S	402800.3,5924627.2	52.8	53.9	174.0	248.7	463.6	272.0	1.0	0.0	---
G	2055.1	B?	402803.4,5925205.2	12.2	6.3	20.2	26.0	35.7	9.9	3.2	29.2	---
H	2069.5	H	402802.9,5925723.5	11.8	16.5	72.2	47.2	117.9	55.1	1.4	22.2	---
I	2083.3	S?	402804.8,5926244.7	18.3	31.7	95.5	94.7	172.4	53.4	1.0	0.0	70.1
J	2112.0	S?	402799.2,5927243.1	25.3	47.6	106.9	150.4	267.8	94.2	1.0	3.8	28.2
K	2133.3	E	402803.2,5928057.2	53.2	38.0	210.3	139.6	293.3	101.8	1.0	0.0	---
L	2136.5	B?	402799.9,5928187.5	7.0	0.0	50.2	11.3	4.0	0.0	4.3	31.6	157.1
M	2142.3	B?	402798.6,5928422.3	10.4	7.4	58.5	54.4	118.7	64.6	2.0	29.5	---
N	2153.3	E	402802.8,5928842.7	52.5	45.2	190.6	153.2	341.7	142.6	1.0	0.1	11.3
O	2157.2	B?	402800.6,5928987.9	9.6	4.0	5.0	9.3	0.9	17.4	2.7	24.1	67.2

Anomalies Summary

Conductor Grade	No. of Responses
7	0
6	0
5	0
4	0
3	2
2	348
1	2
0	4
Total	356

Conductor Model	No. of Responses
L	0
D	1
/	1
\	0
T	0
B	27
H	45
S	260
E	22
M	0
Total	356

APPENDIX F

GLOSSARY

APPENDIX F

GLOSSARY

Note: The definitions given in this glossary refer to the common terminology as used in airborne geophysics.

altitude attenuation: the absorption of gamma rays by the atmosphere between the earth and the detector. The number of gamma rays detected by a system decreases as the altitude increases.

apparent- : the ***physical parameters*** of the earth measured by a geophysical system are normally expressed as apparent, as in "apparent ***resistivity*****"**. This means that the measurement is limited by assumptions made about the geology in calculating the response measured by the geophysical system. Apparent resistivity calculated with ***HEM***, for example, generally assumes that the earth is a ***homogeneous half-space*** – not layered.

amplitude: The strength of the total electromagnetic field. In ***frequency domain*** it is most often the sum of the squares of ***in-phase*** and ***quadrature*** components. In multi-component electromagnetic surveys it is generally the sum of the squares of all three directional components.

analytic signal: The total amplitude of all the directions of magnetic ***gradient***. Calculated as the sum of the squares.

anisotropy: Having different ***physical parameters*** in different directions. This can be caused by layering or fabric in the geology. Note that a unit can be anisotropic, but still **homogeneous**.

anomaly: A localized change in the geophysical data characteristic of a discrete source, such as a conductive or magnetic body: something locally different from the **background**.

B-field: In time-domain **electromagnetic** surveys, the magnetic field component of the (electromagnetic) **field**. This can be measured directly, although more commonly it is calculated by integrating the time rate of change of the magnetic field **dB/dt**, as measured with a receiver coil.

background: The "normal" response in the geophysical data – that response observed over most of the survey area. **Anomalies** are usually measured relative to the background. In airborne gamma-ray spectrometric surveys the term defines the **cosmic**, radon, and aircraft responses in the absence of a signal from the ground.

base-level: The measured values in a geophysical system in the absence of any outside signal. All geophysical data are measured relative to the system base level.

base frequency: The frequency of the pulse repetition for a ***time-domain electromagnetic*** system. Measured between subsequent positive pulses.

bird: A common name for the pod towed beneath or behind an aircraft, carrying the geophysical sensor array.

bucking: The process of removing the strong ***signal*** from the ***primary field*** at the ***receiver*** from the data, to measure the ***secondary field***. It can be done electronically or mathematically. This is done in ***frequency-domain EM***, and to measure ***on-time*** in ***time-domain EM***.

calibration coil: A wire coil of known size and dipole moment, which is used to generate a field of known ***amplitude*** and ***phase*** in the receiver, for system calibration. Calibration coils can be external, or internal to the system. Internal coils may be called Q-coils.

coaxial coils: **[CX]** Coaxial coils in an HEM system are in the vertical plane, with their axes horizontal and collinear in the flight direction. These are most sensitive to vertical conductive objects in the ground, such as thin, steeply dipping conductors perpendicular to the flight direction. Coaxial coils generally give the sharpest anomalies over localized conductors. (See also ***coplanar coils***)

coil: A multi-turn wire loop used to transmit or detect electromagnetic fields. Time varying ***electromagnetic*** fields through a coil induce a voltage proportional to the strength of the field and the rate of change over time.

compensation: Correction of airborne geophysical data for the changing effect of the aircraft. This process is generally used to correct data in ***fixed-wing time-domain electromagnetic*** surveys (where the transmitter is on the aircraft and the receiver is moving), and magnetic surveys (where the sensor is on the aircraft, turning in the earth's magnetic field.

component: In ***frequency domain electromagnetic*** surveys this is one of the two **phase** measurements – ***in-phase or quadrature***. In "multi-component" electromagnetic surveys it is also used to define the measurement in one geometric direction (vertical, horizontal in-line and horizontal transverse – the Z, X and Y components).

Compton scattering: gamma ray photons will bounce off electrons as they pass through the earth and atmosphere, reducing their energy and then being detected by ***radiometric*** sensors at lower energy levels. See also ***stripping***.

conductance: See ***conductivity thickness***

conductivity: [σ] The facility with which the earth or a geological formation conducts electricity. Conductivity is usually measured in milli-Siemens per metre (mS/m). It is the reciprocal of ***resistivity***.

conductivity-depth imaging: see ***conductivity-depth transform***.

conductivity-depth transform: A process for converting electromagnetic measurements to an approximation of the conductivity distribution vertically in the earth, assuming a ***layered earth***. (Macnae and Lamontagne, 1987; Wolfgram and Karlik, 1995)

conductivity thickness: [σ**t**] The product of the ***conductivity***, and thickness of a large, tabular body. (It is also called the "conductivity-thickness product") In electromagnetic geophysics, the response of a thin plate-like conductor is proportional to the conductivity multiplied by thickness. For example a 10 metre thickness of 20 Siemens/m mineralization will be equivalent to 5 metres of 40 S/m; both have 200 S conductivity thickness. Sometimes referred to as conductance.

conductor: Used to describe anything in the ground more conductive than the surrounding geology. Conductors are most often clays or graphite, or hopefully some type of mineralization, but may also be man-made objects, such as fences or pipelines.

coplanar coils: **[CP]** In HEM, the coplanar coils lie in the horizontal plane with their axes vertical, and parallel. These coils are most sensitive to massive conductive bodies, horizontal layers, and the ***halfspace***.

cosmic ray: High energy sub-atomic particles from outer space that collide with the earth's atmosphere to produce a shower of gamma rays (and other particles) at high energies.

counts (per second): The number of ***gamma-rays*** detected by a gamma-ray ***spectrometer.*** The rate depends on the geology, but also on the size and sensitivity of the detector.

culture: A term commonly used to denote any man-made object that creates a geophysical anomaly. Includes, but not limited to, power lines, pipelines, fences, and buildings.

current channelling: See current gathering.

current gathering: The tendency of electrical currents in the ground to channel into a conductive formation. This is particularly noticeable at higher frequencies or early time

channels when the formation is long and parallel to the direction of current flow. This tends to enhance anomalies relative to inductive currents (see also ***induction***). Also known as current channelling.

daughter products: The radioactive natural sources of gamma-rays decay from the original "parent" element (commonly potassium, uranium, and thorium) to one or more lower-energy "daughter" elements. Some of these lower energy elements are also radioactive and decay further. ***Gamma-ray spectrometry*** surveys may measure the gamma rays given off by the original element or by the decay of the daughter products.

dB/dt: As the ***secondary electromagnetic field*** changes with time, the magnetic field [**B**] component induces a voltage in the receiving ***coil***, which is proportional to the rate of change of the magnetic field over time.

decay: In ***time-domain electromagnetic*** theory, the weakening over time of the ***eddy currents*** in the ground, and hence the ***secondary field*** after the ***primary field*** electromagnetic pulse is turned off. In ***gamma-ray spectrometry***, the radioactive breakdown of an element, generally potassium, uranium, thorium, or one of their ***daughter*** products.

decay constant: see time constant.

decay series: In ***gamma-ray spectrometry***, a series of progressively lower energy ***daughter products*** produced by the radioactive breakdown of uranium or thorium.

depth of exploration: The maximum depth at which the geophysical system can detect the target. The depth of exploration depends very strongly on the type and size of the target, the contrast of the target with the surrounding geology, the homogeneity of the surrounding geology, and the type of geophysical system. One measure of the maximum depth of exploration for an electromagnetic system is the depth at which it can detect the strongest conductive target – generally a highly conductive horizontal layer.

differential resistivity: A process of transforming ***apparent resistivity*** to an approximation of layer resistivity at each depth. The method uses multi-frequency HEM data and approximates the effect of shallow layer ***conductance*** determined from higher frequencies to estimate the deeper conductivities (Huang and Fraser, 1996)

dipole moment: [NIA] For a transmitter, the product of the area of a ***coil***, the number of turns of wire, and the current flowing in the coil. At a distance significantly larger than the size of the coil, the magnetic field from a coil will be the same if the dipole moment product is the same. For a receiver coil, this is the product of the area and the number of turns. The sensitivity to a magnetic field (assuming the source is far away) will be the same if the dipole moment is the same.

diurnal: The daily variation in a natural field, normally used to describe the natural fluctuations (over hours and days) of the earth's magnetic field.

dielectric permittivity: **[ε]** The capacity of a material to store electrical charge, this is most often measured as the relative permittivity [ε_r], or ratio of the material dielectric to that of free space. The effect of high permittivity may be seen in HEM data at high frequencies over highly resistive geology as a reduced or negative ***in-phase***, and higher ***quadrature*** data.

drape: To fly a survey following the terrain contours, maintaining a constant altitude above the local ground surface. Also applied to re-processing data collected at varying altitudes above ground to simulate a survey flown at constant altitude.

drift: Long-time variations in the base-level or calibration of an instrument.

eddy currents: The electrical currents induced in the ground, or other conductors, by a time-varying ***electromagnetic field*** (usually the ***primary field***). Eddy currents are also induced in the aircraft's metal frame and skin; a source of ***noise*** in EM surveys.

electromagnetic: **[EM]** Comprised of a time-varying electrical and magnetic field. Radio waves are common electromagnetic fields. In geophysics, an electromagnetic system is one which transmits a time-varying ***primary field*** to induce ***eddy currents*** in the ground, and then measures the ***secondary field*** emitted by those eddy currents.

energy window: A broad spectrum of ***gamma-ray*** energies measured by a spectrometric survey. The energy of each gamma-ray is measured and divided up into numerous discrete energy levels, called windows.

equivalent (thorium or uranium): The amount of radioelement calculated to be present, based on the gamma-rays measured from a **daughter** element. This assumes that the ***decay series*** is in equilibrium – progressing normally.

exposure rate: in radiometric surveys, a calculation of the total exposure rate due to gamma rays at the ground surface. It is used as a measurement of the concentration of all the **radioelements** at the surface. See also: **natural exposure rate**.

fiducial, or fid: Timing mark on a survey record. Originally these were timing marks on a profile or film; now the term is generally used to describe 1-second interval timing records in digital data, and on maps or profiles.

Figure of Merit: **(FOM)** A sum of the 12 distinct magnetic noise variations measured by each of four flight directions, and executing three aircraft attitude variations (yaw, pitch, and roll) for each direction. The flight directions are generally parallel and perpendicular to planned survey flight directions. The FOM is used as a measure of the **manoeuvre noise** before and after **compensation.**

fixed-wing: Aircraft with wings, as opposed to “rotary wing” helicopters.

footprint: This is a measure of the area of sensitivity under the aircraft of an airborne geophysical system. The footprint of an ***electromagnetic*** system is dependent on the altitude of the system, the orientation of the transmitter and receiver and the separation between the receiver and transmitter, and the conductivity of the ground. The footprint of a ***gamma-ray spectrometer*** depends mostly on the altitude. For all geophysical systems, the footprint also depends on the strength of the contrasting ***anomaly***.

frequency domain: An ***electromagnetic*** system which transmits a ***primary field*** that oscillates smoothly over time (sinusoidal), inducing a similarly varying electrical current in the ground. These systems generally measure the changes in the ***amplitude*** and ***phase*** of the ***secondary field*** from the ground at different frequencies by measuring the **in-phase** and **quadrature** phase components. See also ***time-domain***.

full-stream data: Data collected and recorded continuously at the highest possible sampling rate. Normal data are stacked (see ***stacking***) over some time interval before recording.

gamma-ray: A very high-energy photon, emitted from the nucleus of an atom as it undergoes a change in energy levels.

gamma-ray spectrometry: Measurement of the number and energy of natural (and sometimes man-made) gamma-rays across a range of photon energies.

gradient: In magnetic surveys, the gradient is the change of the magnetic field over a distance, either vertically or horizontally in either of two directions. Gradient data is often measured, or calculated from the total magnetic field data because it changes more quickly over distance than the ***total magnetic field***, and so may provide a more precise measure of the location of a source. See also ***analytic signal***.

ground effect: The response from the earth. A common calibration procedure in many geophysical surveys is to fly to altitude high enough to be beyond any measurable response from the ground, and there establish ***base levels*** or ***backgrounds***.

half-space: A mathematical model used to describe the earth – as infinite in width, length, and depth below the surface. The most common halfspace models are ***homogeneous*** and ***layered earth***.

heading error: A slight change in the magnetic field measured when flying in opposite directions.

HEM: Helicopter ElectroMagnetic, This designation is most commonly used for helicopter-borne, ***frequency-domain*** electromagnetic systems. At present, the

transmitter and receivers are normally mounted in a ***bird*** carried on a sling line beneath the helicopter.

herringbone pattern: A pattern created in geophysical data by an asymmetric system, where the **anomaly** may be extended to either side of the source, in the direction of flight. Appears like fish bones, or like the teeth of a comb, extending either side of centre, each tooth an alternate flight line.

homogeneous: This is a geological unit that has the same ***physical parameters*** throughout its volume. This unit will create the same response to an HEM system anywhere, and the HEM system will measure the same apparent ***resistivity*** anywhere. The response may change with system direction (see ***anisotropy***).

HTEM: Helicopter Time-domain ElectroMagnetic, This designation is used for the new generation of helicopter-borne, ***time-domain*** electromagnetic systems.

in-phase: the component of the measured ***secondary field*** that has the same phase as the transmitter and the ***primary field***. The in-phase component is stronger than the ***quadrature*** phase over relatively higher ***conductivity***.

induction: Any time-varying electromagnetic field will induce (cause) electrical currents to flow in any object with non-zero ***conductivity***. (see ***eddy currents***)

induction number: also called the "response parameter", this number combines many of the most significant parameters affecting the ***EM*** response into one parameter against which to compare responses. For a ***layered earth*** the response parameter is $\mu\omega\sigma h^2$ and for a large, flat, ***conductor*** it is $\mu\omega\sigma th$, where μ is the ***magnetic permeability***, ω is the angular ***frequency***, σ is the **conductivity**, t is the thickness (for the flat conductor) and h is the height of the system above the conductor.

inductive limit: When the frequency of an EM system is very high, or the **conductivity** of the target is very high, the response measured will be entirely **in-phase** with no **quadrature** (**phase** angle =0). The in-phase response will remain constant with further increase in conductivity or frequency. The system can no longer detect changes in conductivity of the target.

infinite: In geophysical terms, an "infinite' dimension is one much greater than the ***footprint*** of the system, so that the system does not detect changes at the edges of the object.

International Geomagnetic Reference Field: **[IGRF]** An approximation of the smooth magnetic field of the earth, in the absence of variations due to local geology. Once the IGRF is subtracted from the measured magnetic total field data, any remaining variations are assumed to be due to local geology. The IGRF also predicts the slow changes of the field up to five years in the future.

inversion, or **inverse modeling**: A process of converting geophysical data to an earth model, which compares theoretical models of the response of the earth to the data measured, and refines the model until the response closely fits the measured data (Huang and Palacky, 1991)

layered earth: A common geophysical model which assumes that the earth is horizontally layered – the ***physical parameters*** are constant to ***infinite*** distance horizontally, but change vertically.

magnetic permeability: **[μ]** This is defined as the ratio of magnetic induction to the inducing magnetic field. The relative magnetic permeability [μ_r] is often quoted, which is the ratio of the rock permeability to the permeability of free space. In geology and geophysics, the ***magnetic susceptibility*** is more commonly used to describe rocks.

magnetic susceptibility: **[k]** A measure of the degree to which a body is magnetized. In SI units this is related to relative ***magnetic permeability*** by $k=\mu_r-1$, and is a dimensionless unit. For most geological material, susceptibility is influenced primarily by the percentage of magnetite. It is most often quoted in units of 10^{-6}. In HEM data this is most often apparent as a negative ***in-phase*** component over high susceptibility, high ***resistivity*** geology such as diabase dikes.

manoeuvre noise: variations in the magnetic field measured caused by changes in the relative positions of the magnetic sensor and magnetic objects or electrical currents in the aircraft. This type of noise is generally corrected by magnetic **compensation**.

model: Geophysical theory and applications generally have to assume that the geology of the earth has a form that can be easily defined mathematically, called the model. For example steeply dipping **conductor**s are generally modeled as being **infinite** in horizontal and depth extent, and very thin. The earth is generally modeled as horizontally layered, each layer infinite in extent and uniform in characteristic. These models make the mathematics to describe the response of the (normally very complex) earth practical. As theory advances, and computers become more powerful, the useful models can become more complex.

natural exposure rate: in radiometric surveys, a calculation of the total exposure rate due to natural-source gamma rays at the ground surface. It is used as a measurement of the concentration of all the natural **radioelements** at the surface. See also: **exposure rate**.

noise: That part of a geophysical measurement that the user does not want. Typically this includes electronic interference from the system, the atmosphere (***sferics***), and man-made sources. This can be a subjective judgment, as it may include the response from geology other than the target of interest. Commonly the term is used to refer to high frequency (short period) interference. See also ***drift***.

Occam's inversion: an ***inversion*** process that matches the measured ***electromagnetic*** data to a theoretical model of many, thin layers with constant thickness and varying resistivity (Constable et al, 1987).

off-time: In a ***time-domain electromagnetic*** survey, the time after the end of the ***primary field pulse***, and before the start of the next pulse.

on-time: In a ***time-domain electromagnetic*** survey, the time during the ***primary field pulse***.

overburden: In engineering and mineral exploration terms, this most often means the soil on top of the unweathered bedrock. It may be sand, glacial till, or weathered rock.

Phase, phase angle: The angular difference in time between a measured sinusoidal electromagnetic field and a reference – normally the primary field. The phase is calculated from $\tan^{-1}$(***in-phase / quadrature***).

physical parameters: These are the characteristics of a geological unit. For electromagnetic surveys, the important parameters are ***conductivity, magnetic permeability*** (or ***susceptibility***) and ***dielectric permittivity***; for magnetic surveys the parameter is magnetic susceptibility, and for gamma ray spectrometric surveys it is the concentration of the major radioactive elements: potassium, uranium, and thorium.

permittivity: see ***dielectric permittivity***.

permeability: see ***magnetic permeability***.

primary field: the EM field emitted by a transmitter. This field induces ***eddy currents*** in (energizes) the conductors in the ground, which then create their own ***secondary* fields**.

pulse: In time-domain EM surveys, the short period of intense ***primary*** field transmission. Most measurements (the ***off-time***) are measured after the pulse. **On-time** measurements may be made during the pulse.

quadrature: that component of the measured ***secondary field*** that is phase-shifted 90° from the ***primary field***. The quadrature component tends to be stronger than the ***in-phase*** over relatively weaker ***conductivity***.

Q-coils: see ***calibration coil***.

radioelements: This normally refers to the common, naturally-occurring radioactive elements: potassium (K), uranium (U), and thorium (Th). It can also refer to man-made radioelements, most often cobalt (Co) and cesium (Cs)

radiometric: Commonly used to refer to ***gamma ray*** spectrometry.

radon: A radioactive daughter product of uranium and thorium, radon is a gas which can leak into the atmosphere, adding to the non-geological background of a gamma-ray spectrometric survey.

receiver: the ***signal*** detector of a geophysical system. This term is most often used in active geophysical systems – systems that transmit some kind of signal. In airborne ***electromagnetic*** surveys it is most often a ***coil***. (see also, ***transmitter***)

resistivity: **[ρ]** The strength with which the earth or a geological formation resists the flow of electricity, typically the flow induced by the ***primary field*** of the electromagnetic transmitter. Normally expressed in ohm-metres, it is the reciprocal of ***conductivity***.

resistivity-depth transforms: similar to ***conductivity depth transforms***, but the calculated ***conductivity*** has been converted to ***resistivity***.

resistivity section: an approximate vertical section of the resistivity of the layers in the earth. The resistivities can be derived from the ***apparent resistivity***, the ***differential resistivities***, ***resistivity-depth transforms***, or ***inversions***.

Response parameter: another name for the **induction number**.

secondary field: The field created by conductors in the ground, as a result of electrical currents induced by the ***primary field*** from the ***electromagnetic*** transmitter. Airborne ***electromagnetic*** systems are designed to create and measure a secondary field.

Sengpiel section: a ***resistivity section*** derived using the ***apparent resistivity*** and an approximation of the depth of maximum sensitivity for each frequency.

sferic: Lightning, or the ***electromagnetic*** signal from lightning, it is an abbreviation of "atmospheric discharge". These appear to magnetic and electromagnetic sensors as sharp "spikes" in the data. Under some conditions lightning storms can be detected from hundreds of kilometres away. (see ***noise***)

signal: That component of a measurement that the user wants to see – the response from the targets, from the earth, etc. (See also ***noise***)

skin depth: A measure of the depth of penetration of an electromagnetic field into a material. It is defined as the depth at which the primary field decreases to 1/e of the field at the surface. It is calculated by approximately 503 x $\sqrt{}$(resistivity/frequency). Note that depth of penetration is greater at higher ***resistivity*** and/or lower ***frequency***.

spectrometry: Measurement across a range of energies, where ***amplitude*** and energy are defined for each measurement. In gamma-ray spectrometry, the number of gamma rays are measured for each energy ***window***, to define the ***spectrum***.

spectrum: In ***gamma ray spectrometry***, the continuous range of energy over which gamma rays are measured. In ***time-domain electromagnetic*** surveys, the spectrum is the energy of the **pulse** distributed across an equivalent, continuous range of frequencies.

spheric: see ***sferic***.

stacking: Summing repeat measurements over time to enhance the repeating ***signal***, and minimize the random ***noise***.
stripping: Estimation and correction for the gamma ray photons of higher and lower energy that are observed in a particular ***energy window***. See also ***Compton scattering***.

susceptibility: See ***magnetic susceptibility***.

tau: [τ] Often used as a name for the ***time constant***.

TDEM: ***time domain electromagnetic***.

thin sheet: A standard model for electromagnetic geophysical theory. It is usually defined as a thin, flat-lying conductive sheet, ***infinite*** in both horizontal directions. (see also ***vertical plate***)

tie-line: A survey line flown across most of the ***traverse lines***, generally perpendicular to them, to assist in measuring ***drift*** and ***diurnal*** variation. In the short time required to fly a tie-line it is assumed that the drift and/or diurnal will be minimal, or at least changing at a constant rate.

time constant: The time required for an ***electromagnetic*** field to decay to a value of 1/e of the original value. In ***time-domain*** electromagnetic data, the time constant is proportional to the size and ***conductance*** of a tabular conductive body. Also called the decay constant.

Time channel: In ***time-domain electromagnetic*** surveys the decaying ***secondary field*** is measured over a period of time, and the divided up into a series of consecutive discrete measurements over that time.

time-domain: ***Electromagnetic*** system which transmits a pulsed, or stepped ***electromagnetic*** field. These systems induce an electrical current (***eddy current***) in the ground that persists after the ***primary field*** is turned off, and measure the change

over time of the ***secondary field*** created as the currents ***decay***. See also ***frequency-domain***.

total energy envelope: The sum of the squares of the three ***components*** of the ***time-domain electromagnetic secondary field***. Equivalent to the ***amplitude*** of the secondary field.

transient: Time-varying. Usually used to describe a very short period pulse of ***electromagnetic*** field.

transmitter: The source of the ***signa***l to be measured in a geophysical survey. In airborne ***EM*** it is most often a **coil** carrying a time-varying electrical current, transmitting the ***primary field***. (see also ***receiver***)

traverse line: A normal geophysical survey line. Normally parallel traverse lines are flown across the property in spacing of 50 m to 500 m, and generally perpendicular to the target geology.

vertical plate: A standard model for electromagnetic geophysical theory. It is usually defined as thin conductive sheet, ***infinite*** in horizontal dimension and depth extent. (see also ***thin shee***t)

waveform: The shape of the ***electromagnetic pulse*** from a ***time-domain*** electromagnetic transmitter.

window: A discrete portion of a ***gamma-ray spectrum*** or ***time-domain electromagnetic decay***. The continuous energy spectrum or ***full-stream*** data are grouped into windows to reduce the number of samples, and reduce ***noise***.

Version 1.5, November 29, 2005
Greg Hodges,
Chief Geophysicist
Fugro Airborne Surveys, Toronto

Common Symbols and Acronyms

k Magnetic susceptibility
ε Dielectric permittivity
μ, μ_r Magnetic permeability, relative permeability
ρ, ρ_a Resistivity, apparent resistivity
σ,σ_a Conductivity, apparent conductivity
σ**t** Conductivity thickness
τ Tau, or time constant
Ω**m** ohm-metres, units of resistivity
AGS Airborne gamma ray spectrometry.
CDT Conductivity-depth transform, conductivity-depth imaging (Macnae and Lamontagne, 1987; Wolfgram and Karlik, 1995)
CPI, CPQ Coplanar in-phase, quadrature
CPS Counts per second
CTP Conductivity thickness product
CXI, CXQ Coaxial, in-phase, quadrature
FOM Figure of Merit
fT femtoteslas, normal unit for measurement of B-Field
EM Electromagnetic
keV kilo electron volts – a measure of gamma-ray energy
MeV mega electron volts – a measure of gamma-ray energy 1MeV = 1000keV
NIA dipole moment: turns x current x Area
nT nanotesla, a measure of the strength of a magnetic field
nG/h nanoGreys/hour – gamma ray dose rate at ground level
ppm parts per million – a measure of secondary field or noise relative to the primary or radioelement concentration.
pT/s picoteslas per second: Units of decay of secondary field, dB/dt
S siemens – a unit of conductance
x: the horizontal component of an EM field parallel to the direction of flight.
y: the horizontal component of an EM field perpendicular to the direction of flight.
z: the vertical component of an EM field.

References:

Constable, S.C., Parker, R.L., And Constable, C.G., 1987, Occam's inversion: a practical algorithm for generating smooth models from electromagnetic sounding data: Geophysics, 52, 289-300

Huang, H. and Fraser, D.C, 1996. The differential parameter method for muiltifrequency airborne resistivity mapping. Geophysics, 55, 1327-1337

Huang, H. and Palacky, G.J., 1991, Damped least-squares inversion of time-domain airborne EM data based on singular value decomposition: Geophysical Prospecting, v.39, 827-844

Macnae, J. and Lamontagne, Y., 1987, Imaging quasi-layered conductive structures by simple processing of transient electromagnetic data: Geophysics, v52, 4, 545-554.

Sengpiel, K-P. 1988, Approximate inversion of airborne EM data from a multi-layered ground. Geophysical Prospecting, 36, 446-459

Wolfgram, P. and Karlik, G., 1995, Conductivity-depth transform of GEOTEM data: Exploration Geophysics, 26, 179-185.

Yin, C. and Fraser, D.C. (2002), The effect of the electrical anisotropy on the responses of helicopter-borne frequency domain electromagnetic systems, Submitted to *Geophysical Prospecting*

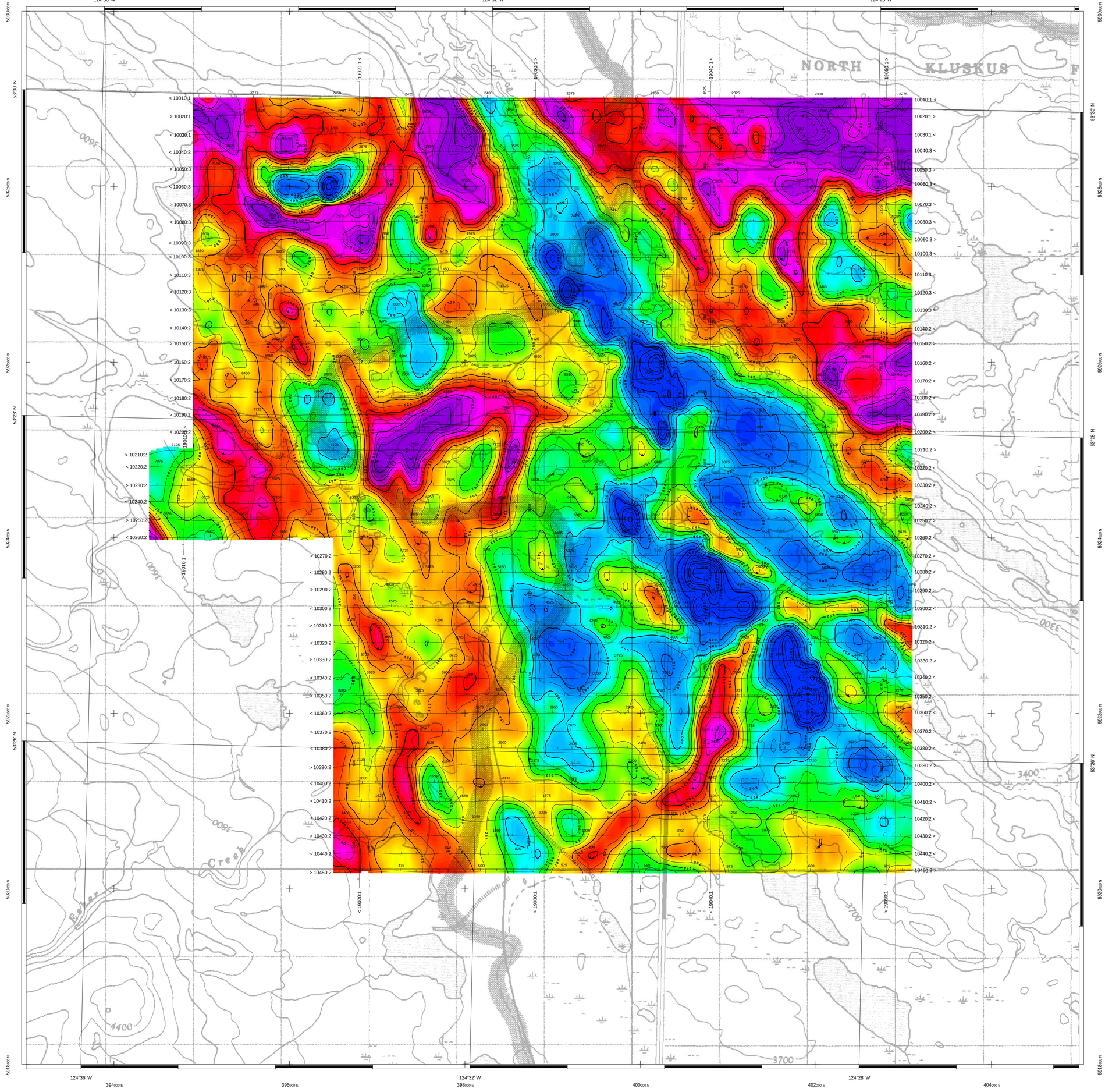

TECHNICAL SUMMARY

Navigation	Differentially-corrected GPS
Data reduction grid interval	40 metres
Terrain clearance	Helicopter 60 m Electromagnetic sensor 35 m Magnetometer 35 m
Data sampling interval	0.1 second
Magnetometer / sensitivity	Cesium / 0.01 nT
Electromagnetic system	DIGHEM^V

Frequency	Sensitivity	Coil Orientation
1000 Hz	.06 ppm	Vertical coaxial
5500 Hz	.12 ppm	Vertical coaxial
900 Hz	.12 ppm	Horizontal coplanar
7200 Hz	.24 ppm	Horizontal coplanar
56000 Hz	.60 ppm	Horizontal coplanar

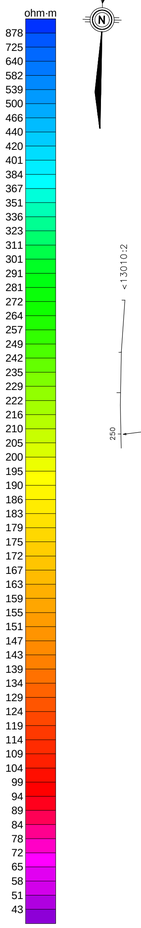

FLIGHT LINES

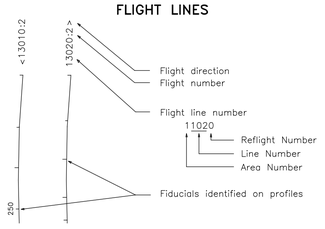

RESISTIVITY CONTOURS

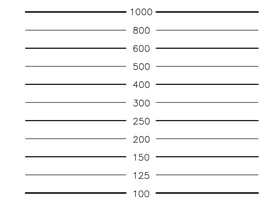

Contours in ohm-m at 10 intervals per decade. Apparent resistivity calculated using a pseudo-layer half-space model (Fraser 1978).

LOCATION MAP

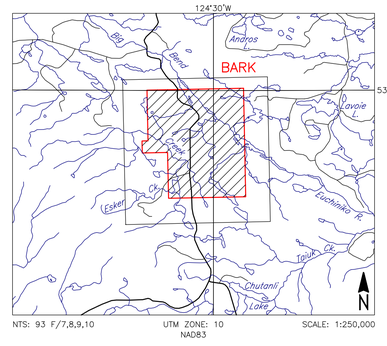

AMARC RESOURCES LTD.

BARK AREA, BC

APPARENT RESISTIVITY 7200 Hz COPLANAR

FUGRO DIGHEM^V SURVEY	NTS: 93 F/7,8,9,10	GEOPHYSICIST:
DATE: JANUARY, 2011	JOB: 10073	SHEET: 1
Fugro Airborne Surveys		

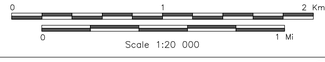

FUGRO AIRBORNE SURVEYS

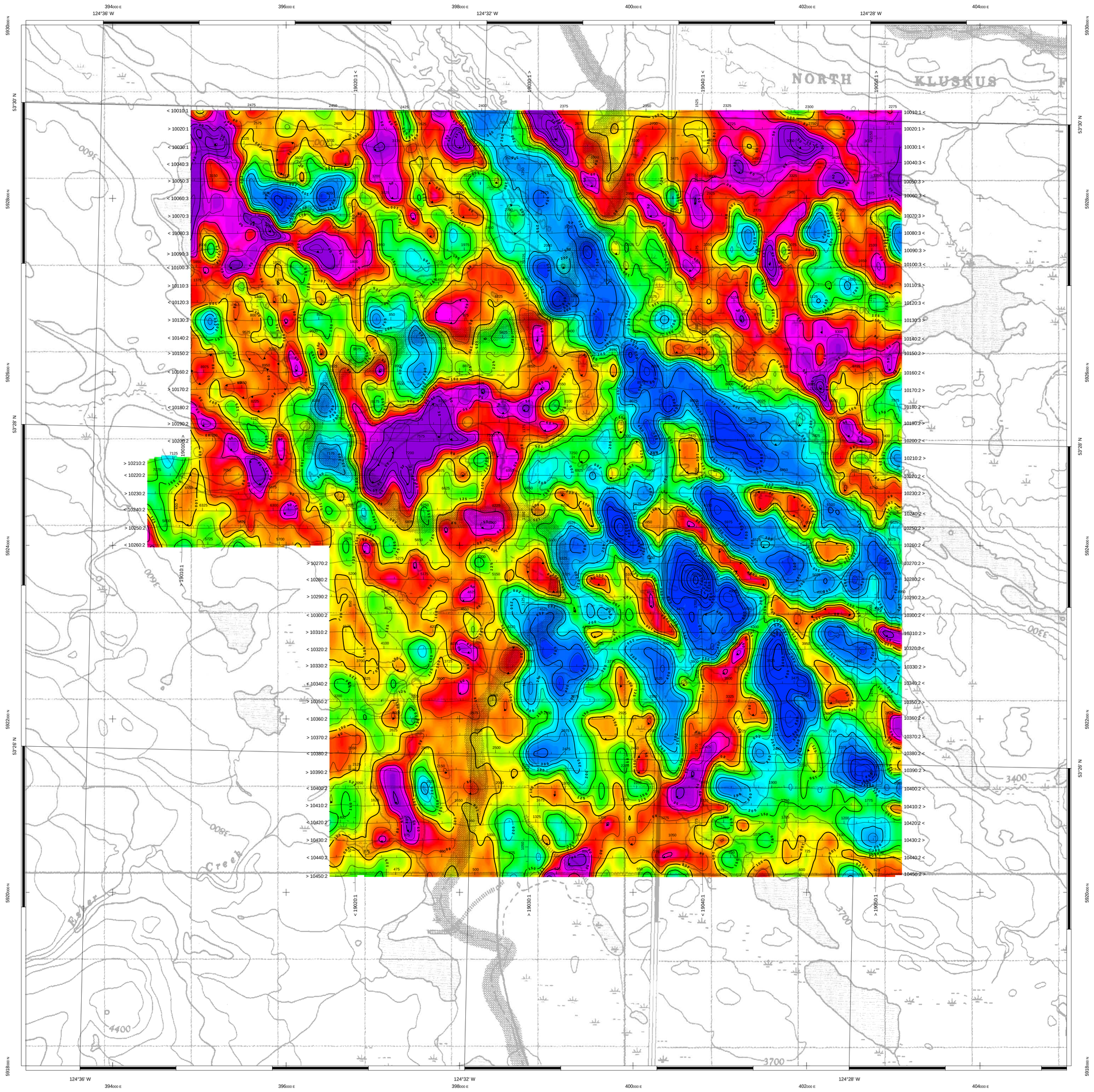

TECHNICAL SUMMARY

Navigation	Differentially-corrected GPS
Data reduction grid interval	40 metres
Terrain clearance	Helicopter 60 m Electromagnetic sensor 35 m Magnetometer 35 m
Data sampling interval	0.1 second
Magnetometer / sensitivity	Cesium / 0.01 nT
Electromagnetic system	DIGHEM^V

Frequency	Sensitivity	Coil Orientation
1000 Hz	.06 ppm	Vertical coaxial
5500 Hz	.12 ppm	Vertical coaxial
900 Hz	.12 ppm	Horizontal coplanar
7200 Hz	.24 ppm	Horizontal coplanar
56000 Hz	.60 ppm	Horizontal coplanar

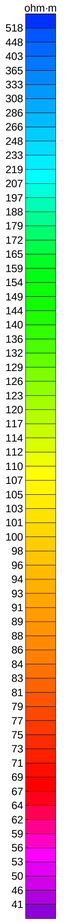

FLIGHT LINES

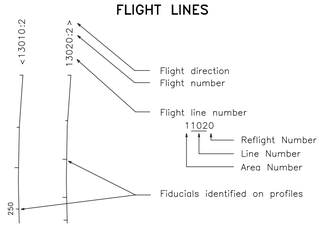

RESISTIVITY CONTOURS

1000
800
600
500
400
300
250
200
150
125
100

Contours in ohm-m at 10 intervals per decade. Apparent resistivity calculated using a pseudo-layer half-space model (Fraser 1978).

LOCATION MAP

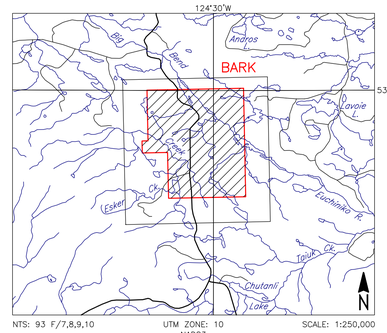

AMARC RESOURCES LTD.

BARK AREA, BC

APPARENT RESISTIVITY
56,000 Hz COPLANAR

FUGRO DIGHEM^V SURVEY	NTS: 93 F/7,8,9,10	GEOPHYSICIST:
DATE: JANUARY, 2011	JOB: 10073	SHEET: 1

Fugro Airborne Surveys

0 1 2 Km

0 1 Mi

Scale 1:20 000

FUGRO AIRBORNE SURVEYS

TECHNICAL SUMMARY

Navigation	Differentially-corrected GPS
Data reduction grid interval	40 metres
Terrain clearance	Helicopter 60 m Electromagnetic sensor 35 m Magnetometer 35 m
Data sampling interval	0.1 second
Magnetometer / sensitivity	Cesium / 0.01 nT
Electromagnetic system	DIGHEM^V

Frequency	Sensitivity	Coil Orientation
1000 Hz	.06 ppm	Vertical coaxial
5500 Hz	.12 ppm	Vertical coaxial
900 Hz	.12 ppm	Horizontal coplanar
7200 Hz	.24 ppm	Horizontal coplanar
56000 Hz	.60 ppm	Horizontal coplanar

nT
469
410
366
334
308
285
266
247
230
211
191
172
154
140
126
114
102
88
74
62
51
40
28
17
5
-7
-19
-30
-43
-55
-66
-76
-85
-92
-99
-106
-112
-119
-125
-131
-137
-142
-148
-154
-161
-168
-174
-180
-187
-194
-202
-210
-217
-226
-234
-241
-248
-258
-267
-278
-292
-306
-323

FLIGHT LINES

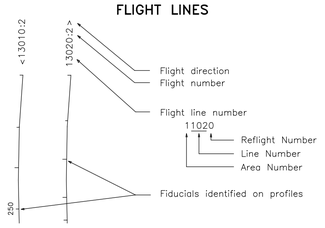

RESIDUAL MAGNETIC FIELD CONTOURS

250 nT
50 nT
10 nT
5 nT
magnetic low

Magnetic inclination within the survey area: 73 degrees N
Magnetic declination within the survey area: 19 degrees E

LOCATION MAP

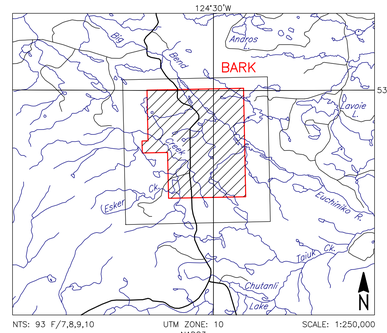

AMARC RESOURCES LTD.

BARK AREA, BC

RESIDUAL MAGNETIC FIELD

IGRF Removed

FUGRO DIGHEM^V SURVEY	NTS: 93 F/7,8,9,10	GEOPHYSICIST:
DATE: JANUARY, 2011	JOB: 10073	SHEET: 1

Fugro Airborne Surveys

0 1 2 Km
0 1 Mi
Scale 1:20 000

FUGRO AIRBORNE SURVEYS

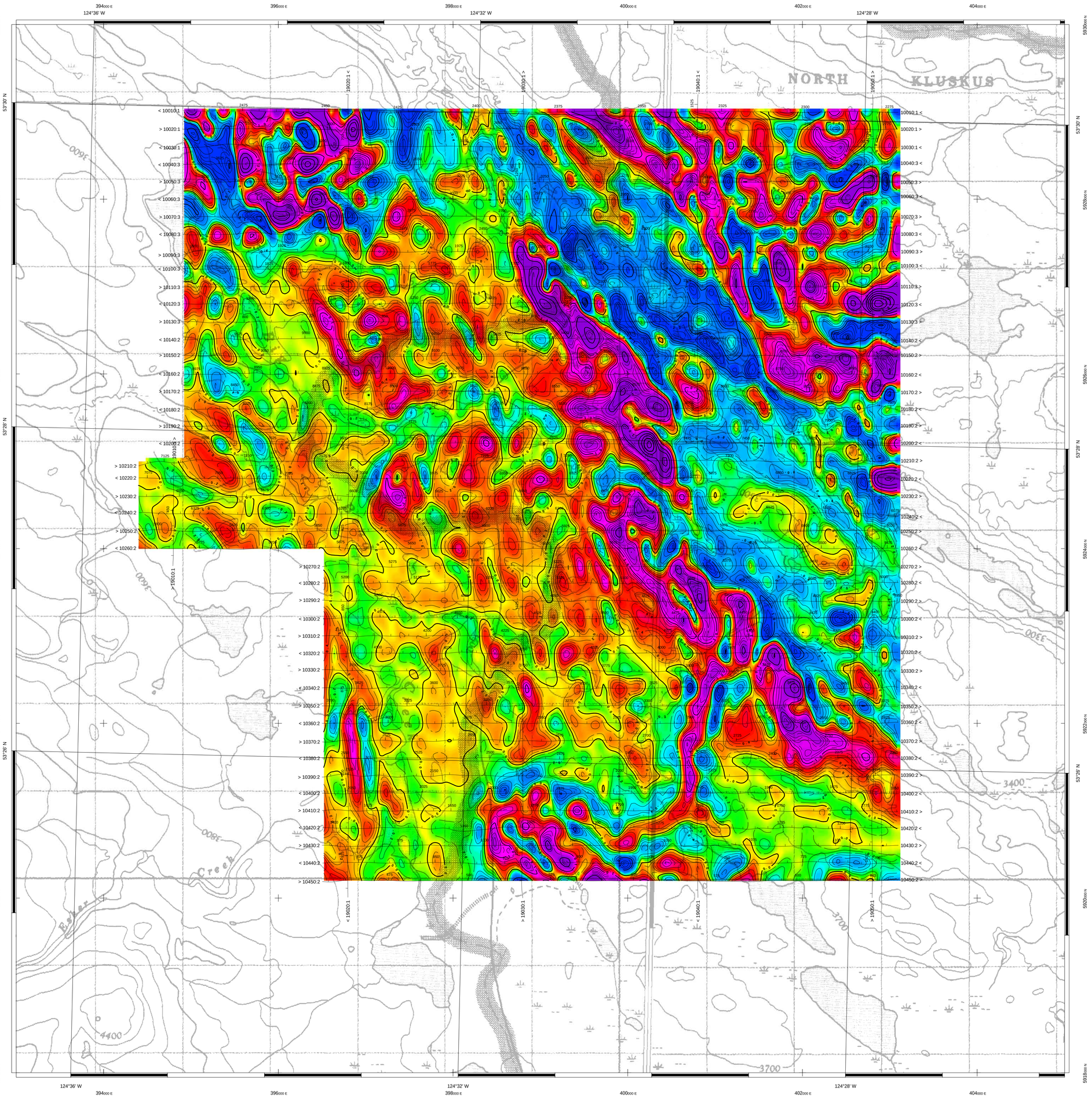

TECHNICAL SUMMARY

Navigation	Differentially–corrected GPS
Data reduction grid interval	40 metres
Terrain clearance	Helicopter 60 m Electromagnetic sensor 35 m Magnetometer 35 m
Data sampling interval	0.1 second
Magnetometer / sensitivity	Cesium / 0.01 nT
Electromagnetic system	DIGHEM^V

Frequency	Sensitivity	Coil Orientation
1000 Hz	.06 ppm	Vertical coaxial
5500 Hz	.12 ppm	Vertical coaxial
900 Hz	.12 ppm	Horizontal coplanar
7200 Hz	.24 ppm	Horizontal coplanar
56000 Hz	.60 ppm	Horizontal coplanar

nT/m
1.96
1.59
1.34
1.15
0.99
0.87
0.76
0.66
0.59
0.52
0.47
0.42
0.38
0.34
0.31
0.28
0.26
0.23
0.21
0.18
0.16
0.14
0.12
0.11
0.09
0.08
0.06
0.05
0.03
0.02
0.01
-0.01
-0.02
-0.03
-0.04
-0.05
-0.06
-0.08
-0.09
-0.10
-0.12
-0.13
-0.15
-0.17
-0.19
-0.21
-0.23
-0.25
-0.28
-0.31
-0.34
-0.37
-0.41
-0.45
-0.49
-0.54
-0.58
-0.63
-0.69
-0.77
-0.87
-0.98
-1.14

FLIGHT LINES

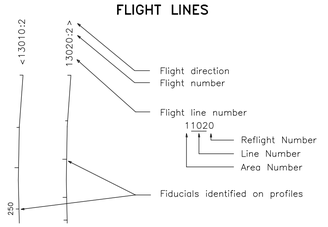

CALCULATED VERTICAL GRADIENT CONTOURS

5.0 nT/metre
1.0 nT/metre
0.2 nT/metre
0.1 nT/metre

LOCATION MAP

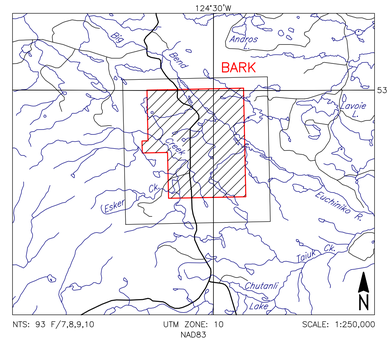

NTS: 93 F/7,8,9,10 UTM ZONE: 10 NAD83 SCALE: 1:250,000

AMARC RESOURCES LTD.

BARK AREA, BC

CALCULATED VERTICAL MAGNETIC GRADIENT

FUGRO DIGHEM^V SURVEY	NTS: 93 F/7,8,9,10	GEOPHYSICIST:
DATE: JANUARY, 2011	JOB: 10073	SHEET: 1

Fugro Airborne Surveys

0 1 2 Km
0 1 Mi
Scale 1:20 000

FUGRO AIRBORNE SURVEYS

394000 E
396000 E
398000 E
400000 E
402000 E
404000 E
124°36' W
124°32' W
124°28' W
5930000 N
5928000 N
5926000 N
5924000 N
5922000 N
5920000 N
5918000 N
53°30' N
53°28' N
53°26' N

NORTH KLUSKUS

Esker Creek

< 10010:1 | 10010:1 <
> 10020:1 | 10020:1 >
< 10030:1 | 10030:1 <
< 10040:3 | 10040:3 <
> 10050:3 | 10050:3 >
< 10060:3 | 10060:3 <
> 10070:3 | 10070:3 >
< 10080:3 | 10080:3 <
> 10090:3 | 10090:3 >
< 10100:3 | 10100:3 <
> 10110:3 | 10110:3 >
< 10120:3 | 10120:3 <
> 10130:3 | 10130:3 >
< 10140:2 | 10140:2 <
> 10150:2 | 10150:2 >
< 10160:2 | 10160:2 <
> 10170:2 | 10170:2 >
< 10180:2 | 10180:2 <
> 10190:2 | 10190:2 >
< 10200:2 | 10200:2 <
> 10210:2 | 10210:2 >
< 10220:2 | 10220:2 <
> 10230:2 | 10230:2 >
< 10240:2 | 10240:2 <
> 10250:2 | 10250:2 >
< 10260:2 | 10260:2 <
> 10270:2 | 10270:2 >
< 10280:2 | 10280:2 <
> 10290:2 | 10290:2 >
< 10300:2 | 10300:2 <
> 10310:2 | 10310:2 >
< 10320:2 | 10320:2 <
> 10330:2 | 10330:2 >
< 10340:2 | 10340:2 <
> 10350:2 | 10350:2 >
< 10360:2 | 10360:2 <
> 10370:2 | 10370:2 >
< 10380:2 | 10380:2 <
> 10390:2 | 10390:2 >
< 10400:2 | 10400:2 <
> 10410:2 | 10410:2 >
< 10420:2 | 10420:2 <
> 10430:2 | 10430:2 >
< 10440:2 | 10440:2 <
> 10450:2 | 10450:2 >

< 19010:1 | > 19010:1
< 19020:1 | > 19020:1
< 19030:1 | > 19030:1
< 19040:1 | > 19040:1
< 19050:1 | > 19050:1

TECHNICAL SUMMARY

Navigation	Differentially-corrected GPS
Data reduction grid interval	40 metres
Terrain clearance	Helicopter 60 m Electromagnetic sensor 35 m Magnetometer 35 m
Data sampling interval	0.1 second
Magnetometer / sensitivity	Cesium / 0.01 nT
Electromagnetic system	DIGHEM^V

Frequency	Sensitivity	Coil Orientation
1000 Hz	.06 ppm	Vertical coaxial
5500 Hz	.12 ppm	Vertical coaxial
900 Hz	.12 ppm	Horizontal coplanar
7200 Hz	.24 ppm	Horizontal coplanar
56000 Hz	.60 ppm	Horizontal coplanar

ELECTROMAGNETIC ANOMALIES

Grade	Anomaly	Conductance
7	●	>100 siemens
6	◕	50–100 siemens
5	◑	20–50 siemens
4	◔	10–20 siemens
3	⊕	5–10 siemens
2	○	1–5 siemens
1	◌	< 1 siemens
–	✳	Questionable anomaly

Anomaly identifier: C H
Interpretive symbol

Interpretive symbol		Conductor model
	B	Bedrock conductor
	D	Narrow bedrock conductor ("thin dike")
	S	Conductive cover ("horizontal thin sheet")
	H	Broad conductive rock unit, deep conductive weathering, thick conductive cover ("half-space")
	E	Edge of broad conductor ("edge of half space")
□	L	Culture, e.g. power line, metal building or fence
△	M	Magnetite

FLIGHT LINES WITH EM ANOMALIES

< 13010:2 | > 13020:2
120
11020
A D
F B
100

- Flight direction
- Flight number
- Flight line number
- Reflight Number
- Line Number
- Area Number
- Fiducials identified on profiles
- Dip direction
- EM anomaly (see EM legend)
- Conductor axis (on EM maps only)
- Arcs indicate the conductor has a thickness > 10m
- Magnetic correlation in nT

LOCATION MAP

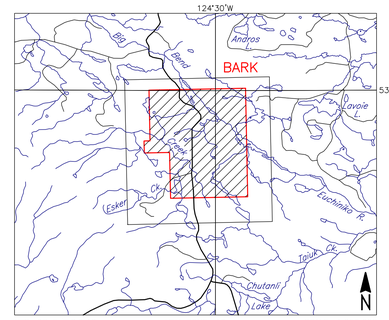

NTS: 93 F/7,8,9,10 | UTM ZONE: 10 NAD83 | SCALE: 1:250,000

AMARC RESOURCES LTD.

BARK AREA, BC

ELECTROMAGNETIC ANOMALIES

FUGRO DIGHEM^V SURVEY	NTS: 93 F/7,8,9,10	GEOPHYSICIST:
DATE: JANUARY, 2011	JOB: 10073	SHEET: 1

Fugro Airborne Surveys

0 1 2 Km
0 1 Mi
Scale 1:20 000

FUGRO AIRBORNE SURVEYS